# Performance Analysis of SCM Optical Transmission Link for Fiber-to-the-Home

# EECS891

By

Anthony Leung

BSEE University of Missouri-Rolla

Submitted to the Department of Electrical Engineering and Computer Science
and the Faculty of the Graduate School of the University of Kansas
in partial fulfillment of the requirements for the degree of
Master of Science

_____
Professor in Charge

_____

_____

_____
Date EECS891 Project Submitted

# ABSTRACT

After years of anticipation, organizations such as ILECS, CLECS and municipalities are deploying Fiber to the Home networks in various communities across the states. A Fiber to the Home (FTTH) network is a residential communications infrastructure where fibers run all the way to the subscriber premises.

Recent FTTH field test trials were demonstrated last year using low cost CWDM passive optical network with three (3) optical channels to support Broadband Services. Wavelength 1550nm was used to broadcast TV programs, wavelength 1490nm was used to transmit downstream data and wavelength 1310nm was used for upstream digital data transmission.

The idea of this project is to study another approach using SCM-based optical network to transmit 78 CATV and 1Gb/s digital data from central office to subscriber premises using one (1) optical channel.

The goal of this project is to evaluate the physical transmission quality of analog and digital signal using SCM approach. Therefore, this study will look at

1) CATV carrier-to-noise ratio (CNR) in SCM externally modulation optical link.

2) Digital data Q-Value in SCM externally modulation optical link.

3) The characteristic of fiber nonlinear crosstalk such as Stimulated Raman Scattering (SRS), Cross Phase Modulation (XPM) and Four-wave mixing (FWM) in SCM externally modulation optical link

4) The impact of fiber nonlinear crosstalk on CATV CNR & Digital data Q-Value performance.

**ACKNOWLEDGEMENTS**

**TABLE OF CONTENTS**

# LIST OF FIGURES

# LIST OF TABLES

**CHAPTER 1: INTRODUCTION**

**1.1     Background**

This project studies and examines the transmission performance of SCM Optical

Network to support Broadband Services such as cable TV programs and Broadband Internet

access.  After years of anticipation, organizations such as ILECS, CLECS and municipalities are

deploying Fiber to the Home networks in various communities across the states.  A Fiber to the

Home (FTTH) network is a residential communications infrastructure where fibers run all the

way to the subscriber premises.

FTTH networks differ from past residential telecommunications infrastructure such as the

telephone and cable TV networks.  Those networks were built to support specific applications;

namely, telephone service and cable television.  Nowadays, cable modem and DSL technologies

are used to adapt these existing networks to provide broadband Internet access.  The current

cable modem and DSL broadband services are sufficient for today's applications, however, these

technologies will soon face bandwidth limitation challenges to provide next generation

broadband service to customers over coaxial cable and twisted-copper pair wiring.  To address

these issues, ATM-PON and Ethernet PON FTTH solutions have been proposed in recent years.

ATM-PON and Ethernet PON are based on the common network architecture, but adopt

different transfer technologies to support integrated services and multiple protocols.  ATM-PON

and Ethernet PON both use Time Division Multiple Access (TDMA) based media access control

(MAC) protocol for upstream transmission.

In TDM-based PON, some of the fiber and transceiver-in-feeder networks are shared by

end-users, and only low-cost, passive power splitters are on the light paths between Central

Office (CO) and end users.  This enables cost sharing of a transceiver and reduces maintenance

cost significantly.  On the other hand, the TDM-based MAC protocols for collision-free upstream transmission are rather complicated, so the future upgrade of TDM-PON could be a major challenge.  Any change in line rate and frame format for upgrade requires a change of MAC protocol and thereby the equipment in the network.  In addition to upstream transmission protocol issue, transmission clocks of each customer premises are different from one another. Therefore, reset and synchronization should be done within the overhead period of each upstream slot, which is a very challenging task especially at high speed.  Furthermore, Video Broadcasting is one of important services that access network must deliver.  While cable TV service providers provide data services via cable modems in addition to broadcast video services, telephone providers cannot deliver comparable video broadcasting with the current TDM-based system.  Therefore, broadcast video overlay has become one of major driving force for WDM-based system.

WDM-based network shares many benefits of TDM-based system.  In addition, WDM efficiently exploits the large capacity of optical fiber without much change in infrastructure and can provide a virtual point-to-point connection to each end-user, which is totally independent of line rate and frame format.

The recent WDM-based FTTH network uses 1550 nm wavelength for CATV video stream, 1490nm for digital data downstream and 1310nm upstream TDMA as shown in figure 1-1.
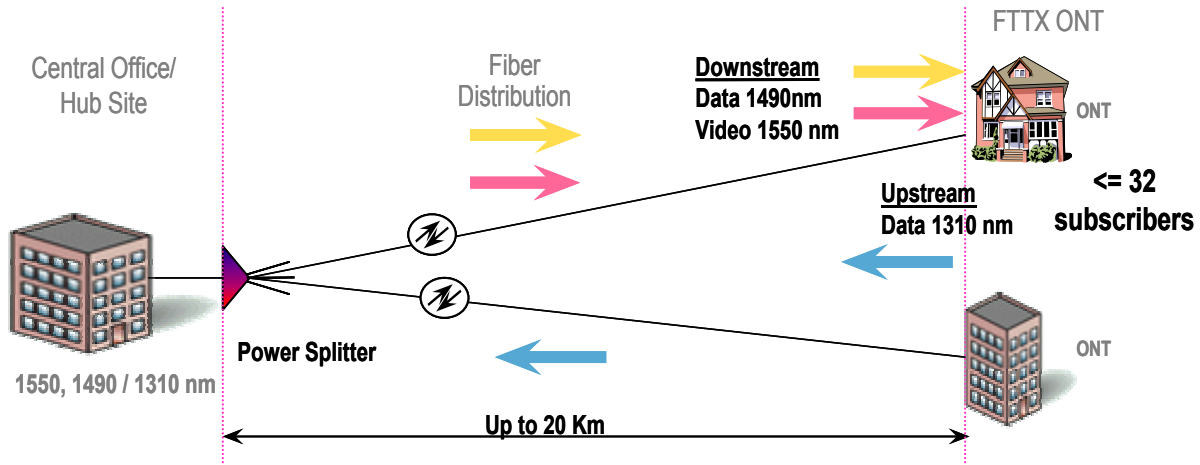
**Figure 1-1  FTTH WDM Solution**

In terms of system design, this approach requires WDM filters, additional lasers and photodiodes at CO and end-users.  It is not efficient for bandwidth utilization and the difficulty of this architecture is the more demanding 1310nm TDMA upstream transmission resulting from the increase of the sharing ratio.

## 1.2    Project Purpose and Motivation

The goal of this project is to study another approach using sub-carrier multiplexing (SCM) Optical Network as shown in figure 1-2.
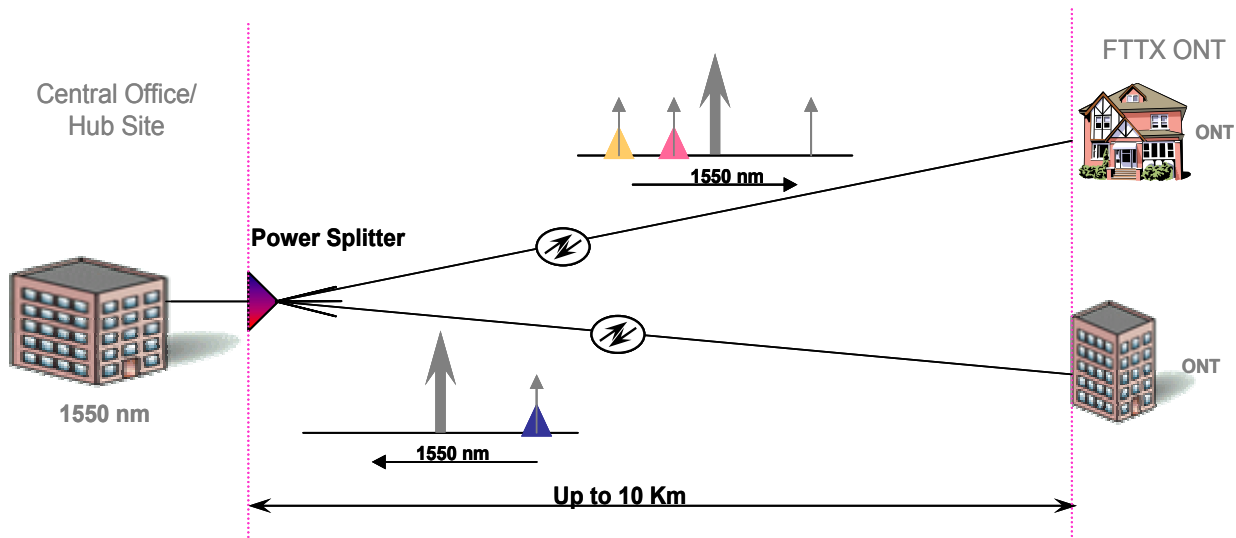


**Figure 1-2 SCM/WDM Architecture**

Because of the simplicity and stability of microwave and RF devices, SCM over WDM can combine different RF channels (analog & digital signals) closely with each other in electrical domain, and then modulate onto an optical carrier.   In this study, 78 NTSC standard analog video streams and 1Gb/s digital data are mixed by different microwave frequencies and combined together in the electrical domain before modulating onto one wavelength using optical single sideband modulation.  This composite signal is modulated at the lower sideband of the optical carrier.  In addition, a microwave frequency is modulated at the upper sideband of optical carrier.  At the end-users, an optical filter (fabry-Perot Interferometer) and optical circulator can be used to separate the optical subcarriers at the upper and lower sideband of optical carrier.  The optical subcarriers at the lower sideband of optical carrier will then demodulate into electrical domain for CATV broadcasting and downstream digital data transmission.  The optical subcarriers at the upper sideband of optical carrier can be used as an optical source for end-user upstream digital data transmission.

The goal of this project is to examine the transmission performance of SCM/WDM network transmitting1Gb/s data and 78 CATV Analog video streams under one wavelength. Therefore, this project will examine the CATV Carrier-to-Noise Ratio (CNR), the digital data receiver Q values, the characteristic of fiber nonlinear characteristic as well as the impact of fiber nonlinear crosstalk to CATV analog and digital transmission performance.

**1.3    Project Organization**

This project is organized into 6 chapters.  In chapter 2, the SCM over WDM based architecture, using 90 degree hybrid coupler and a Mach-Zender Modulator for optical single-side band modulation (OSSB), will be presented.  In chapter 3, the analytical calculation of video stream Carrier-to-Noise Ratio (CNR) and Digital Q-Value in optical systems based on a SCM externally modulated optical link concept model is presented.  In chapter 4, a detailed analysis of Carrier-to-Noise Ratio (CNR) for analog video transmission and digital data Q-value as well as an overview of the effect of using Dual Parallel linearized external modulator to suppress third-order nonlinear distortion will be examined.  In chapter 5, Stimulated Raman Scattering (SRS), Cross Phase Modulation (XPM) & Four-wave mixing will be presented and a detailed analysis of resulting nonlinear crosstalk that impacts on the CATV CNR & digital Q-Value of SCM/WDM network will be studied.  And finally, in chapter 6, the results of the above analysis are summarized and the problems that need further study are discussed and prospected.

# CHAPTER 2: SCM ARCHITECTURE

In this chapter, the architecture of SCM, using 90 degrees hybrid coupler and MZ modulator,

between the central office (CO) and the end-user network is presented in Figure 2-1
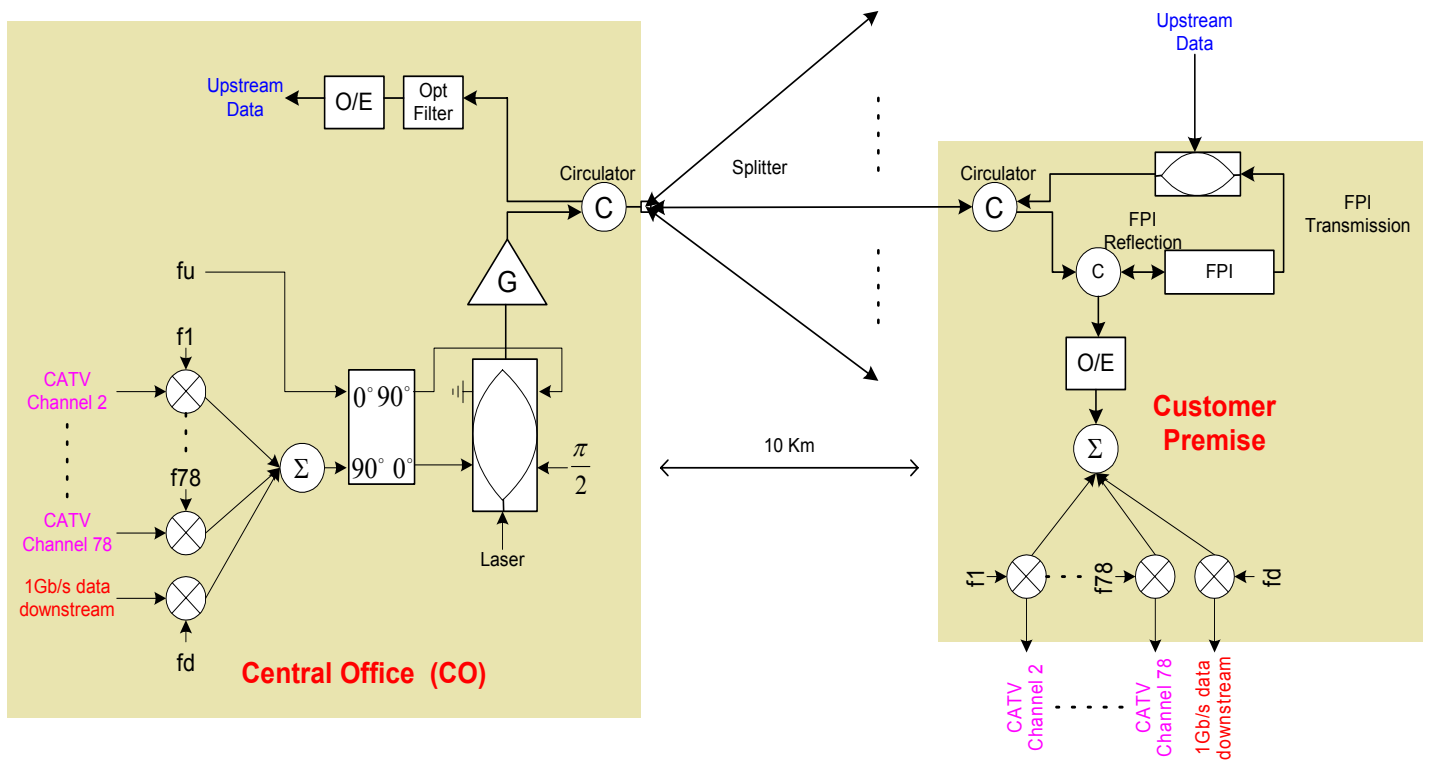


**Figure 2-1: SCM Diagram**

As shown in Figure 2-1, 78 NTSC standard analog video streams and 1Gb/s digital data are

mixed by different microwave frequencies and combined together in electrical domain before

being modulated onto one wavelength using optical single sideband modulation.  The composite

signal is modulated at the lower sideband of the optical carrier.  In addition, a microwave

frequency is modulated at the upper sideband of optical carrier and delivered to the end users.  At

the end-users, an optical filter (fabry-Perot Interferometer) and optical circulator can be used to

separate the optical subcarriers at the upper and lower sideband of optical carrier.  The optical

subcarriers at the lower sideband of optical carrier demodulate into electrical domain for CATV

broadcasting and downstream digital data transmission.  The optical subcarriers at the upper

sideband of optical carrier are used as an optical source at the end-user for upstream digital data transmission.

## 2.1    Subcarrier Modulation

In SCM optical transmission systems, a large variety of modulation scheme become feasible because all those modulation and demodulation can be done in microwave domain.

### 2.1.1   Analog AM-VSB Modulation

The standard modulation format for NTSC analog video stream is AM-VSM (Amplitude-modulation with vestigial sideband modulation).  Amplitude modulation with vestigial sideband (AM-VSB) modulation up converts each video stream on an allocated CATV frequency. The NTSC standard analog video stream has two major components, picture carrier and audio subcarrier.  The TV luminance and the 3.58 MHz chrominance subcarrier amplitude modulates an IF carrier (such as 55.25MHz, 61.25MHz, etc), then, an asymmetrically filter is used to filter portion of the upper sideband of the amplitude modulated signal such that the upper sideband edge is 1.25MHz above the IF carrier and the lower sideband edge is 4.75MHz below the IF carrier.

The output expression for VSB-AM is $s(t) = (Ac \cdot m(t) \cdot \cos(\omega_c t)) * h(t)$, where $m(t)$ is the video stream input, $h(t)$ is the sideband filter, and $\cos(\omega_c t)$ is the microwave frequency.  A separate mixer is needed for each video subcarrier channel at own microwave frequency.  A sinusoidal signal, $\cos(\omega_m t)$, is used to represent video stream input for approximation. Therefore, the output expression for a 78 VSB-AM modulated signal can be rewritten as

$$s_i(t) = \sum_{i=1}^{78} Ac_i \cdot \cos(\omega_{ci} - \omega_{mi})t$$

.

### 2.1.2　Digital Modulation

The Q value of digital data transmission performance of this study is based on the BPSK, QPSK & ASK (OOK) modulation schemes.  The baseband signal is modulated to a subcarrier frequency by a carrier suppress mixer.

The expression for the output of such a mixer is $y(t) = x(t) \cdot \cos(\omega_c t)$, where $\cos(\omega_c t)$ is the microwave carrier of downlink digital data and *x(t)* is the baseband signal. The baseband signal, *x(t),* can set as bipolar (+1,-1) for BPSK modulated signal, or unipolar (0, 1) for ASK modulated signal.

### 2.2　　Optical single-side band Modulation & Mach-Zehnder modulator

After SCM modulation, all subcarriers are combined together by a wideband microwave power coupler to modulate lightwave from the laser.  In this study, external intensity modulation/direct detection is used to support lightwave analog video and digital data transmission.

There are two main classes of external modulators available for external intensity modulation: the Mach-Zehnder (MZ) interferometer and the electroabsorption (EA) modulator. Compared to EA modulator, the MZ modulator is modulator choice for a vast majority of system manufacturers because of its lower insertion loss, controlled frequency chirp and its well behaved on/off characteristics.  The MZ device relies on the electro-optic effects to manipulate the optical phase differently between the two interferometer branches to effect 'on/off' switching.  Here the switch voltage is commonly referred to as $V_\pi$ and Lithium Niobate (LiNbO$_3$) is the most common used material.

The conventional MZ modulator consists of waveguides forming two Y junctions in an electro-optic material with coplanar electrodes over the waveguides. The voltage response of MZ modulator can be described as [4]

$$P_{out} = \left(\frac{P_{in} \cdot L_a}{4}\right) \cdot \left|e^{[j(\omega t - \beta_1 l + \theta)]} + e^{[j(\omega t - \beta_2 L)]}\right|^2 = (P_{in}L_a) \cdot \cos^2\left[\frac{\Delta\beta L - \theta}{2}\right] \qquad \textbf{(2-1)}$$

where $P_{in}$ is the average input optical power, $L_a$ is the 3-dB waveguide loss at the combiner Y-junction, $\omega$ is the optical carrier frequency, $\theta$ is the static bias phase shift between the two arms, and $\Delta Bl = (\beta 1 - \beta 2)L = \dfrac{\pi V(t)}{V_\pi}$ is the applied voltage-induced phase difference between the two arms.

In order to minimize the impact of fiber chromatic dispersion and to increase the optical bandwidth efficiency, optical single-side band (OSSB) modulation is used. The OSSB signal can be generated using MZ modulator. The output of the MZ modulator can be written as [1] & [5]

$$E_o(t) = \frac{A}{2}\left\{\cos[\omega_c t + \gamma\pi + \beta\pi\cos\omega_i t] + \cos[\omega_c t + \beta\pi\cos(\omega_i t + \theta)]\right\} \qquad \textbf{(2-2)}$$

The first and second term of the equation represent the phase modulation of upper and lower arm of MZ modulator. This two phase modulated optical wave then recombines resulting in amplitude modulation, where $\cos(\omega_i t)$ is the modulating RF signal and $\cos(\omega_i t + \theta)$ is the phase shifted modulating RF signal, $\omega$ is modulation signal frequency, $\gamma = \dfrac{V_{dc}}{V_\pi}$ is the bias of one arm, and $\beta\pi = \dfrac{V_{ac}}{V_\pi}\pi$ is the optical modulation index.

To obtain optical single side band, the phase difference of the modulating RF signal on each MZ modulator arm is $\theta = \dfrac{\pi}{2}$. In addition, the applied dc Voltage, $V_{dc}$, drives to one half of swinging voltage, $V_{J1}$, to bias the MZ Modulator at the quadrature point to obtain $\dfrac{\pi}{2}$ phase difference between two MZ modulator arms. By biasing the MZ Modulator at the quadratue point, the even order nonlinear distortions are cancelled. The equation in (2-2) can be expanded in terms of Bessel functions to give

$$E_o(t) = \frac{A}{2}\left\{ \cos\left[ \omega_c t + \frac{V_{dc}}{V_\pi}\pi + \frac{V_{ac}}{V_\pi}\pi\cos\omega_i t \right] + \cos\left[ \omega_c t + \frac{V_{ac}}{V_\pi}\pi\cos(\omega_i t + \theta) \right] \right\}$$

$$E_o(t) = \frac{A}{2}\left\{ J_0(\frac{V_{ac}}{V_\pi}\pi)(\cos\omega_c t - \sin\omega_c t) - 2J_1(\frac{V_{ac}}{V_\pi}\pi)\cos(\omega_c + \omega_i)t \right\}$$

$$(2\text{-}3)$$

The first term is the optical carrier at wavelength $\lambda_c = \dfrac{2\pi c}{\omega_c}$, while the second term is a lower sideband at the optical frequency $\omega_c + \omega_i$.

Furthermore, in order to double the information capacity transmitting different information in the two sidebands of the same optical carrier, a 4-port 90-degree RF hybrid is used along with dual electrode LiNbO3 Mach Zehnder modulator as shown in Figure 2-1.

The 90-degree RF hybrid coupler has two input and two output ports. When signal A enters port 1, the signal power is divided equally between ports 3 and 4. The output signal at port 3 will have a –90 degree phase shift and no phase shift at port 4. At the same time, when signal B enters port 2, the output signal at port 4 will have –90 degree phase shift and no phase shift at port 3. Nothing is coupled from port 2 to port 1.

When combining RF hybrid coupler and a MZ modulator, several types of optical modulations can be obtained as summarized in Table 2-1:

$$\sin(\omega_s t + \psi)$$

Opt In      Opt Out

$$\sin(\omega_s t) \quad \theta$$
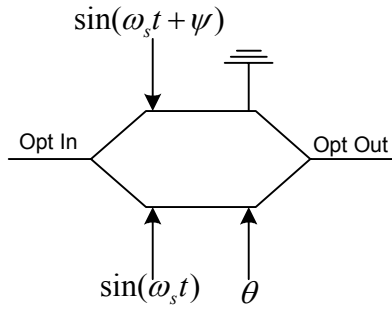
| | Optical $\Delta\theta = -\dfrac{\pi}{2}$ | Optical $\Delta\theta = \pi$ | Optical $\Delta\theta = \dfrac{\pi}{2}$ |
|---|---|---|---|
| RF $\Delta\psi = -\dfrac{\pi}{2}$ | $\omega_0 \quad \omega_0{+}\omega_S$ | | $\omega_0{-}\omega_S \quad \omega_0$ |
| RF $\Delta\psi = \pi$ | $\omega_0{-}\omega_S \quad \omega_0 \quad \omega_0{+}\omega_S$ | $\omega_0{-}\omega_S \quad \omega_0 \quad \omega_0{+}\omega_S$ | $\omega_0{-}\omega_S \quad \omega_0 \quad \omega_0{+}\omega_S$ |
| RF $\Delta\psi = \dfrac{\pi}{2}$ | $\omega_0{-}\omega_S \quad \omega_0$ | | $\omega_0 \quad \omega_0{+}\omega_S$ |

Table 2-1: Optical SSB & DSB Modulation

In this project, the composite signal, which carries analog video streams and 1Gb/s data, is first sent to the input port 1 of the 90-degree hybrid coupler. The outputs of hybrid coupler are then sent to the two arms of a balanced dual arm modulator with pi/2 phase shift. A continuous wave laser diode at 1550nm is externally modulated with this composite signal by the Mach-Zender Modulator and the signal output is then input to an erbium doped-fiber amplifier (EDFA) to increase the optical power to 17dBm. As the result of OSSB modulation, the composite signal is translated to the lower sideband of the output optical spectrum.

In addition, a RF carrier is sent to the second input port of the 90-degree hybrid. As the result of OSSB modulation, this RF subcarrier translates to the upper sideband of the output

optical spectrum.  This optical subcarrier will be delivered to the end-users as the optical source

for upstream transmission.

The output of MZ modulator can be express as

$$E(t) = \frac{E_i}{2}\left\{ J_0(\frac{\pi A}{V_\pi})[\cos(\omega_c t) - \sin(\omega_c t)]\right\}$$
$$- E_i\left\{ J_1(\frac{\pi A}{V_\pi})\cos(\omega_c + \sum_{i=1}^{78}(\omega_i - \omega_m))t\right\}$$
$$- E_i\left\{ J_1(\frac{\pi A}{V_\pi})x(t)\cos(\omega_c + \omega_d)t\right\}$$
$$- E_i\left\{ J_1(\frac{\pi A}{V_\pi})\cos(\omega_c - \omega_u)t\right\}$$

(2-4)

where the first term is the optical carrier at wavelength $\lambda_c = \frac{2\pi c}{\omega_c}$, the second and third terms

represents 78 video signal and digital data at lower sideband of optical carrier, respectively.  The

digital data *x(t)* is (-1,1) for BPSK, $\{\frac{1}{\sqrt{2}}, -\frac{1}{\sqrt{2}}\}$ for QPSK, and (0,1) for ASK modulation.  The

last term represents the dc optical subcarrier at upper sideband of optical carrier.

## 2.3 Nonlinear Distortion of Conventional MZ Modulator

The voltage response of MZ modulator in equation (2-1) is

$$P_{out} = (P_{in}L_a)\cdot\cos^2\left[\frac{\Delta\beta L - \theta}{2}\right] = \frac{P_{in}L_a}{2}\left(1 + \cos\left[\frac{V(t)}{V_\pi}\pi - \theta\right]\right),$$

When the MZ modulator is bias at quadrature point, the phase bias between two arms of the

modulator is $\theta = \frac{\pi}{2}$.  The transfer function of the MZ modulator is expressed as a sine wave-like

function of the input voltage.  For this reason, signal distortion is always found in a MZ

modulator output.  In other words, when multiple carrier frequencies pass through a nonlinear

device such as a conventional MZ modulator, signal products other than the original frequencies are produced.  In analog video transmissions, many channels are allocated close to one another. As a result, signal distortion in a channel can cause an interference problem with other channels. Two nonlinear terms generated by MZ modulator are composite second order (CSO) and composite triple beat (CTB).

In a multichannel system, the number of CSO terms increase linearly as the number of channels increase, whereas for CTB terms, it increases as $N^2$.  Figure 2-2 shows the CSO ($f_a \pm f_b$) Intermodulation product terms for a 78-channel system where the terms $f_a - f_b$ are clearly seen to be dominant at the lower end of the multichannel spectrum while at the upper edge the type $f_a + f_b$ that dominates.  In this case, the number of second-order IM products that fall right on the first CATV channel is $N_{CSO} = 69$.

Figure 2-3 shows the CTB ($f_a \pm f_b \pm f_c$) Intermodulation product terms for a 78-channel system where the maximum value of CTB occurs at the centers of the channel groups and where the number of third-order IM products that fall right on the channel number 38 is $N_{CTB}=2185$.

Figure 2-2 Second order product count vs. Channel Number)
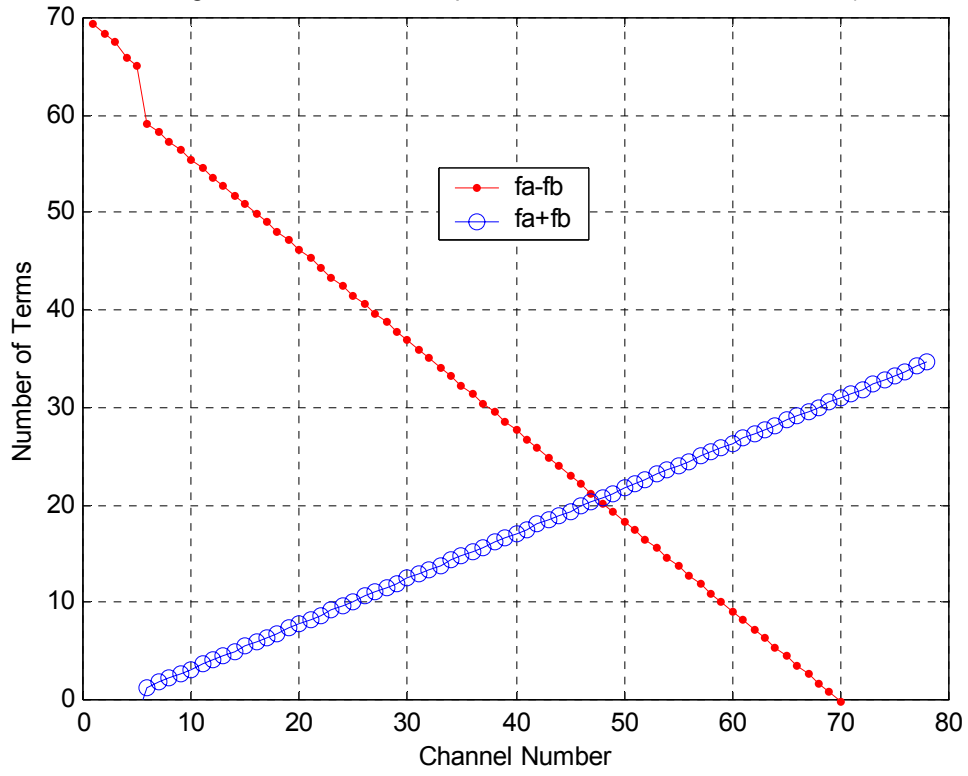


Figure 2-3 Third order product count vs. Channel Number)
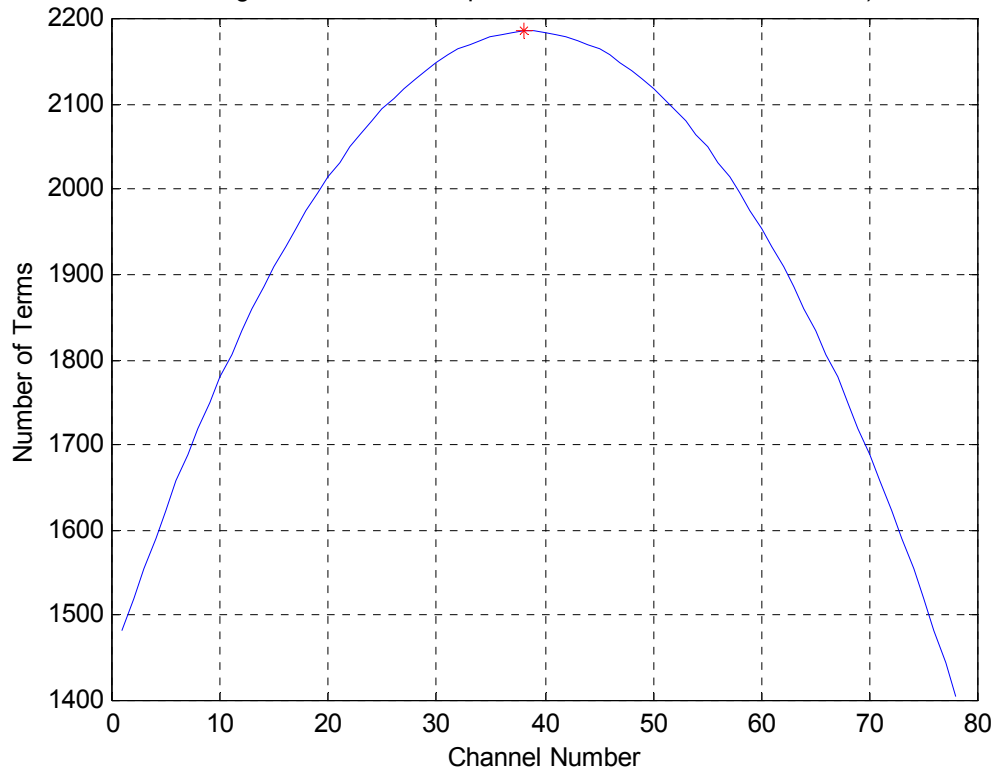
In general, second and other high even-order distortions of the MZ modulators can be eliminated by optimization of the driving bias point at quadrature point. Reference [4] demonstrates CSO products can be cancelled by setting the dc applied voltage $V_{dc}$ equal to $mV_\pi$, $(m = 0,\pm1, \pm 2, ...)$ on a dual outputs BBI modulator.

In this project, a conventional MZ modulator with a single output is used and the derivation of composite second order (CSO) and composite triple beat (CTB) is detailed in Appendix 2. The power ratio of composite second order (CSO) to carrier is:

$$\frac{CSO}{C} = \left\{\frac{2[J_1(\frac{\pi A}{V_\pi})]^2[J_0(\frac{\pi A}{V_\pi})]^{N-2}}{2J_1(\frac{\pi A}{V_\pi})[J_0(\frac{\pi A}{V_\pi})]^{N-1}}\right\}^2 N_{CSO} \cdot \{\frac{\cos(\frac{\pi}{V_\pi}V_{dc})}{\sin(\frac{\pi}{V_\pi}V_{dc})}\}^2 \qquad \textbf{(2-5)}$$

This formula clearly shows that when the applied dc Voltage is equal to

$mV_\pi$, $(m = \pm\frac{1}{2}, \pm\frac{3}{2}, ...)$, the CSO distortion is cancelled out. In other words, by setting the

applied dc Voltage equal to $\frac{V_\pi}{2}$, all even-order distortion are cancelled and the bias phase shift

between the two arms of modulator is $\frac{\pi}{2}$. The power ratio of composite triple beat (CTB) to

carrier is:

$$\frac{CTB}{C} = \left\{\frac{2[J_1(\frac{\pi A}{V_\pi})]^3[J_0(\frac{\pi A}{V_\pi})]^{N-3}}{2J_1(\frac{\pi A}{V_\pi})[J_0(\frac{\pi A}{V_\pi})]^{N-1}}\right\}^2 N_{CTB} \cdot \{\frac{\sin(\frac{\pi}{V_\pi}V_{dc})}{\sin(\frac{\pi}{V_\pi}V_{dc})}\}^2 \qquad \textbf{(2-6)}$$

When the optical modulation index is $\chi = \dfrac{\pi A}{V\pi} \ll 1$, we can approximate $J_0(\chi) = 1$ [4] and

$J_1(\chi) = \dfrac{\chi}{2}$ [4] and equation (2-6) can be simplified as $\dfrac{CTB}{C} = \left(\dfrac{x}{2}\right)^4 \cdot N_{CTB}$, where $N_{CTB}$ is the

product count of third-order intermodulations in a particular channel.

Figure 2-4 calculates the worst case of CSO/C and CTB/C as a function of bias voltage offset with an optical modulation index (OMI) equal to 5%. It is clear from figure 2-4 that when the applied dc voltage is bias at $mV_\pi$, $(m = \pm\dfrac{1}{2}, \pm\dfrac{3}{2}, ...)$, which known as Q-point, we can as expected, obtain the best CSO/C distortion ratio. Also notice that when the bias voltage is offset slightly from the Q-point, the second-order distortion (CSO/C) increases sharply while the third-order distortion (CTB/C) remains constant.



Figure 2-4 CTB/C, CSO/C vs. Applied DC bias voltage with OMI=5%)
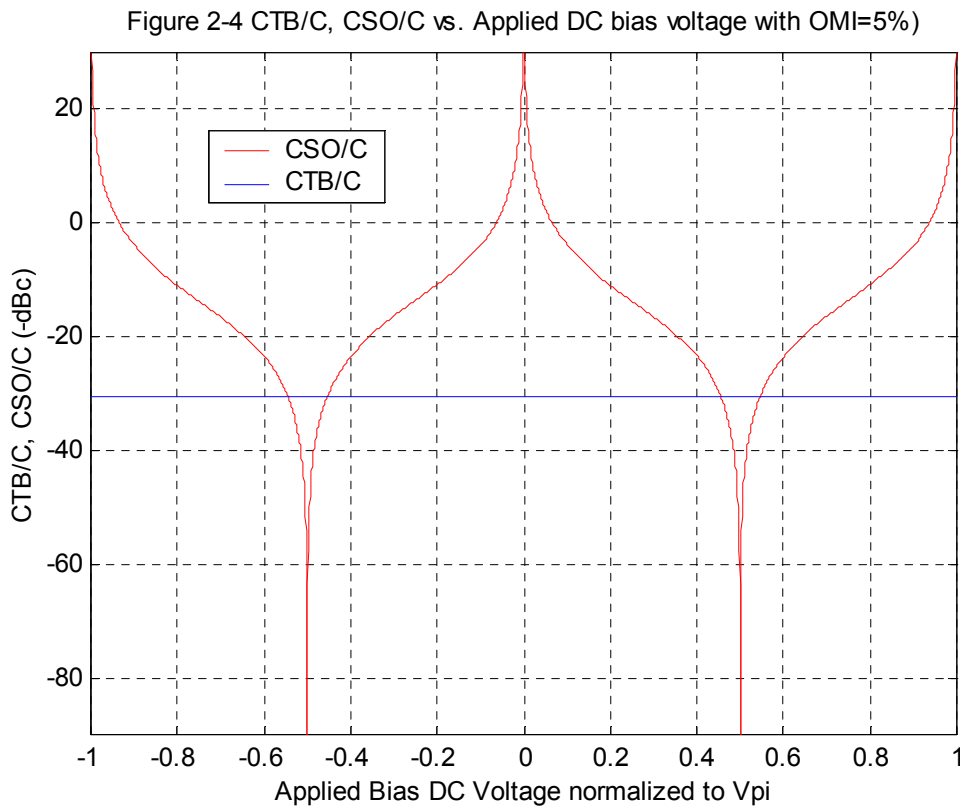
Though the second-order distortion generated by MZ Modulator can be suppressed by biasing the Modulator at Q point, the strong third-order distortion remains unchanged at CATV Channel 38 with -30.5dBc at 5%OMI.

Figure 2-5 illustrate the third-order nonlinear distortion vs. optical modulation index (OMI). The CTB is -58dBc at OMI = 1% and -30.5dBc at OMI = 5%. It is clear that there is a trade off between the signal amplitude and the distortion. The higher the optical modulation index (OMI) is, the higher the signal amplitude; but the distortion is also higher.



Figure 2-5 Composite Triple Beat/Carrier vs. OMI
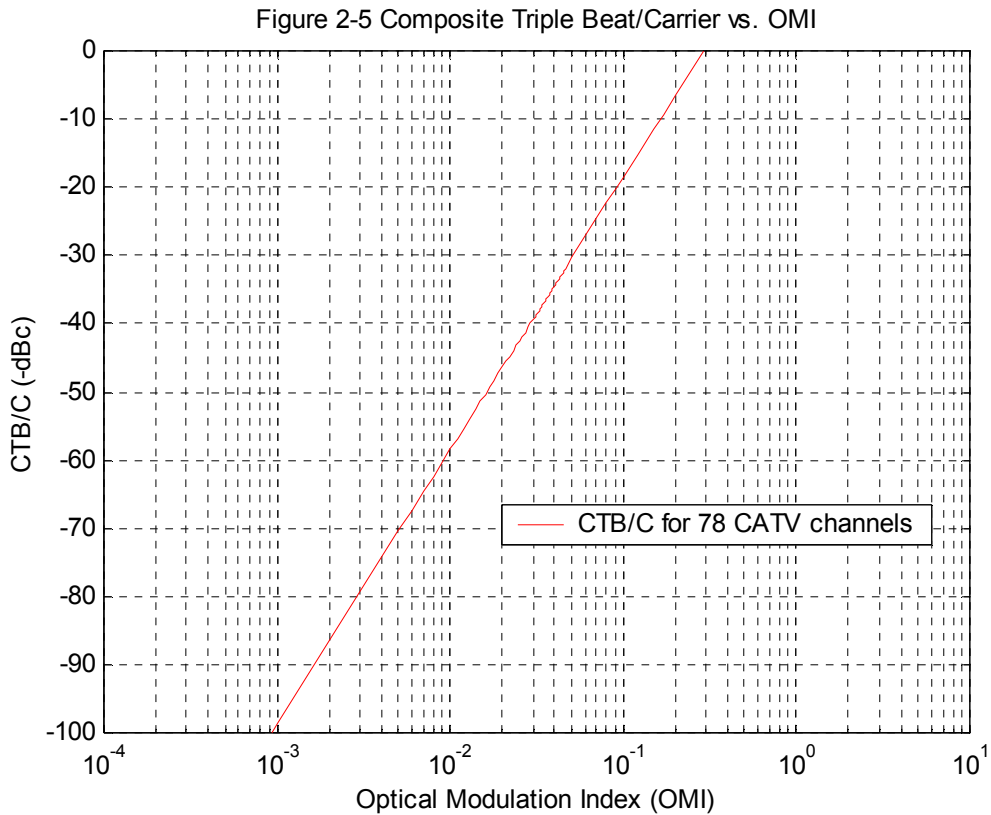
## CHAPTER 3: OPTICAL LINK MODEL FOR CNR AND Q-VALUE CALCULATION

### 3.1    Analog and Digital Optical Link Model

In analyzing the performance of analog systems, one usually calculates the Carrier-to-Noise Ratio (CNR) which is expressed as the ratio of the signal power to the total noise power. In analyzing the performance of digital system, one usually calculates the Bit Error Rate (BER), or Q-Value.

In order to guarantee a good CNR value, the receiver should have low intrinsic noise and the detectable signal power should be sufficiently high to dominate this noise power.  Other noise contributions are PIN-receiver shot noise, laser RIN noise, signal-ASE noise generated by the EDFA booster amplifier, laser clipping, as well as the composite triple beat (CTB) nonlinear whose distortions can seriously degrade transmission performance.

The FCC requires CNR > 43 dB and distortions such as CSO & CTB > 51dBc under FCC specification Section 76.605(a).  Most systems are design for approximately 48dB CNR at the end-of-line to account for house amps and bigger TV screens.

The typical digital data specifications requires the BER be 1e-9 or Q value = 6 or better. In this project, the target value for CNR and BER is shown in table 3-1.

| Parameter | FCC Requirement | Typical Value | Project Target Value |
|-----------|----------------|---------------|---------------------|
| Carrier/Noise (CNR) | > 43dB [Section 76.605 (a) (7)] | 48dB  +/- 2dB | 50dB |
| Composite Second Order | > 51dBc [Section 76.605 (a) (8)] | -53dBc +/- 2dB | -60dBc |
| Composite Triple Beat | > 51dBc [Section 76.605 (a) (8)] | -53dBc +/- 2dB | -60dBc |
| Digital Q-Value | 6 | 6 | 6 |

**Table 3-1        Signal Quality Target Values**

In the following section we give an analytical estimation of CATV CNR & Digital Q-Value Calculation in optical systems based on a SCM externally modulated optical link concept model as shown below.
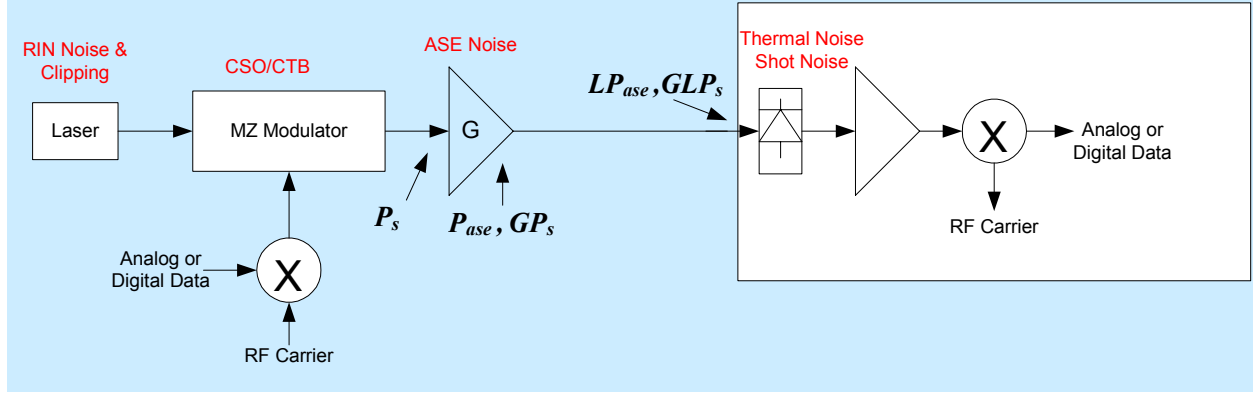


**Figure 3-1: Concept model of SCM system for CNR and Q-Value Calculation**

### 3.1.1 Signal power in Optical System

It has been shown in [4] that an intensity modulator has a voltage – optical intensity relationship that can be expressed as (see section 2.2)

$$P_s = P_o \cdot \cos^2\left[\frac{\dfrac{\pi V(t)}{V_\pi} - \theta}{2}\right] = \frac{P_o}{2} + \frac{P_o}{2}\cos(\frac{\pi V(t)}{V_\pi} - \theta)\,] \tag{3-1}$$

At quadrature bias, the static phase shift is $\dfrac{\pi}{2}$ and so the expression of equation 3-1 can be rewritten as

$$P_s = \frac{P_o}{2} + \frac{P_o}{2}\sin(\frac{\pi V(t)}{V_\pi}) \tag{3-2}$$

In this project, the multiple sub-carrier signals can be represented by the following equation:

$$V(t) = \sum_{i=1}^{78}\cos(\omega_i - \omega_{mi})t + x(t) \cdot \cos(\omega_d t) + \cos(\omega_u t), \tag{3-3}$$

where the first term is 78 CATV video signals, the second term is digital data and the last term is

RF subcarrier. By substitute equation (3-3) into (3-2), we have

$$P_s = \frac{P_o}{2} + \frac{P_o}{2} \sin(\frac{\pi}{V_\pi} \left[ \sum_{i=1}^{78} \cos(\omega_i - \omega_{mi})t + x(t) \cdot \cos(\omega_d t) + \cos(\omega_u t) \right])$$
 **(3-4)**

Using Bessel Expansions as below:

$$\sin\left[ \frac{\pi}{V_\pi} \left( \sum_{i=1}^{N} A\cos(\omega_i t + \phi_i) \right) \right]$$

$$= \left\{ \sum_{n_i=-\infty}^{\infty} \sum_{n_2=-\infty}^{\infty} \cdots \sum_{n_N} J_{n_2}(\frac{\pi A}{V_\pi}) \cdot J_{n_2}(\frac{\pi A}{V_\pi}) \ldots J_{n_N}(\frac{\pi A}{V_\pi}) \cos[n_1(\omega_1 + \phi_1) + \ldots n_N(\omega_N + \varphi_N)] \right\}$$

the carrier and the multiple sub-carrier signals can be express as

$$P_s = \frac{P_o}{2} + \frac{P_o}{2}[2 \cdot J_0(\frac{\pi V}{V_\pi})^1 J_0(\frac{\pi V}{V_\pi})^{N-1}] \left[ \sum_{i=1}^{78} \cos(\omega_i - \omega_{mi})t + x(t) \cdot \cos(\omega_d t) + \cos(\omega_u t) \right]$$

$$P_s = \frac{P_o}{2} \left[ 1 + 2 \cdot J_0(\frac{\pi V}{V_\pi})^1 J_0(\frac{\pi V}{V_\pi})^{N-1}] \left[ \sum_{i=1}^{78} \cos(\omega_i - \omega_{mi})t + x(t) \cdot \cos(\omega_d t) + \cos(\omega_u t) \right] \right]$$

**(3-5)**

At the receiver, the receiver power is $P_p = P_s GL$, where $G$ is the gain of the optical Booster

Amplifier and $L$ is the loss factor between the Booster amplifier and the photodetector which

includes transmission loss, coupling loss and power splitting loss.

$$P_p = \frac{P_o GL}{2} \left[ 1 + 2 \cdot J_0(\frac{\pi V}{V_\pi})^1 J_0(\frac{\pi V}{V_\pi})^{N-1}] \left[ \sum_{i=1}^{78} \cos(\omega_i - \omega_{mi})t + x(t) \cdot \cos(\omega_d t) + \cos(\omega_u t) \right] \right]$$

**(3-6)**

The DC term of the photocurrent is $I = R \cdot \frac{P_o GL}{2}$. Obviously, the useful signal photo-current for

the *k-th* CATV channel is

$$I_k = I \cdot 2 \cdot J_0(\frac{\pi V}{V_\pi})^1 J_0(\frac{\pi V}{V_\pi})^{N-1} \cdot \cos(\omega_k - \omega_{mk})t$$
 **(3-7)**

Assumed that the modulation depth per channel is small by making the approximations cited in [4]

$$J_0(\frac{\pi V}{V_\pi}) = \frac{m}{2}, \quad J_0(\frac{\pi V}{V_\pi})^{N-1} \approx 1$$

The average carrier power of channel $k$ at the receiver is

$$< I_{ch}^2 > = < I^2 2 \cdot J_1(\frac{\pi V}{V_\pi})^2 J_0(\frac{\pi V}{V_\pi})^{2N-2} |\cos(\omega_k - \omega_{mk})t|^2 > = \frac{I^2 m^2}{2} \tag{3-8}$$

### 3.1.2 Noise Contributions in Optical Systems

There are typically six types of dominant noise that impair the detected signal in SCM systems. They are: (1) Thermal Noise; (2) Shot noise from photo-diode; (3) Relative Intensity Noise (RIN) within laser; (4) Amplified Spontaneous Emission (ASE) noise from Booster Amplifier; (5) Clipping noise from the nonlinear distortion result from clipping of the laser output; and (6) Intermodulation Distortion (CSO & CTB) from the nonlinear distortion of MZ modulator. Each is described as follows:

**Thermal Noise:** Thermal noise is generated in resistive elements of the link including the photo-diode and the modulator. Its mean square current value is given by [3]:

$$< I_{th}^2 > = \frac{4 \cdot K \cdot T \cdot B}{R} \tag{3-9}$$

where K is Boltzmann's constant, T is the absolute temperature, B is the video stream bandwidth and R is the load resistance value.

**Shot Noise:** Shot noise is generated when an optical signal is incident on the photo-detector and is given by [3]: $< I_{sh}^2 > = 2 \cdot q \cdot (I + I_d) \cdot B$ (3-10)

where $q$ is the electronic charge, $I$ is the mean optically generated current and $I_d$ is the photo-detector dark current.

**Relative Intensity Noise (RIN):** Relative Intensity Noise is generated by spontaneous emission within the laser source and is dependent on material, structural and modulation parameters. The contribution of the source RIN to the noise current at the detector for a CW laser is given by [3]:

$$< I_{RIN}{}^2 >= I^2 \cdot RIN \cdot B \qquad (3\text{-}11)$$

**Clipping :** When transporting multiple signals in SCM network, the modulated composite input signal is only weakly clipped by laser so that the desirable CNR and low CTB/CSO values are obtained. Clipping sets the fundamental limitation on how much the laser can be clipped for composite input signal. Clipping is given by [4]:

$$Clipping^{-1} = \left[ \sqrt{2\pi} \frac{\left(1 + 6\mu^2\right)}{\mu^3} e^{\frac{1}{2\mu^2}} \right]^{-1}, \quad \mu = m\sqrt{\frac{N}{2}} \qquad (3\text{-}12)$$

where $N$ is the number of SCM channels and $m$ is the optical modulation index per channel.

**Intermodulation Distortion:** As mentioned in Section 2-3, the transfer function of the MZ modulator is expressed as a sine wave-like function of the input voltage. For this reason, signal distortion is always found in a MZ modulator output. Two nonlinear terms generated by MZ modulator are composite second order (CSO) and composite triple beat (CTB).
In this project, the OSSB modulation is generated by biased the MZ modulator at Q-point, which results in canceling CSO distortion. The composite triple beat (CTB) is given by:

$$\frac{CTB}{C} = \left(\frac{x}{2}\right)^4 \cdot N_{CTB} \qquad (3\text{-}13)$$

**Booster Amplifier Noise:** When an amplifier is added to the system, the two major noise terms generated from the amplifier are the signal-spontaneous beat noise, $< i^2{}_{sig=sp} >$ and the spontaneous-spontaneous beat noise, $< i^2{}_{sp=sp} >$. As shown in figure 3-1, the output of the

Booster Amplifier contains the average amplified signal power as $P_sG$ and ASE power

as $P_{ase} = 2\eta_{sp}hf(G-1)B_O$. Factor of 2 at ASE power are horizontal and vertical polarization. At

the input of the receiver, the average input signal is $I_p = L \cdot R \cdot P_sG$ and the ASE input signal

is $I_{ase} = L \cdot R \cdot 2\eta_{sp}hf(G-1)B_O$, where L is the loss factor between the Booster amplifier and the

photo-detector.

The signal-spontaneous beat noise is defined as a beat product between the signal and the ASE

noise. It can express as [4]

$$<i^2{}_{sig-sp}> = 2 \cdot \left\{ 2I_p \cdot \frac{I_{ase}}{2B_o} \right\} = 4R^2L^2 \left\{ P_sGhfn_{sp}(G-1) \right\} \qquad \textbf{(3-14)}$$

The spontaneous-spontaneous beat noise is defined as a beat product between the ASE noise

within optical bandwidth. It can express as [4]

$$<i^2{}_{sp=sp}> = 2 \cdot \left\{ (\frac{I_{ase}}{2})^2 - (\frac{I_{ase}}{2})^2 \right\} / B_o = 4R^2h^2f^2n_{sp}{}^2(G-1)G \cdot L^2B_o \qquad \textbf{(3-15)}$$

It is clear that the sp-sp beat noise in equation (3-15) depends on optical bandwidth, which

implies that optical filter can be used to eliminate sp-sp beat noise. In equation (3-14), we see

that the CNR depends on the amplifier input optical power. The optical loss before an optical

amplifier can seriously degrade the CNR, but optical loss after an optical amplifier does not

affect CNR because of the optical loss in signal-spontaneous noise power is in parallel to the

optical loss in signal power at the receiver. In other words, using a booster amplifier offers

better CNR than in-line and preamplifier.

## 3.2  Analog Carrier-to-Noise Ratio (CNR) Calculation

Assuming that all of these noise sources are uncorrelated, the total Carrier-to-Noise Ratio

(CNR) for the downstream Analog Video signal can be expressed by:

$$CNR_{total}^{-1} = CNR_{RIN}^{-1} + CNR_{Thermal}^{-1} + CNR_{shot}^{-1} + CNR_{ASE}^{-1} + CNR_{Clipping}^{-1} + CNR_{CTB}^{-1}$$

$$CNR_{total}^{-1} = [\frac{m^2 I_p^{\ 2}}{2RIN \cdot I_p^{\ 2}B}]^{-1} + [\frac{m^2 I_p^{\ 2}}{\frac{8KTB}{R}}]^{-1} + [\frac{m^2 I_p^{\ 2}}{4qI_pB}]^{-1} + [\frac{m^2 I_s}{8hfn_{sp}RB}]^{-1} + [\frac{\sqrt{2\pi}\left(1+6\mu^2\right)e^{\frac{1}{2\mu^2}}}{\mu^3}]^{-1} + [\frac{16}{m^4 \cdot N_{ctb}}]^{-1}$$

**(3-16)**

The total noise becomes the sum of above components, and since some of these components are signal dependent, the limiting noise is dependent on the received optical power. The first three noise terms of equation 3-16 can be summarized as followed:

- Thermal noise limited - increasing the optical power transmitted by 1dB will generally improve the CNR at the receiver by ~ 1dB.

- Shot noise limited - a 1dB increase in optical power will improve the CNR by 0.5dB.

- RIN limited - no benefit to increase optical power.

## 3.3 Digital Q Value Calculation

Digital communications systems have many advantages over analog systems brought about by the need to detect the presence or absence of a pulse rather than measure the absolute pulse shape. Such detection can be made with reasonable accuracy even if the pulses are distorted and noisy.

The receiver samples the incoming optical pulses at a rate equal to the bit rate of transmission and a decision, which is usually performed by setting a threshold level, is made as to whether each pulse corresponds to a "1" or "0" for ASK system or "1" or "-1" for BPSK system.

The quality of a digital communication system is specified by its BER or Q value. The BER is specified as the average probability of incorrect bit identification. In general, the higher

the received Q-value, the lower the BER probability will be.  The relationship between BER and

Q-value can be express as [3]

$$BER = \frac{1}{2}\left[1 - erf\left(\frac{Q}{\sqrt{2}}\right)\right] \approx \frac{1}{\sqrt{2\pi}} \frac{e^{-\frac{Q^2}{2}}}{Q},$$

From equation (3-6), the useful signal photo-current for the digital channel is

$$I_p = I \cdot m \cdot x(t) \cdot \cos(\omega_d t),$$

where $x(t) = \{-1, 1\}$ for BPSK, $\{\frac{1}{\sqrt{2}}, -\frac{1}{\sqrt{2}}\}$ for QPSK and $\{1, 0\}$ for ASK system

The receiver Q value for BPSK and ASK system can be approximated as

$$Q_{BPSK} = \frac{I_P(1) - I_P(-1)}{2\sigma} \tag{3-17}$$

$$Q_{QPSK} = \frac{I_P(\frac{1}{\sqrt{2}}) - I_P(-\frac{1}{\sqrt{2}})}{2\sigma} \tag{3-18}$$

$$Q_{ASK} = \frac{I_P(1) - I_P(0)}{2\sigma} \tag{3-19}$$

where σ is the square root of total noise in an optical receiver, which is the composite of the

signal shot noise, the thermal noise, Laser RIN noise, and ASE Booster amplifier noise.

## CHAPTER 4: Analysis and Performance of SCM Optical Link

This following section examines the physical layer transmission performance of SCM/WDM Optical Link.

### 4.1    Optical Power Budget

This section analyzes the optical link power budget between the CO and the end users. As shown in Figure 2.1, the Central Office has SCM modulators, a 1550nm laser, a MZ external modulator and a Booster Amplifier for the downlink path. An optical power splitter is used to distribute the power into a number of end-users. Each end-user has an optical circulator, an optical filter, a modulator and SCM de-modulators.

In order to maintain optical power budget, low loss LC connectors as well as optical circulators are used. Although cheaper optical couplers can replace circulators, circulators are less optical loss (< 1dB), while optical couplers automically imply a 3 to 4 dB loss in power budget. The simple optical power link budget for downlink represented by:

$$P_{budget} = L_C + \alpha L + 10 \cdot \log(N) + M \qquad \qquad \textbf{(4-1)}$$

where *Lc* is the total circulators loss, $\alpha = 0.22$ dB/km is the fiber loss for SM fiber and *L=10km* is the fiber length, *N* is the number of end-users and *M* is the Operation Margin.

Since the combined loss of MZ modulator (5dB) and Booster Amplifier coupling & isolator loss (2dB) with the Gain of Booster Amplifier, the actual output after Booster Amplifier is 17dBm. The above link budget uses current commercial available optical component values and includes a 2dB system margin as shown in Table 4-1. The optical budget vs. number of end-users is plotted in figure 4-1.

Central Office (CO)

Customer Premis
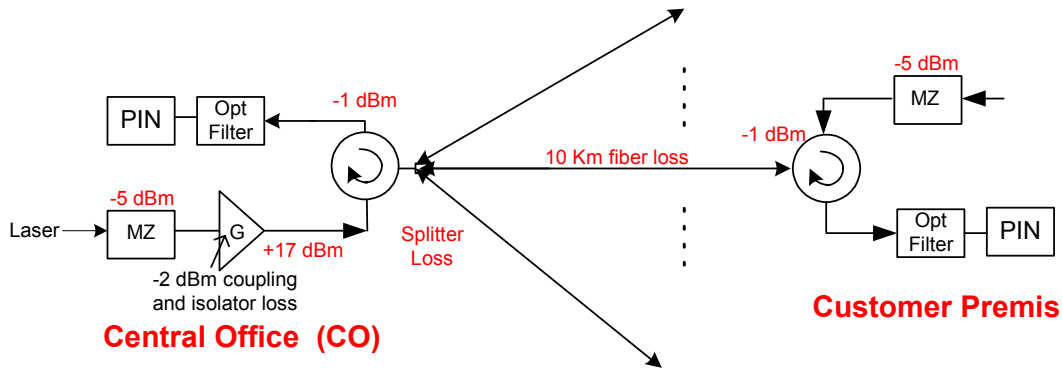
| Laser | MZ Modulator | Booster Amplifier | Photodiode |
|---|---|---|---|
| Power = 6, 8 &10dBm | Loss=5dB | Input Power from -1, 1 & 3dBm | Responsivity = 0.8, 0.9A/W |
| Wavelength = 1550nm | Bandwidth = 20GHz | Output Power = 17dBm | BW = 6MHz (CATV) |
| RIN=-155, -160dB/Hz | | Noise Figure = 5dB | BW = 0.75GHz (Digital) |
| | | nsp = 1.5849 | T=300K, Kb=1.38e-23 |
| | | Coupling and Isolator loss = 2dB | Resistance = 1000 ohms |

**Table 4-1        Optical Device Parameters**



Figure 4-1: Requirement Power Budget (dB) verus the number of End Users
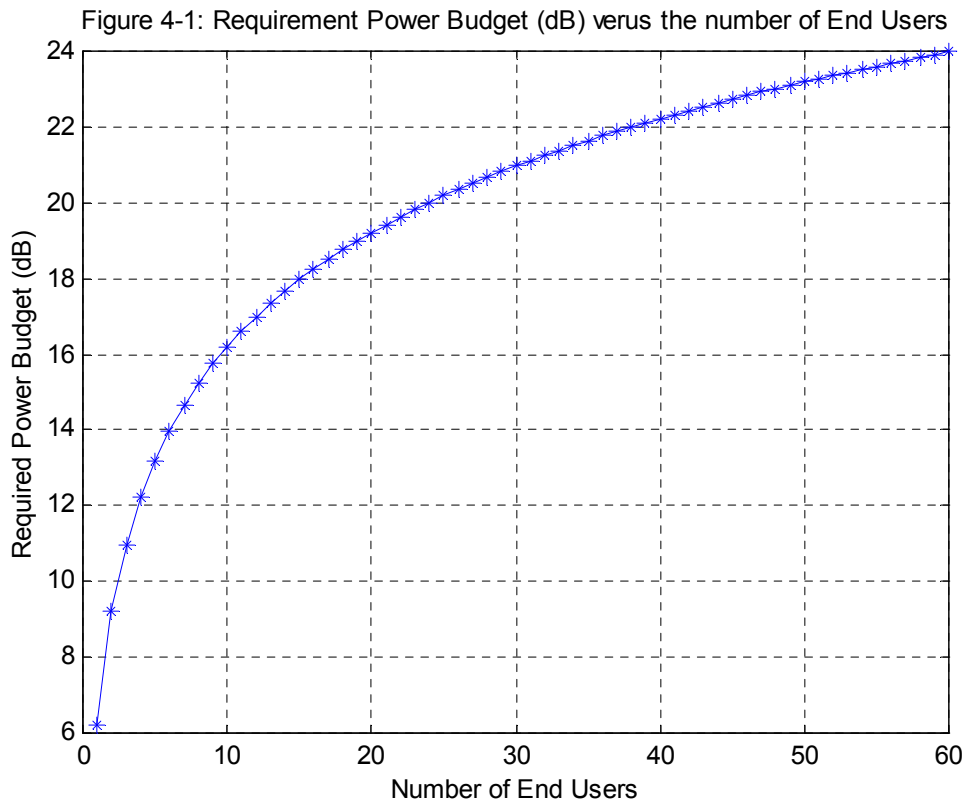
**RMS modulation index (M)**

In general, the signal current at each subcarrier channel is fully dependent upon the optical modulation index (OMI), "*m*", which is a measure of the ratio of the peak modulation of the individual channel to the average optical power. For a SCM system with 4 subcarrier channels, the maximum OMI for each channel is 25%.

In common CATV systems, the modulation index (OMI) is twice or more of the reciprocal of the channel number, i.e., summation of all the modulation indexes will give over 100% modulation. System manufacturers reply upon the fact that the individual channels are not modulated coherently and the signals add up statistically, seldom reaching 100% OMI, as a consequence, the laser is operating in its linear region. In this project, the SCM network, which is composed of 78 video subcarrier channels and 1 digital subcarrier channel, the rms modulation index (M) is defined as $M_{rms} = m\sqrt{N}$; where *m* is the OMI for each channel and *N* is the total number of subcarrier channel.

## 4.2    CATV Carrier-to-Noise Ratio (CNR)

Figure 4-2 shows the CNR across 78 video Channel.  This data is obtained based on the optical power budget of one (1) end-user connected to CO.  The optical link loss is 6.2dB, other parameters used are: RIN=-155dB/Hz, Laser Power = 6dBm & R = 0.8 A/W.



Figure 4-2: CNR across 78 Video Channel)
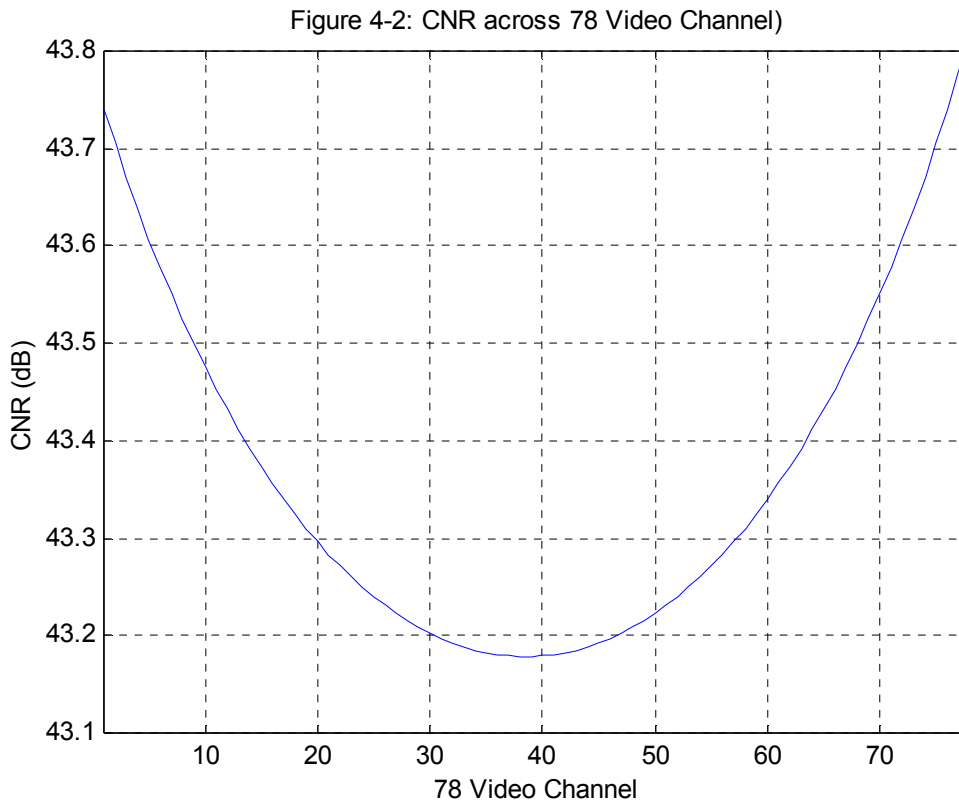
Figure 4-3 shows Video Channel CNR vs. OMI.  One thing that should be noted from these curves is that CNR is computed by taking into account thermal, shot, and ASE noise increase as the signal power increases or, the optical modulation index (OMI) increases.  On the other hand, CNR is computed with third-order nonlinear distortion (CTB) and laser clipping noise decreases at high OMI because these two noise terms become significantly dominant at high OMI.

Figure 4-3 CNR vs OMI with one Remote Unit
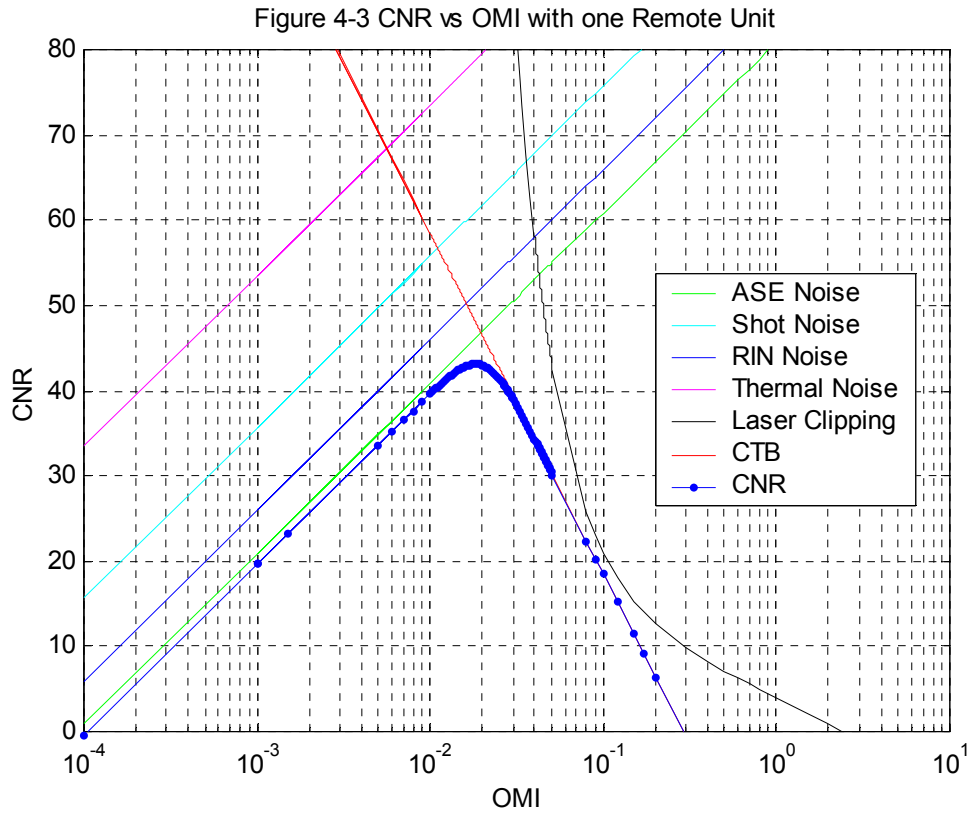
From this analysis, we can summarize as followed:

- The maximum CNR is 43.1 dB at OMI 1.84% & C/CTB = 47dB

- If disregarding the CTB noise term for the moment, CNR can be improved to 50dB by increasing the OMI to 3.4%. However when OMI increases to 4.32%, Clipping noise becomes dominant and the maximum CNR is 52.3dB.

Figure 4-4 shows the scalability of the proposed SCM optical network using varied parameters.

| Parameters | Line 1 | Line 2 | Line 3 | Line 4 |
|---|---|---|---|---|
| Input power at Booster Amplifier | -1dBm | 1dBm | 1dBm | 3dBm |
| Laser RIN | -155dB/Hz | -155dB/Hz | -160dB/Hz | -160dB/Hz |
| Photodiode Responsivity | 0.8 A/W | 0.8 A/W | 0.9A/W | 0.9 A/W |
| Fiber distance | 10km | 10km | 10km | 10km |



Figure 4-4 CNR vs Number End-Users
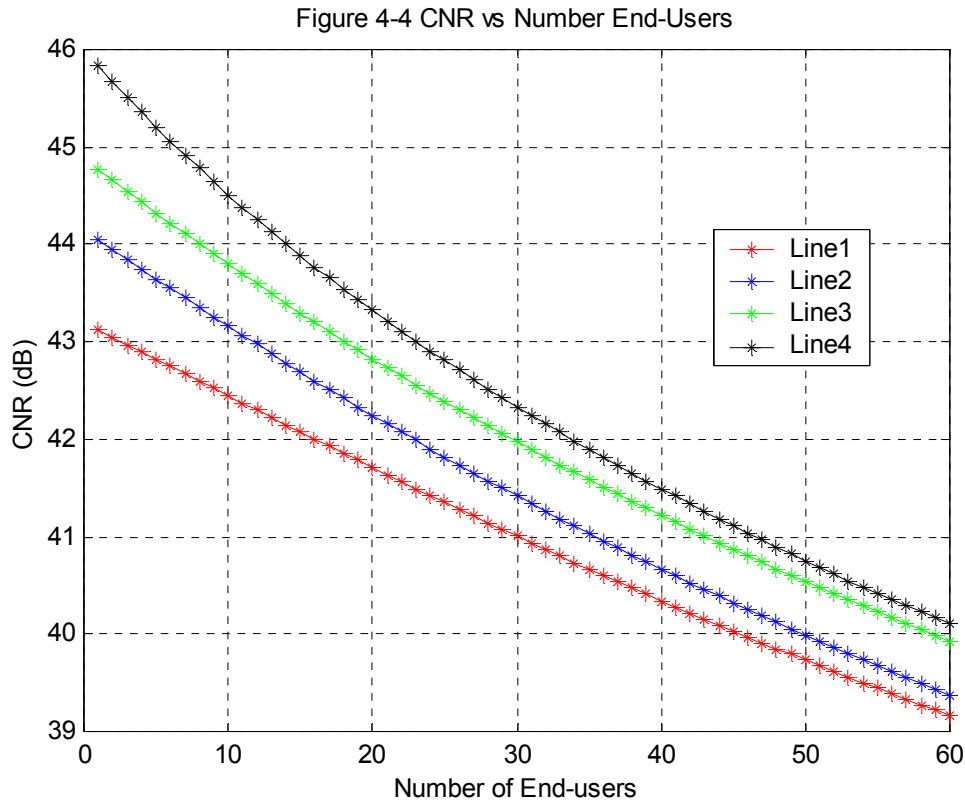
In this analysis, the downstream performance can be improved easily by increasing the output power of the lasers (input power of Booster Amplifier) at low optical power budget (Few End-Users).  At large optical power budget (many End-Users), the overall downstream performance can be improved by increasing RIN and Photodiode Responsivity values.

This network scalability cannot improve further as the third order nonlinear distortion (CTB) severely limits the overall CNR performance; and it is clear that it cannot be used in practical CATV network without reduced CTB noise.

## 4.3    Dual Parallel Linearized External Modulators

The basic configuration of optical dual parallel linearization technique is shown below
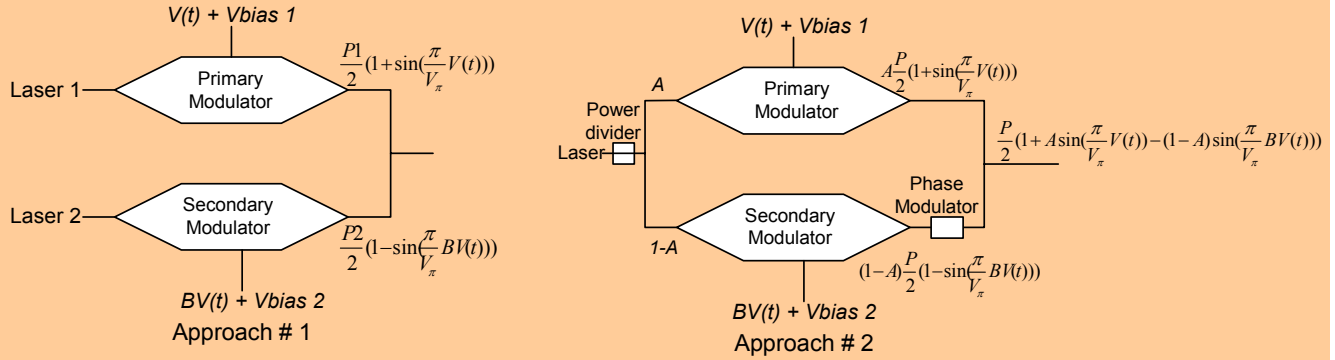


Figure 4-5:  Dual Parallel MZ Modulator

In [6], by providing less optical power and higher RF drive power to the secondary modulator, the secondary modulator has higher OMI and greater distortion. By providing more optical power to the primary MZ modulator, the third-order distortion products created in the secondary modulator can be made to cancel the distortion products from the primary modulator with a small cancellation of the fundamental signal.  There are two approaches to implement dual parallel modulators. The first approach is to use separate optical sources for each of the modulators and then recombined incoherently. The second approach is to use a single optical source launched into the two modulators and recombined the output signals coherently. A phase modulator is required in one of the two MZ output paths to maintain 180 degrees between primary and secondary signals.    The transfer function of the DPMZ can be expressed as [6]

$$
\frac{P_{out}}{P_{in}} = A\cos^2\left[\frac{\dfrac{\pi V(t)}{V_\pi} - \dfrac{\pi}{2}}{2}\right] + (1-A)\cos^2\left[\frac{B\dfrac{\pi V(t)}{V_\pi} - \dfrac{3\pi}{2}}{2}\right] = \frac{1}{2}\left(1 + A\sin\frac{\pi V(t)}{V_\pi} - (1-A)\sin\frac{B\pi V(t)}{V_\pi}\right)
$$

**(4-2)**

where A is the splitting ratio of the input power divider and B is the ratio of RF drive power.

Assuming $V(t)$ is a multi-sinusoidal signal, using trigonometric identities and Bessel functions, the amplitude of the fundamental carrier with frequency $\omega_k$ can be expressed as

$$\frac{P_{\omega_k}}{P_{in}} = AJ_1(\frac{\pi A}{V_\pi})J_0(\frac{\pi A}{V_\pi})^{N-1} - (1-A)J_1(B\frac{\pi A}{V_\pi})J_0(B\frac{\pi A}{V_\pi})^{N-1} \tag{4-3}$$

and the amplitude of the third-order intermodulation component of the frequency $\omega_i+\omega_j+\omega_k$ can be expressed as

$$\frac{P_{\omega_k+\omega_j+\omega_k}}{P_{in}} = AJ_1(\frac{\pi A}{V_\pi})^3 J_0(\frac{\pi A}{V_\pi})^{N-3} - (1-A)J_1(B\frac{\pi A}{V_\pi})^3 J_0(B\frac{\pi A}{V_\pi})^{N-3} \tag{4-4}$$

It is easy to show that the third-order intermoduloation product can be cancelled when

$$A = \frac{J_1(B\frac{\pi A}{V_\pi})^3 J_0(B\frac{\pi A}{V_\pi})^{N-3}}{J_1(\frac{\pi A}{V_\pi})^3 J_0(\frac{\pi A}{V_\pi})^{N-3} + J_1(B\frac{\pi A}{V_\pi})^3 J_0(B\frac{\pi A}{V_\pi})^{N-3}} \tag{4-5}$$

The expressions can be simplified by assuming that the modulation depth/channel is small and by making the approximations [2]

$$\frac{J_1(Bm)}{J_0(Bm)} = B\frac{m}{2} \qquad \text{and} \qquad J_0(Bm)^N \approx \exp(-B^2m^2N/4) \approx 1, \quad \text{when } m \text{ is extremely small}$$

From equation (4-5), we easily find the optimize value of optical power splitting ratio (A) , the RF drive power (B) and the modulation index (OMI) to minimize third order intermodulation product.  Figure 4-6 shows the variation of the values of optical power splitting ratio required to attain minimum third order intermodulation product for different values of B and OMI.

Figure 4-6 DPMZ Power Divider Ratio vs. OMI
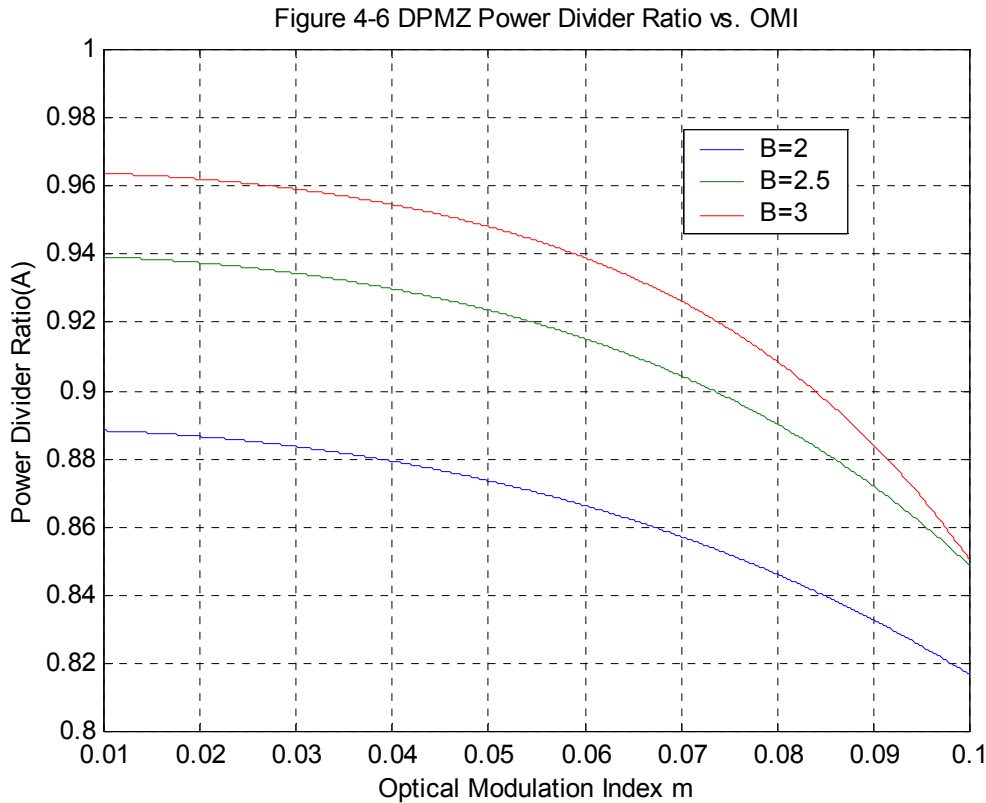
In section 4.2, we summarized that in order to meet 50dB or higher CNR, OMI should be in the range of 3.4% to 4.3%. When OMI is higher than 4.3%, clipping noise becomes dominant. In this case, we focused on the power splitting ratio in the OMI range of 3.4% to 4.3% and summarize it as followed:

- When B=2, we are interested in the optical power splitting ratio in the range of 0.87 to 0.89
- When B=2.5, we are interested in the optical power splitting ratio in the range of 0.92 to 0.94
- When B=3, we are interested in the optical power splitting ratio in the range of 0.94 to 0.97

As a result, Figures 4-7 to 4-9 show the calculated third-order intermodulation performance of the linearized modulator with different values of parameters A and B compared to nonlinearized modulator.

Figure 4-7 C/CTB Performance with B=2 and A=0.87, 0.88 & 0.89
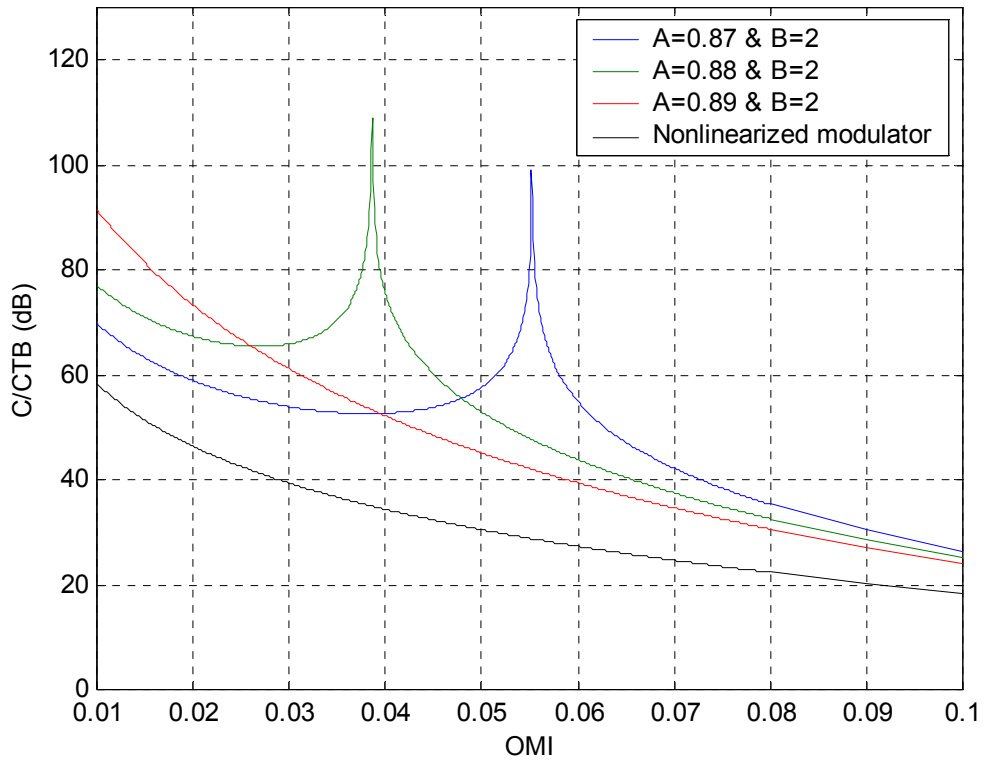


Figure 4-8 C/CTB Performance with B=2.5 and A=0.92, 0.93 & 0.94
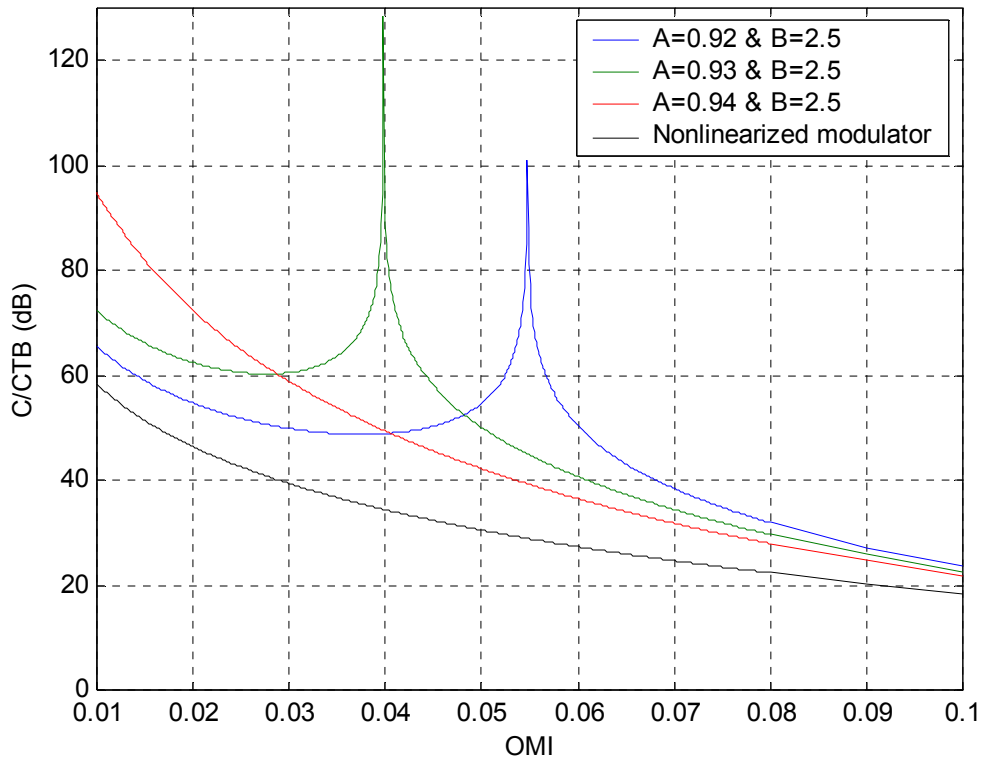
Figure 4-9 C/CTB Performance with B=3 and A=0.94, 0.95, 0.96 & 0.97
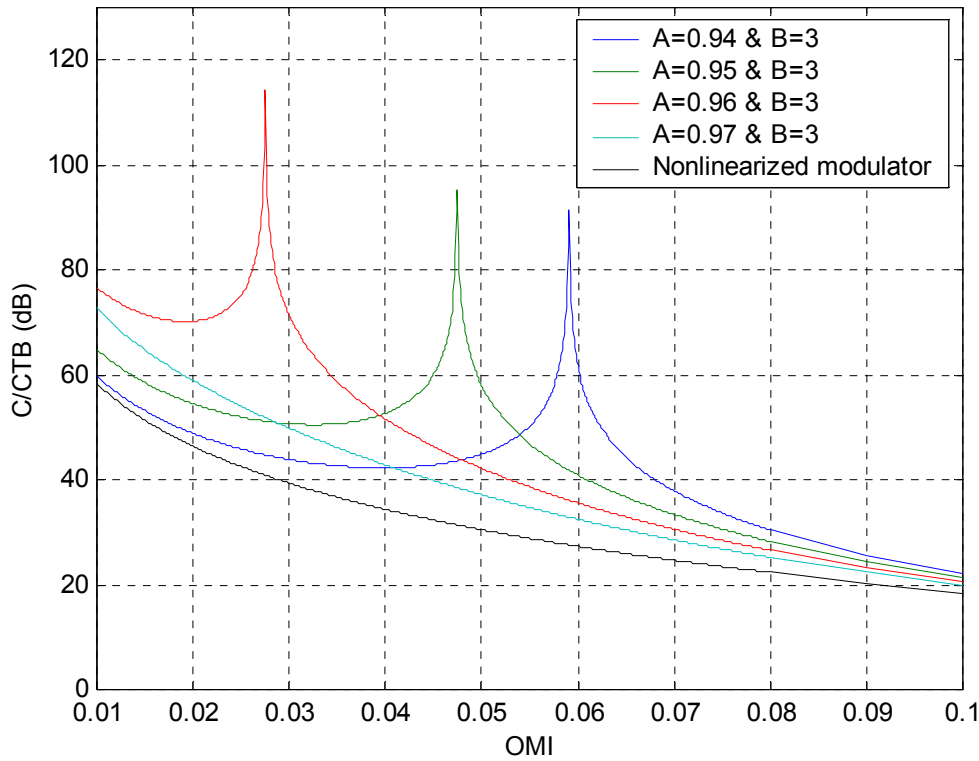
From the above analysis, we optimize the linearized MZ modulator parameters to meet 60dB

C/CTB target. As a result, three (3) sets of parameters are selected to use to reduce CTB for the

analysis of CNR performance. The C/CTB for these three sets of parameter is plotted in figure

4-10 as a function of OMI. As can be seen, very large improvements in C/CTB are achieved.

| | | | | |
|---|---|---|---|---|
| Case I | A=0.88 | B=2 | OMI = 1% - 4.5% | CTB/C > 60 dB |
| Case II | A=0.93 | B=2.5 | OMI = 1% - 4.4% | CTB/C > 60 dB |
| Case III | A=0.96 | B=3 | OMI = 1% - 3.4% | CTB/C > 60 dB |

Figure 4-10 Three Cases study
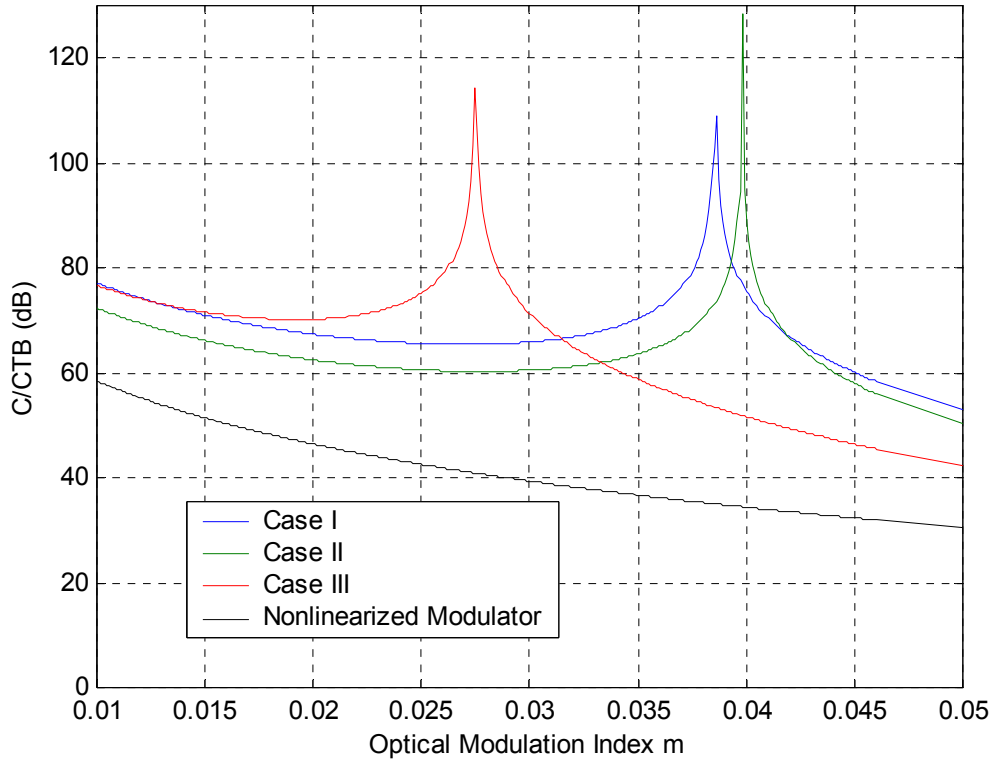
Once the third-order distortions are cancelled or reduced, the fifth-order distortion becomes

dominant.  Therefore, it is important to include fifth-order distortion analysis in this discussion.

The power ratio of fifth-order distortion to carrier is:

$$\frac{CIR_5}{C} = \left| \frac{AJ_1(\frac{\pi A}{V_\pi})^5 J_0(\frac{\pi A}{V_\pi})^{N-5} - (1-A)J_1(B\frac{\pi A}{V_\pi})^5 J_0(B\frac{\pi A}{V_\pi})^{N-5}}{AJ_1(\frac{\pi A}{V_\pi})^1 J_0(\frac{\pi A}{V_\pi})^{N-1} - (1-A)J_1(B\frac{\pi A}{V_\pi})^1 J_0(B\frac{\pi A}{V_\pi})^{N-1}} \right|^2 \cdot \frac{N^4}{12} \qquad \textbf{(4-6)}$$

The Carrier-to-intermodulation product ratio, which includes third order and fifth order

distortion, is presented in figure 4-11 for Case I, II & III.

Figure 4-11 Carrier to Third & Fifth order distortion vs. OMI
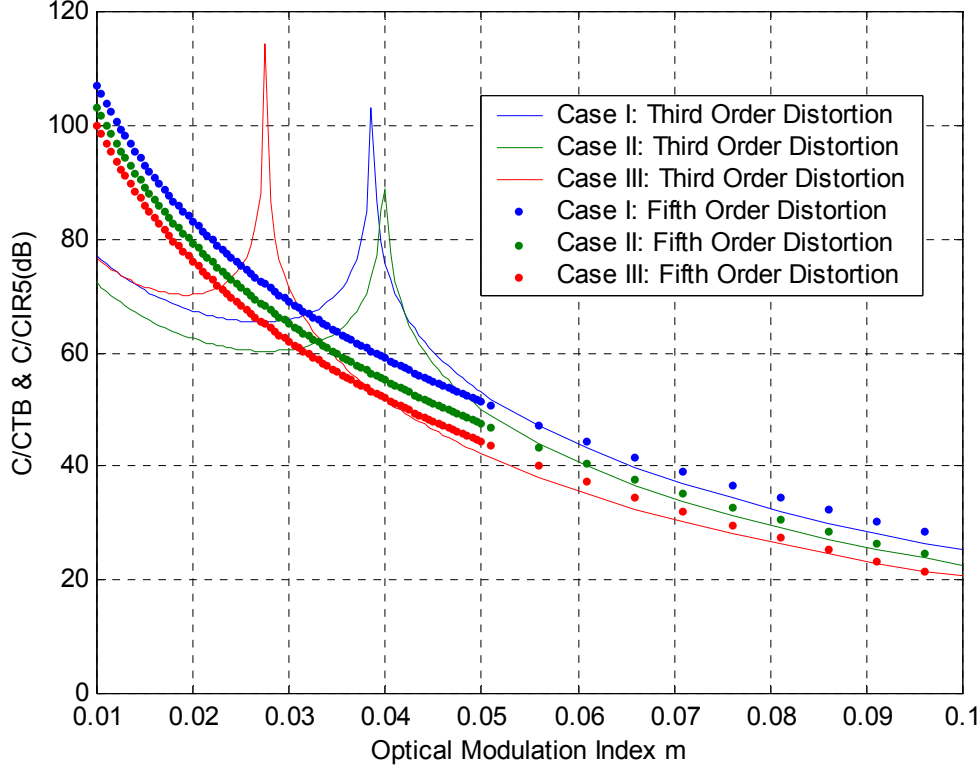
The third and fifth order distortion have similar severe distortion as OMI increases as shown in figure 4-11. The photo-current expression for *kth*-CATV channel after using DPMZ modulator can be derived as follows:

$$I_k = I \cdot \left\{ \left[ 2AJ_0(\frac{\pi V}{V_\pi})^1 J_0(\frac{\pi V}{V_\pi})^{N-1} \cdot \cos(\omega_k - \omega_{mk})t \right] - \left[ 2(1-A)J_0(B\frac{\pi V}{V_\pi})^1 J_0(B\frac{\pi V}{V_\pi})^{N-1} \cdot \cos(\omega_k - \omega_{mk})t \right] \right\}$$

**(4-7)**

Assuming the modulation index/channel is small and by making the approximations [2]

$$\frac{J_1(Bm)}{J_0(Bm)} = B\frac{m}{2} \qquad \text{and} \qquad J_0(Bm)^N \approx \exp(-B^2 m^2 N/4)$$

The average carrier power of channel *k* at the receiver

$$\text{is} < I_{ch}^2 > = \frac{I^2 m^2 e^{-2m^2 N/4} A^2}{2} - \frac{I^2 (Bm)^2 e^{-2Bm^2 N/4}(1-A)^2}{2} \qquad \textbf{(4-8)}$$

### 4.3.1 CNR Performance using Linearized MZ Modulator

**Case I – Linearized Modulator**

The following section analyzes CNR performance using Case I linear MZ modulator (A=0.88 & B=2) with RIN=-155dB/Hz, Laser power = 6dBm & R=0.8 A/W. We first analyze the impact of RIN, Thermal, Shot and ASE noise after applying Case I Linear MZ modulator. Figure 4-12 shows RIN, Thermal, Shot and ASE noise are degraded an average of 1.5dB. This is due to optical power splitting loss use in parallel MZ modulators.



Figure 4-12 Shot, ASE, Thermal & RIN Noises
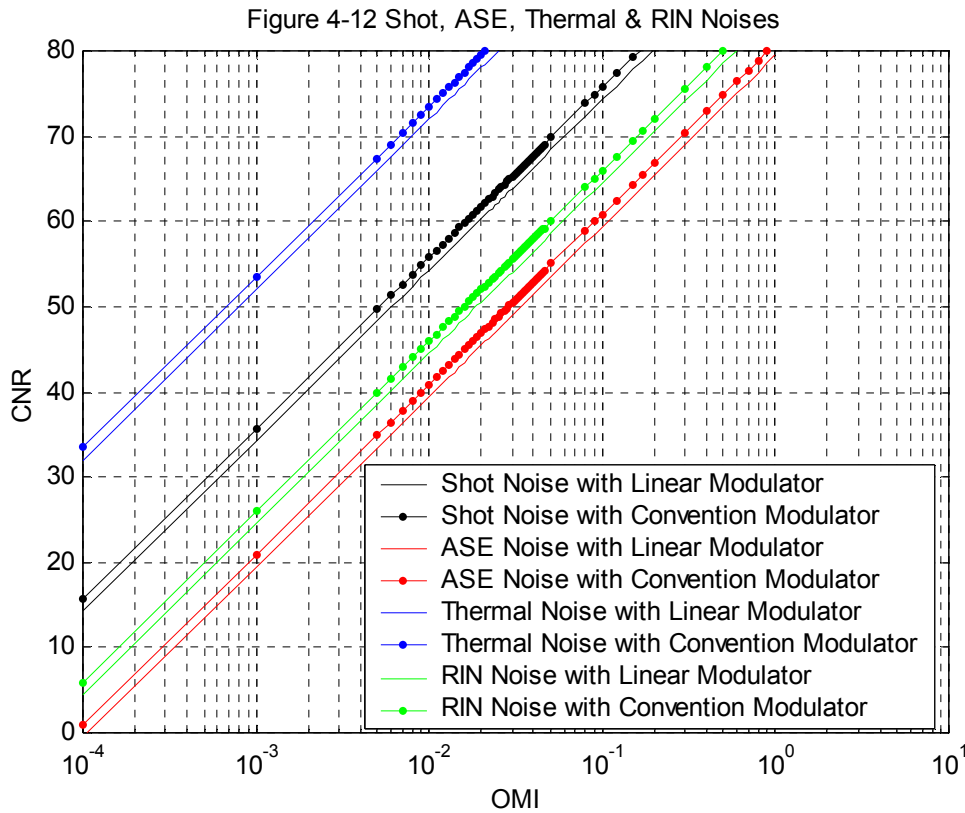
Figure 4-13 shows the overall improvement of CNR vs. OMI with a total of eight (8) End-Users connected to CO and the optical link loss of 15.23dB. The result shows that after using a Linear Modulator (A=0.88, B=2), this proposed SCM network can support up to 8 end-users that meet CNR = 50dB & C/CTB=60.4695 dB at OMI = 4.48%

Figure 4-13:CNR vs OMI using Case I linearized Modulator
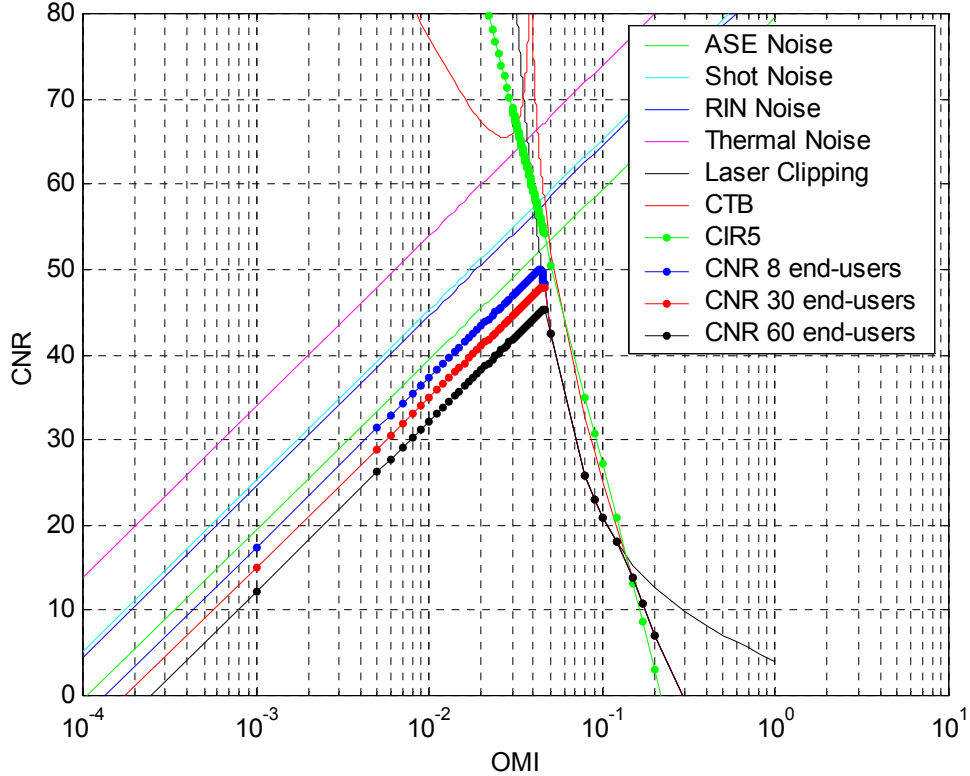
**Case II – Linearized MZ Modulator**

The overall improvement of CNR using Case II Linearized MZ Modulator, RIN=-155dB/Hz, R=0.8A/W & laser power 6dBm, is plotted in Figure 4-14.  This network can support up to 12 end-users that meets CNR = 50dB & C/CTB=61.9 dB at OMI = 4.34%.   Even though Case I and II have similar analytical results in reducing third order distortion. Case II provides a better CNR performance because of the power splitting loss in Case II is less than Case I.

**Case III – Linearized MZ Modulator**

In figure 4-15, Case III Modulator with A=0.96 & B=3 is examined. The maximum CNR is 49.5 dB. The third order distortion is dominant after OMI 3.4%. The overall CNR performance can be improved by increasing laser power, laser RIN & receiver reponsivitiy values.

Figure 4-14:CNR vs OMI using Case II linearized Modulator
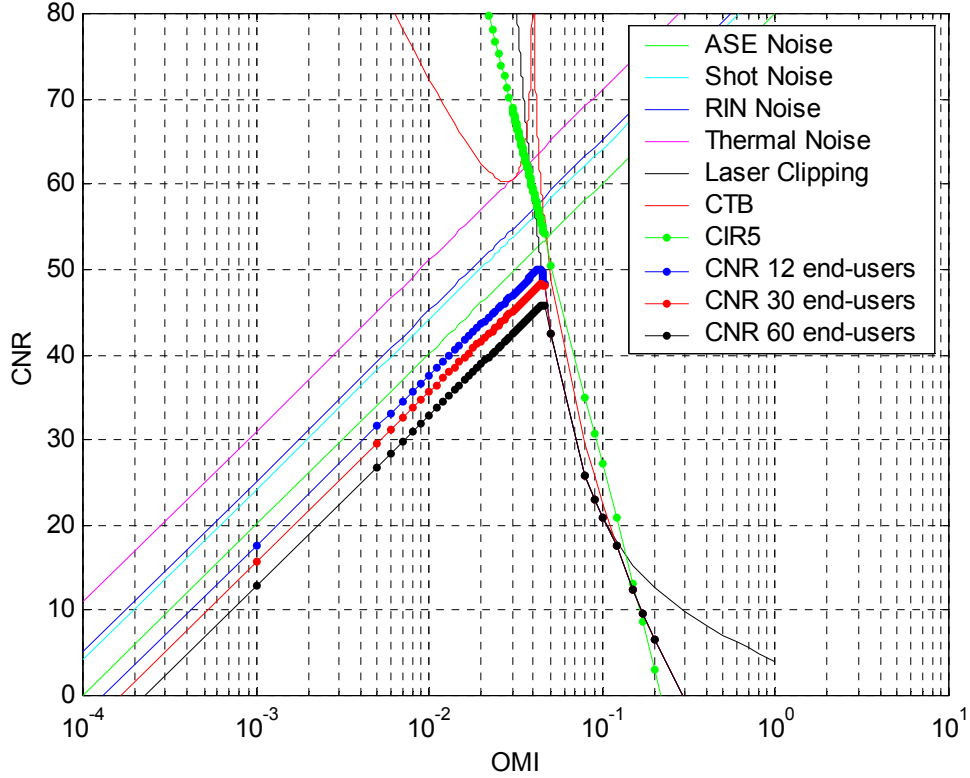


Figure 4-15:CNR vs OMI using Case III linearized Modulator
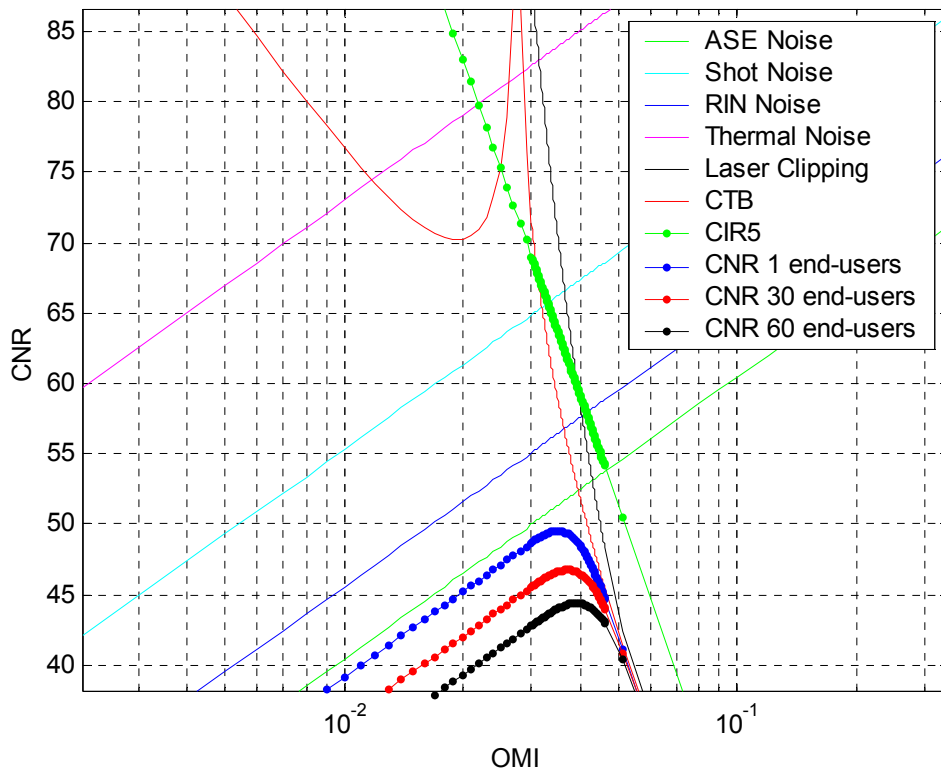
### 4.3.2 Network Scalability comparison between Case I, II & III Linear Modulator

**Network Scalability using Case I - Linear Modulator**

| PARAMETERS | Line 1 | Line 2 | Line 3 | Line 4 |
|---|---|---|---|---|
| **Case I : MZ Modulator** | A=0.88 & B=2 | A=0.88 & B=2 | A=0.88 & B=2 | A=0.88 & B=2 |
| Input power at Booster Amplifier | -1dBm | 1dBm | 1dBm | 3dBm |
| Laser RIN | -155dB/Hz | -155dB/Hz | -160dB/Hz | -160dB/Hz |
| Photodiode Responsivity | 0.8 A/W | 0.8 A/W | 0.9A/W | 0.9 A/W |
| Fiber distance | 10km | 10km | 10km | 10km |
| **RESULTS** | | | | |
| No. of End-Users > 50dB CNR | **8** | **15** | **22** | **27** |
| CNR per Channel | 50 dB | 50.1163 dB | 50.0553dB | 50.0079 dB |
| C/CTB per Channel | 60.4695 dB | 60.6555dB | 60.65dB | 60.655dB |
| OMI per Channel | 4.48 % | 4.47 % | 4.47 % | 4.47% |
| Receiver Optical Channel Power | -13.647dBm | -16.37dBm | -18dBm | -18.9dBm |



Figure 4-16 CNR vs Number End-Users using Case I Linear Modulator
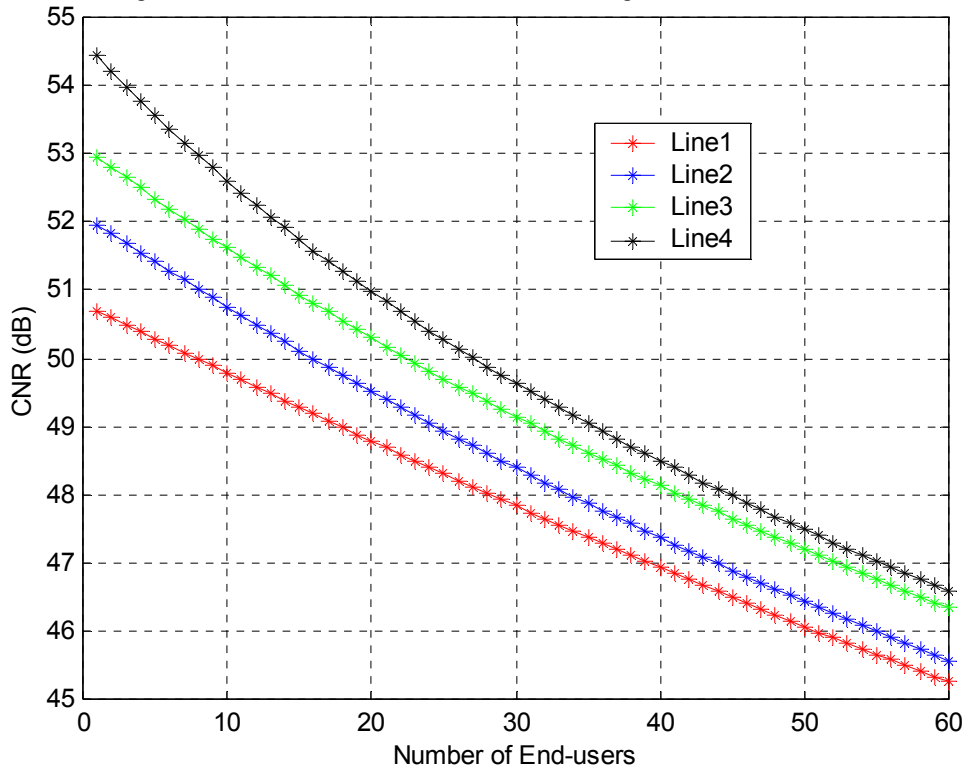
**Network Scalability using Case II - Linear Modulator**

| PARAMETERS | Line 1 | Line 2 | Line 3 | Line 4 |
|---|---|---|---|---|
| **Case II: MZ Modulator** | A=0.93 & B=2.5 | A=0.93 & B=2.5 | A=0.93 & B=2.5 | A=0.93 & B=2.5 |
| Input power at Booster Amplifier | -1dBm | 1dBm | 1dBm | 3dBm |
| Laser RIN | -155dB/Hz | -155dB/Hz | -160dB/Hz | -160dB/Hz |
| Photodiode Responsivity | 0.8 A/W | 0.8 A/W | 0.9A/W | 0.9 A/W |
| Fiber distance | 10km | 10km | 10km | 10km |
| **RESULTS** | | | | |
| No. of End-Users > 50dB CNR | **12** | **19** | **26** | **30** |
| CNR per Channel | 50.036 dB | 50.085 dB | 50.043dB | 50.08 dB |
| C/CTB per Channel | 61.9 dB | 61.89dB | 61.89dB | 61.89dB |
| OMI per Channel | 4.34 % | 4.34 % | 4.34 % | 4.34% |
| Receiver Optical Channel Power | -14.8dBm | -16.8dBm | -18.1dBm | -18.8dBm |



Figure 4-17 CNR vs Number End-Users using Case II Linear Modulator
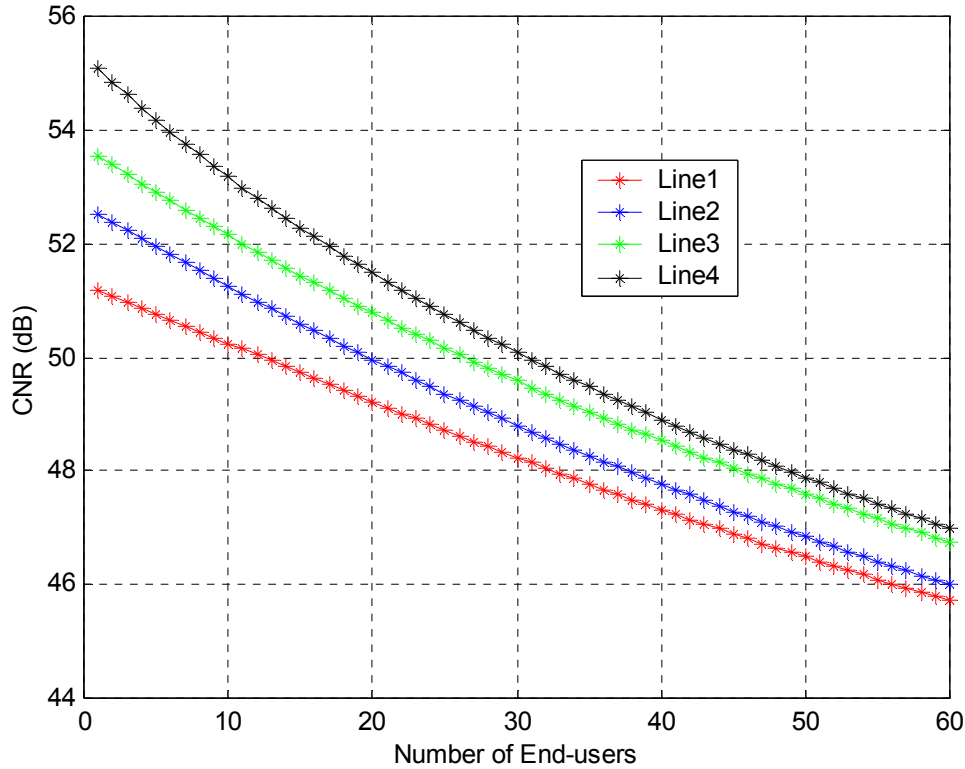
**Network Scalability using Case III - Linear Modulator**

| Parameters | Line 1 | Line 2 | Line 3 | Line 4 |
|---|---|---|---|---|
| **Case III: MZ Modulator** | A=0.96 & B=3 | A=0.96 & B=3 | A=0.96 & B=3 | A=0.96 & B=3 |
| Input power at Booster Amplifier | -1dBm | 1dBm | 1dBm | 3dBm |
| Laser RIN | -155dB/Hz | -155dB/Hz | -160dB/Hz | -160dB/Hz |
| Photodiode Responsivity | 0.8 A/W | 0.8 A/W | 0.9A/W | 0.9 A/W |
| Fiber distance | 10km | 10km | 10km | 10km |
| **RESULTS** | | | | |
| No. of End-Users > 50dB CNR | **0** | **6** | **12** | **18** |
| CNR per Channel | 49.47 dB | 50.062 dB | 50.1182dB | 50.05 dB |
| C/CTB per Channel | 60.0191 dB | 60.0191dB | 60.0191dB | 60.0191dB |
| OMI per Channel | 3.43 % | 3.43 % | 3.43 % | 3.43% |
| Receiver Optical Channel Power | -4.6dBm | -12.38dBm | -15.9dBm | -17.6dBm |



Figure 4-18 CNR vs Number End-Users using Case III Linear Modulator
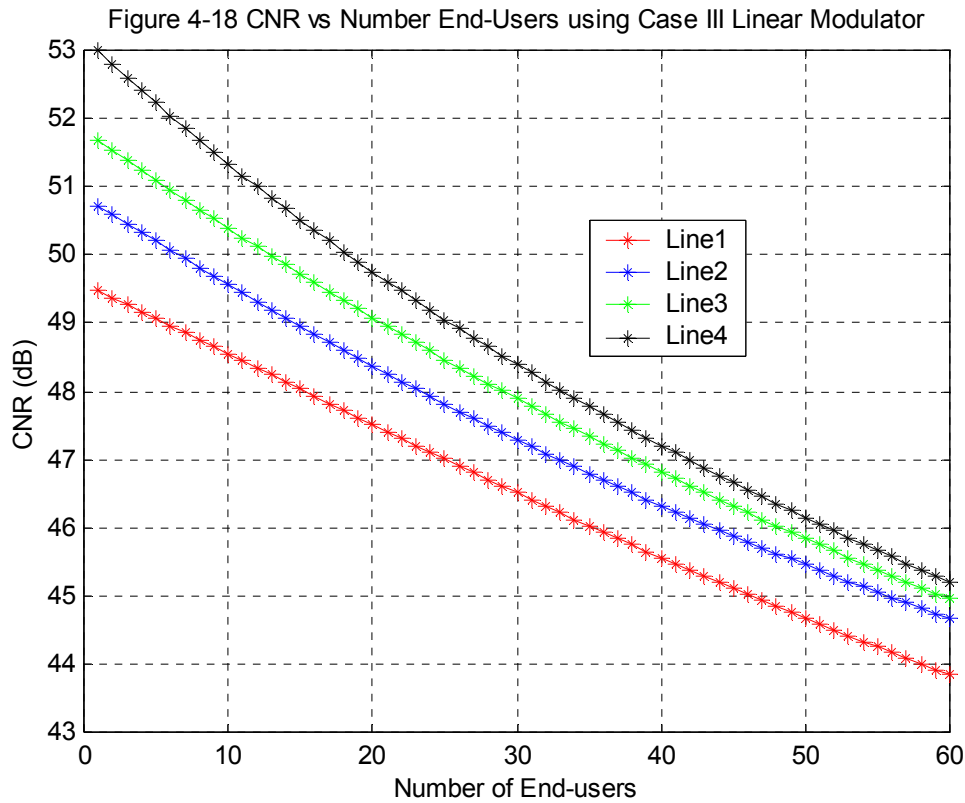
From the above analysis, it is clear that using Case II linearized Modulator, which has the optical power splitter value of 0.93 for the primary modulator and RF power ratio of 2.5 for the secondary modulator, has the best performance compared to Linearized Modulator in Case I & Case III.

## 4.4 Digital Signal Q-Value Using Linearized MZ Modulator

Using a linearized DPMZ modulator approach, the useful signal photo-current at the receiver expressed in equation (3-16) can be modified as follows:

$$I_p = I \cdot \left\{ \left[ 2AJ_1(\frac{\pi V}{V_\pi})J_0(\frac{\pi V}{V_\pi})^{N-1} \cdot x(t) \cdot \cos(\omega_d)t \right] - \left[ 2(1-A)J_1(B\frac{\pi V}{V_\pi})J_0(B\frac{\pi V}{V_\pi})^{N-1} \cdot x(t) \cdot \cos(\omega_d)t \right] \right\}$$

**(4-9)**

and the output of the demodulator is

$$I_p = I \cdot \left\{ \left[ 2AJ_1(\frac{\pi V}{V_\pi})J_0(\frac{\pi V}{V_\pi})^{N-1} \cdot x(t) \right] - \left[ 2(1-A)J_1(B\frac{\pi V}{V_\pi})J_0(B\frac{\pi V}{V_\pi})^{N-1} \cdot x(t) \right] \right\}$$

Assuming the modulation index/channel is small and by making the approximations [2]

$$\frac{J_1(Bm)}{J_0(Bm)} = B\frac{m}{2} \qquad \text{and} \qquad J_0(Bm)^N \approx \exp(-B^2 m^2 N / 4)$$

the Q value for BPSK, QPSK & ASK is:

$$Q_{BPSK} = \frac{I_P(1) - I_P(-1)}{\sigma(1) + \sigma(-1)} = \frac{2 \cdot I \cdot \left\{ \left[ 2A(\frac{m}{2})e^{-m^2 N/4} \right] - \left[ 2(1-A)(\frac{Bm}{2})e^{-B^2 m^2 N/4} \right] \right\}}{2(\sigma_{Shot} + \sigma_{RIN} + \sigma_{Thermal} + \sigma_{ASE})} \qquad \textbf{(4-10)}$$

$$Q_{QPSK} = \frac{I_P(\frac{1}{\sqrt{2}}) - I_P(-\frac{1}{\sqrt{2}})}{\sigma(\frac{1}{\sqrt{2}}) + \sigma(-\frac{1}{\sqrt{2}})} = \frac{I \cdot \left\{ \left[ 2A(\frac{m}{2})e^{-m^2 N/4} \right] - \left[ 2(1-A)(\frac{Bm}{2})e^{-B^2 m^2 N/4} \right] \right\}}{\sqrt{2} \cdot (\sigma_{Shot} + \sigma_{RIN} + \sigma_{Thermal} + \sigma_{ASE})} \qquad \textbf{(4-11)}$$

$$Q_{ASK} = \frac{I_P(1) - I_P(0)}{\sigma(1) + \sigma(0)} = \frac{I \cdot \left\{ \left[ 2A(\frac{m}{2})e^{-m^2 N/4} \right] - \left[ 2(1-A)(\frac{Bm}{2})e^{-B^2 m^2 N/4} \right] \right\}}{2(\sigma_{Shot} + \sigma_{RIN} + \sigma_{Thermal} + \sigma_{ASE})} \qquad \textbf{(4-12)}$$

$$\sigma_{Shot} = \sqrt{2qIB} \quad \sigma_{RIN} = \sqrt{I^2 RINB} \quad \sigma_{Thermal} = \sqrt{\frac{4KBT}{R_T}} \quad \sigma_{ASE} = \sqrt{4n_{sp}hfBR^2 G^2 L^2 P_s}$$

Because digital data is multiplexed together with 78 analog video streams in electrical domain and then optical modulated into one wavelength, the optical modulation index used in digital data is the same as other 78 analog video streams.  The Q-Value for BPSK, QPSK & ASK is examined based on the following parameter listed below.

| Parameter | Set 1 | Set 2 | Set 3 |
|---|---|---|---|
| **Linear MZ Modulator** | A=0.88 & B=2 | A=0.93 & B=2.5 | A=0.96 & B=3 |
| Input power at Booster Amplifier | 3dBm | 3dBm | 3dBm |
| Laser RIN | -160dB/Hz | -160dB/Hz | -160dB/Hz |
| Photodiode Responsivity | 0.9 A/W | 0.9 A/W | 0.9A/W |
| Fiber distance | 10km | 10km | 10km |
| No. of End-Users | 27 | 30 | 18 |
| OMI / Channel | 4.47% | 4.34% | 3.43% |
| Receiver Optical Channel Power | -18.9dBm | -18.8dBm | -17.6dBm |
| **RESULTS** | | | |
| BPSK Q-Value | **14.3** | **15.7** | **16.9** |
| QPSK Q-Value | **10.1** | **11** | **11.9** |
| ASK Q-Value | **7.2** | **7.8** | **8.4** |



Figure 4-19 "Set 1"
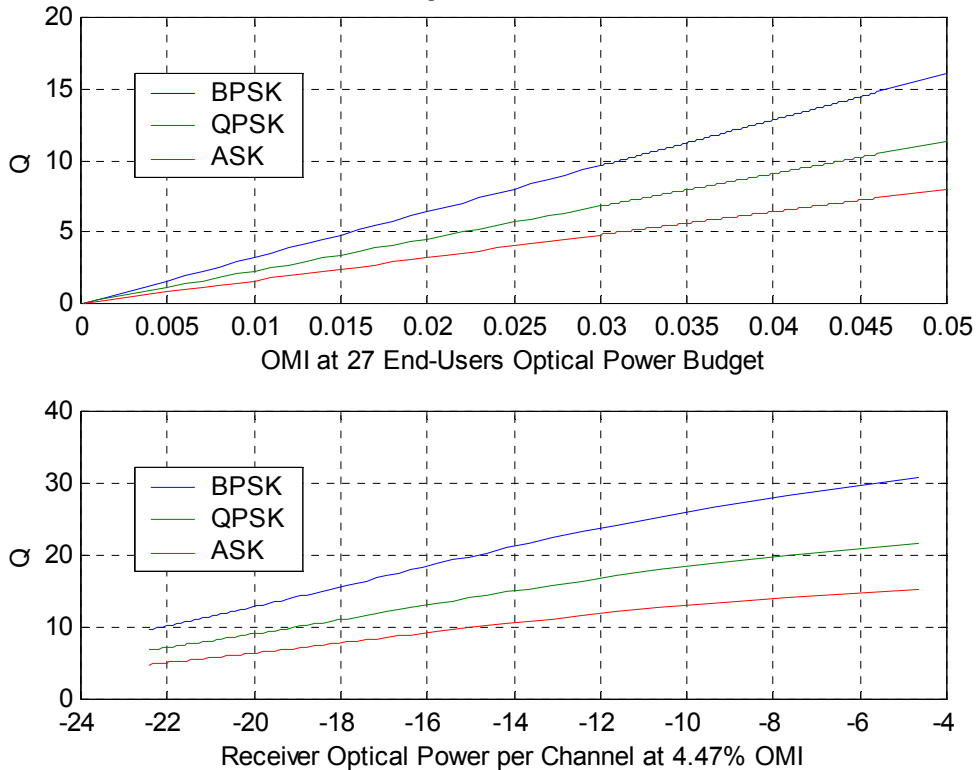
Figure 4-20 "Set 2"
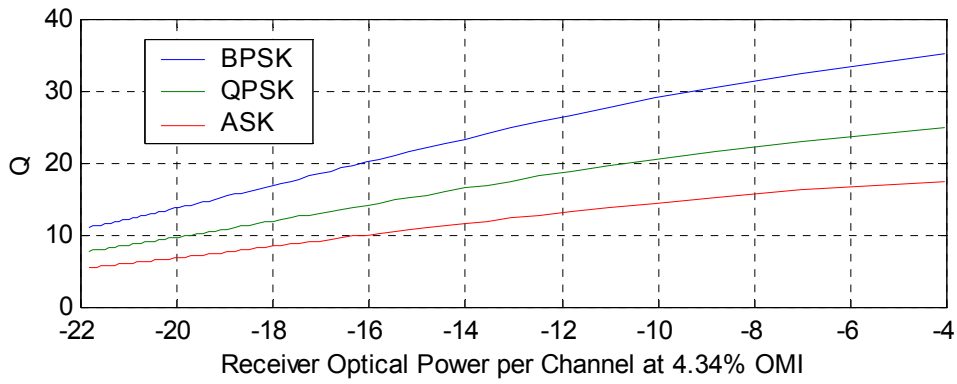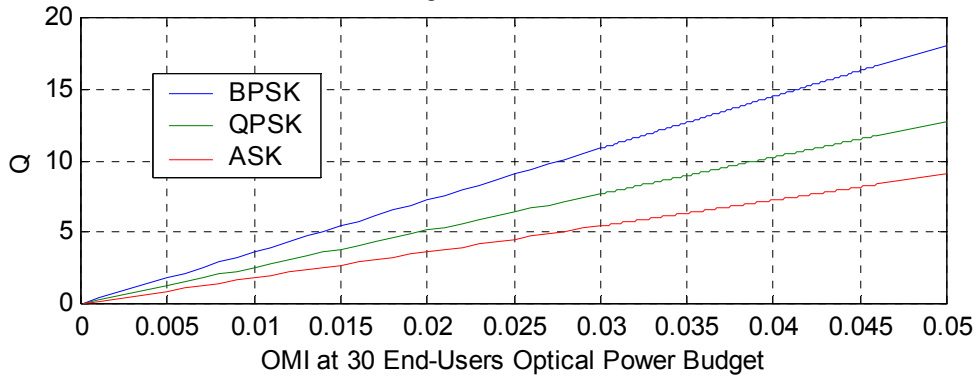




Figure 4-21 "Set 3"
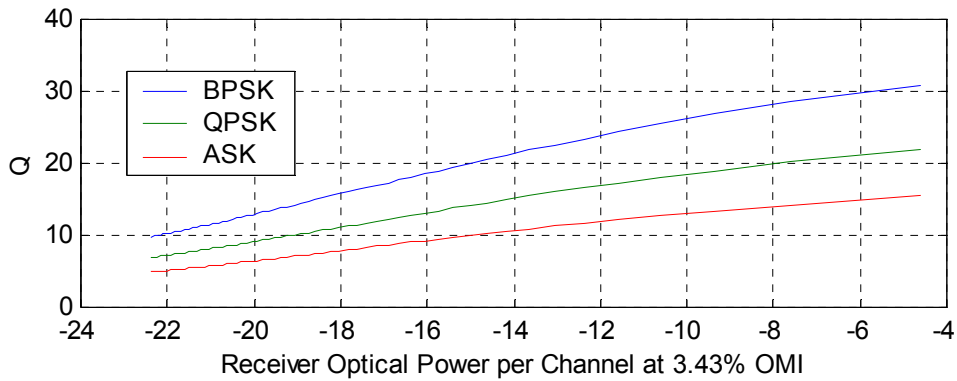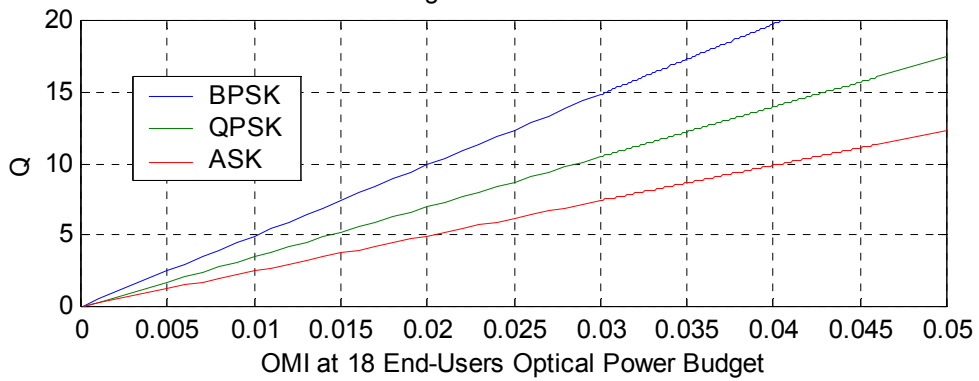
# CHAPTER 5: Fiber Nonlinear Crosstalk

In addition to transmitter and receiver noises in optical systems, fiber nonlinear crosstalk can significantly degrade the transmission system performance. There are two basic fiber nonlinear mechanisms. The first mechanism that causes fiber nonlinearities is the scattering phenomena, which produces Stimulated Raman Scattering. The second mechanism arises from the refractive index of glass being dependent on the optical power going through the material. This results in producing Cross Phase Modulation (XPM) and Four-Wave Mixing (FWM) crosstalk

## 5.1      Stimulated Raman Scattering (SRS) Crosstalk Frequency Response

Stimulated Raman Scattering (SRS) is a nonlinear phenomenon found in wavelength-division multiplexed (WDM) transmission system. As shown in figure 5-1, where the shorter wavelength channels are robbed of power and that power feeds the longer wavelength channel. [9]
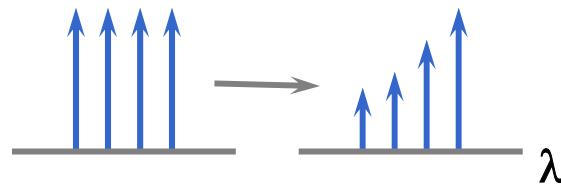
**Figure 5-1**

This phenomenon is similar to the operation of EDFAs where a 980nm pump wavelength provides the energy that amplifies the signals in the longer wavelength such as at 1550nm region.

As for the crosstalk interaction between pump channel and signal channel in the SCM/WDM system, assuming pump channel has a shorter wavelength than probe channel, the most significant crosstalk term is due to the SRS interaction between pump channel optical carrier and probe channel subcarriers. As for the interaction between signal channel optical

carrier and pump channel subcarriers, an optical power loss occurs , but does not contribute to SRS crosstalk.  In addition, each subcarrier comprises only a small fraction of the total optical power. The SRS interaction between subcarriers in different WDM channels is relatively weak compared to the SRS interactions between the subcarriers (in any given WDM channel) and the optical carrier (of any other WDM channel).

A formal approach to determining SRS crosstalk levels is to solve the coupled propagation equations for the optical intensity I at wavelengths $\lambda 1$ and $\lambda 2$ [10].

$$\frac{\partial I_1}{\partial z} + \frac{1}{v_1}\frac{\partial I_1}{\partial t} = (gI_2 - \alpha)I_1 \tag{5-1}$$

$$\frac{\partial I_2}{\partial z} + \frac{1}{v_2}\frac{\partial I_2}{\partial t} = (-gI_1 - \alpha)I_2 \tag{5-2}$$

where z is the distance along the fiber, g is the Raman gain (loss) coefficient and $v$ is the group velocity of each channel in the fiber.  Assuming $\lambda 2 < \lambda 1$ (channel 2 is designated as pump channel and channel 1 as probe channel).

By neglecting the SRS term, $gI_2$, on the right hand side of (5-1) and solving for $I_1$; then substituting $I_1$ into (5-2) and solving for $I_2$ are gets [10]:

$$
\begin{aligned}
P_2(0,\mu_2) &= P_2(0,\mu_2)e^{-\alpha z} \cdot \exp\left[-\frac{g}{A_{eff}}\int_0^z P_1(0,\mu_2 + d_{12}z^{'})e^{-\alpha z^{'}}dz^{'}\right] \\
P_2(0,\mu_2) &\approx P_2(0,\mu_2)e^{-\alpha z} \cdot \left[1 - \frac{g}{A_{eff}}\int_0^z P_1(0,\mu_2 + d_{12}z^{'})e^{-\alpha z^{'}}dz^{'}\right]
\end{aligned}
\tag{5-3}
$$

where $d_{12} = \left|\frac{1}{v_1} - \frac{1}{v_2}\right|$ is the group velocity mismatch between the pump and signal channels and

$$\mu_2 = t - \frac{z}{v_2}.$$

A similar approach can be used to solve for $I_1$ by neglecting the SRS term, $-gI_1$ on the right hand side of (5-2) and solving for $I_2$, then substituting $I_2$ into (5-1) to get

$$P_1(0,\mu_1) \approx P_1(0,\mu_1)e^{-\alpha z} \cdot \left[1 + \frac{g}{A_{eff}} \int_0^z P_2(0,\mu_1 + d_{12}z')e^{-\alpha z'}dz'\right] \qquad (5\text{-}4)$$

**Crosstalk due to SRS for steady light**

We first assume channel 1 & 2 are unmodulated signal and they both have the same average optical power of $P_1(0,t) = P_2(0,t) = P_o$



λ2                    λ1
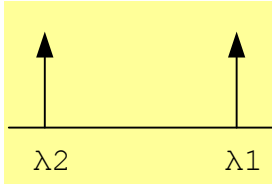
$$P_2(0,\mu_2) \approx P_2(0,\mu_2)e^{-\alpha z}\left[1 - \frac{g}{A_{eff}}\int_0^z P_1(0,\mu_2 + d_{12}z')e^{-\alpha z'}dz'\right] = P_o e^{-\alpha z}\left\{1 - \frac{g}{A_{eff}}P_o\left|\frac{1-e^{-\alpha z}}{\alpha}\right|\right\} \quad (5\text{-}5)$$

$$P_1(0,\mu_1) \approx P_1(0,\mu_1)e^{-\alpha z}\left[1 + \frac{g}{A_{eff}}\int_0^z P_2(0,\mu_1 + d_{12}z')e^{-\alpha z'}dz'\right] = P_o e^{-\alpha z}\left\{1 + \frac{g}{A_{eff}}P_o\left|\frac{1-e^{-\alpha z}}{\alpha}\right|\right\} \quad (5\text{-}6)$$

The first term in equations (5-5) & (5-6) represents carrier power after fiber loss; and, the second term in equations (5-5) & (5-6) is attributed to carrier power loss or gain due to SRS interaction. Therefore, the steady-light described the SRS interaction between pump channel and probe channel optical carrier to express the amplification (depletion) of the probe channel (pump channel) carrier power, but not its interference which leads to crosstalk.

**Crosstalk due to SRS for modulated light**

This case assume channel 1 (probe channel) has modulated signal $P_1(0,t) = P_0(1 + m\cos(\omega t))$ & channel 2 is unmodulated signal as shown below:
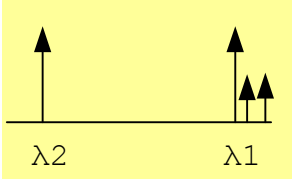
In [10], $P_2(0,\mu_2) = P_0 e^{-\alpha z} \cdot \left[ 1 - \frac{g}{A_{eff}} \int_0^z P_0 e^{-\alpha z'} dz' - \frac{g}{A_{eff}} \int_0^z P_0 m \cos(\omega\mu_2 + \omega d_{12} z') e^{-\alpha z'} dz' \right]$ **(5-7)**

$$P_2(0,\mu_2) = P_0 e^{-\alpha z} \cdot \left[ 1 - \frac{g}{A_{eff}} P_o \left| \frac{1-e^{-\alpha z}}{\alpha} \right| - \frac{g}{A_{eff}} P_0 m \frac{\sqrt{1+e^{-2\alpha z} - 2e^{-\alpha z} \cos(\omega d_{12}z)}}{\sqrt{\alpha^2 + (d_{12}\omega)^2}} \cos(\omega\mu_2 + \Theta_{srs}) \right]$$

$$where \quad \Theta_{srs} = \tan^{-1}\left(\frac{-\omega d_{12}}{-\alpha}\right) + \tan^{-1}\left(\frac{e^{-\alpha z} \sin(\omega d_{12}z)}{e^{-\alpha z} \cos(\omega d_{12}z) - 1}\right)$$

In equation (5-7), the first term corresponds to the carrier power after fiber loss. The second term corresponds to the interaction between the optical carriers, this result in optical dc power gain or loss. The third term is the crosstalk as the result of modulation depletion through SRS interaction between pump channel optical carrier and signal channel subcarrier.

The electrical crosstalk suffered by the subcarrier in the probe channel due to SRS is [10]:

$$Crosstalk(SRS) = \frac{\left| -P_0 e^{-\alpha z} \frac{P_0 m g}{A_{eff}} \frac{\sqrt{1+e^{-2\alpha z} - 2e^{-\alpha z} \cos(\omega d_{12}z)}}{\sqrt{\alpha^2 + (d_{12}\omega)^2}} \right|^2}{\left| P_o m e^{-\alpha z} \left\{ 1 + \frac{g}{A_{eff}} P_o \left| \frac{1-e^{-\alpha z}}{\alpha} \right| \right\} \right|^2} \approx \left| -\frac{g P_0}{A_{eff}} \frac{\sqrt{1+e^{-2\alpha z} - 2e^{-\alpha z} \cos(\omega d_{12}z)}}{\sqrt{\alpha^2 + (d_{12}\omega)^2}} \right|^2$$

**(5-8)**

On the other hand, assuming channel 2 (pump channel) has modulated signal

$P_2(0,t) = P_0(1 + m\cos(\omega t))$ & channel 1 is the unmodulated signal as shown below.
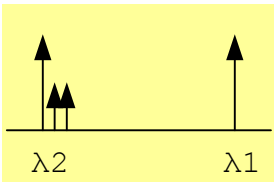


then, the electrical crosstalk suffered by subcarrier in pump channel due to SRS is:

$$Crosstalk(SRS) = \frac{\left| P_0 e^{-\alpha z} \dfrac{P_0 mg}{A_{eff}} \dfrac{\sqrt{1 + e^{-2\alpha z} - 2e^{-\alpha z} \cos(\omega d_{12} z)}}{\sqrt{\alpha^2 + (d_{12}\omega)^2}} \right|^2}{\left| P_o m e^{-\alpha z} \left\{ 1 - \dfrac{g}{A_{eff}} P_o \left| \dfrac{1 - e^{-\alpha z}}{\alpha} \right| \right\} \right|^2} \approx \left| \frac{gP_0}{A_{eff}} \frac{\sqrt{1 + e^{-2\alpha z} - 2e^{-\alpha z} \cos(\omega d_{12} z)}}{\sqrt{\alpha^2 + (d_{12}\omega)^2}} \right|^2$$

**(5-9)**

SRS-induced crosstalk is present in both the short and long wavelength channels, as long as the

change in the average crosstalk power caused by SRS is negligible, its magnitude is independent

on which signal is used as pump for Raman gain. [10]

Figure 5-2 illustrates SRS vs. Modulation Frequency Response with three different frequency

separations (1nm, 4nm & 8nm). The optical power per channel is 10dBm with 10km SM fiber,

D=17ps/nm/km, and the slope of Raman gain is 5e-15 m/W/THz.



Figure 5-2 SRS Frequency Response
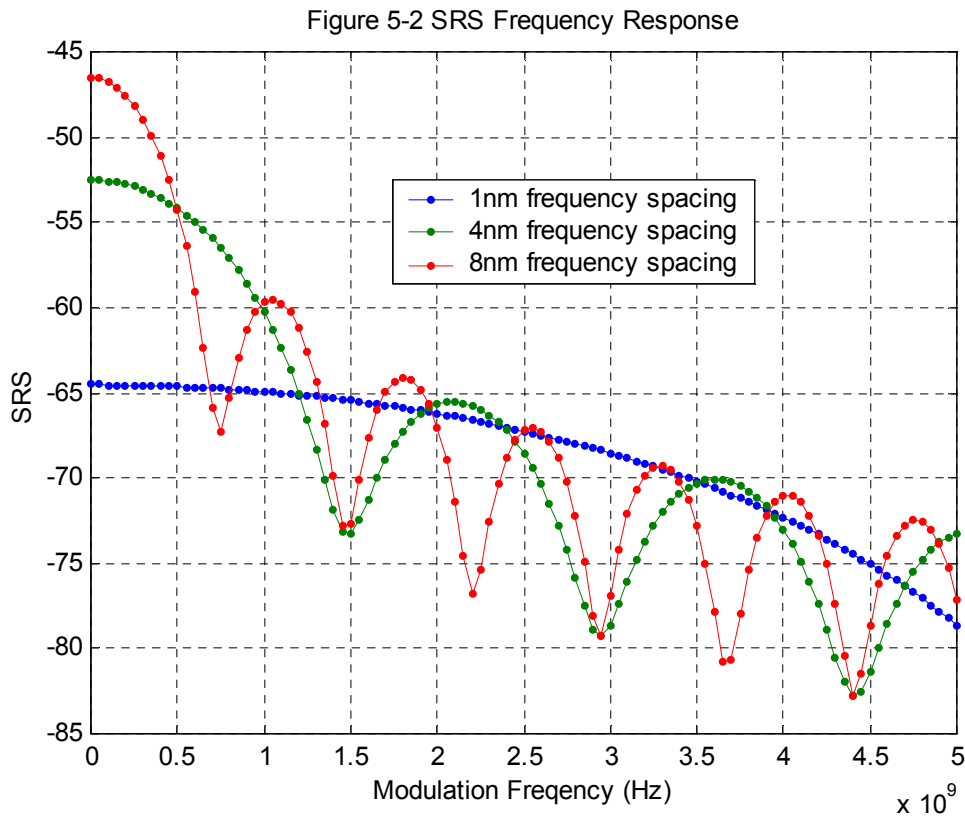
We can summarize the characteristic of SRS Crosstalk Frequency Response as followed:

- As Frequency Separation (Wavelength Separation) increases, SRS crosstalk increases.

- SRS crosstalk decreases as modulation frequency increases when frequency separation > 1nm & SRS crosstalk stays constant as modulation frequency increases when frequency separation is small, such as when less than 0.5nm.

- SRS crosstalk is dominant at large frequency separation with small modulation frequency.

## 5.2    Cross Phase Modulation (XPM) Crosstalk Frequency Response

Cross Phase Modulation (XPM) is a type of nonlinear crosstalk caused by the Kerr effect in optical fibers.  The intensity modulation of one optical carrier can modulate the phases of other copropagating optical signals in the same fiber; and, in the absence of fiber dispersion, does not affect Intensity Modulation system.  However, in the presence of fiber dispersion, the phase modulation converts to intensity modulation that leads to crosstalk and degradation of the IMDD system performance. The analytical expression of XPM induced crosstalk is obtained by using nonlinear wave propagation equation as shown in reference [10] & [11].  Here the pump channel as a modulated optical signal and the probe channel as an unmodulated optical signal are copropagating in the same optical fiber.



Pump
Channel K

Probe
Channel J
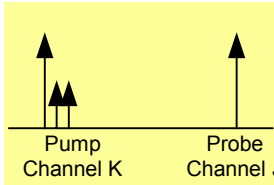
$$\frac{\partial A_j(t,z)}{\partial z} + \frac{\alpha}{2} A_j(t,z) + \frac{1}{v_j}\frac{\partial A_j(t,z)}{\partial t} + \frac{i\beta_2}{2}\frac{\partial^2 A_j(t,z)}{\partial^2 t} = i\gamma_j[2P_k(t - d_{jk}z, z)]A_j(t,z)$$

**(5-10)**

Translating this propagation equation (5-10) into the frequency domain using Fourier transformation becomes equation 5-11.

$$\frac{\partial A_j(\Omega,z)}{\partial z} = \left\{ -(\frac{\alpha}{2} + \frac{i\Omega}{v_j}) + i\gamma_j 2P_k(\Omega,0)e^{i\Omega d_{jk}z}e^{-\alpha z} + \frac{i\beta_2\Omega^2}{2} \right\} A_j(\Omega, z) \qquad \textbf{(5-11)}$$

The first term on the right hand side of (5-11) accounts for attenuation and linear phase delay. The second term accounts for phase modulation in the probe channel $j$ induced by the pump channel k and depends on the pump channel $k$ power and fiber nonlinearity.

In a short fiber section, dz, the crosstalk phase modulation in the probe signal induced by the pump signal can be linearized under the small signal approximation [10],[11]  In addition, because of chromatic dispersion of the fiber, the crosstalk phase modulation generated at z=z' is converted into an amplitude modulation at the end of fiber z=L.  Integrating all XPM contributions along the fiber such as fiber loss, linear phase delay, phase modulation, phase modulation to intensity modulation conversion, the total intensity noise at the end of fiber z=L can be obtained as shown in reference [10], [11]

$$\Delta A_j(\Omega, L) = -2P_j(0)e^{-(\alpha - i\Omega/v_j)z} \int_0^L 2\gamma_j P_k(\Omega,0)e^{-(\alpha - i\Omega d_{jk})z} \sin[\beta_2\Omega^2(L-z)/2]dz$$

$$\Delta A_j(\Omega, L) = P_j(L)e^{-\frac{i\Omega}{v_j}L} 2\gamma_j P_k(\Omega,0)\left\{ \frac{e^{\frac{i\beta_2\Omega^2 L}{2}} - e^{(-\alpha + i\Omega d_{jk})L}}{i(\alpha - i\Omega d_{jk} + i\beta_2\Omega^2/2)} - \frac{e^{\frac{i\beta_2\Omega^2 L}{2}} - e^{(-\alpha + i\Omega d_{jk})L}}{i(\alpha - i\Omega d_{jk} - i\beta_2\Omega^2/2)} \right\}$$

and the XPM induced electrical power spectral density in the probe channel j is

$$\Delta P_j(\Omega, L) = \left| \frac{\Delta A_j(\Omega, L)}{P_j(L)} \right|^2$$

$$\Delta P_j(\Omega, L) = \left| 2\gamma_j P_k(\Omega,0)\left\{ \frac{e^{\frac{i\beta_2\Omega^2 L}{2}} - e^{(-\alpha + i\Omega d_{jk})L}}{i(\alpha - i\Omega d_{jk} + i\beta_2\Omega^2/2)} - \frac{e^{\frac{i\beta_2\Omega^2 L}{2}} - e^{(-\alpha + i\Omega d_{jk})L}}{i(\alpha - i\Omega d_{jk} - i\beta_2\Omega^2/2)} \right\} \right|^2 \qquad \textbf{(5-12)}$$

Figure 5-3 illustrates XPM vs. Modulation Frequency Response with three different frequency separations (1nm, 4nm & 8nm).  The average optical channel power is 10dBm with 10km SM fiber, D=17ps/nm/km.

Figure 5-3 XPM Frequency Response
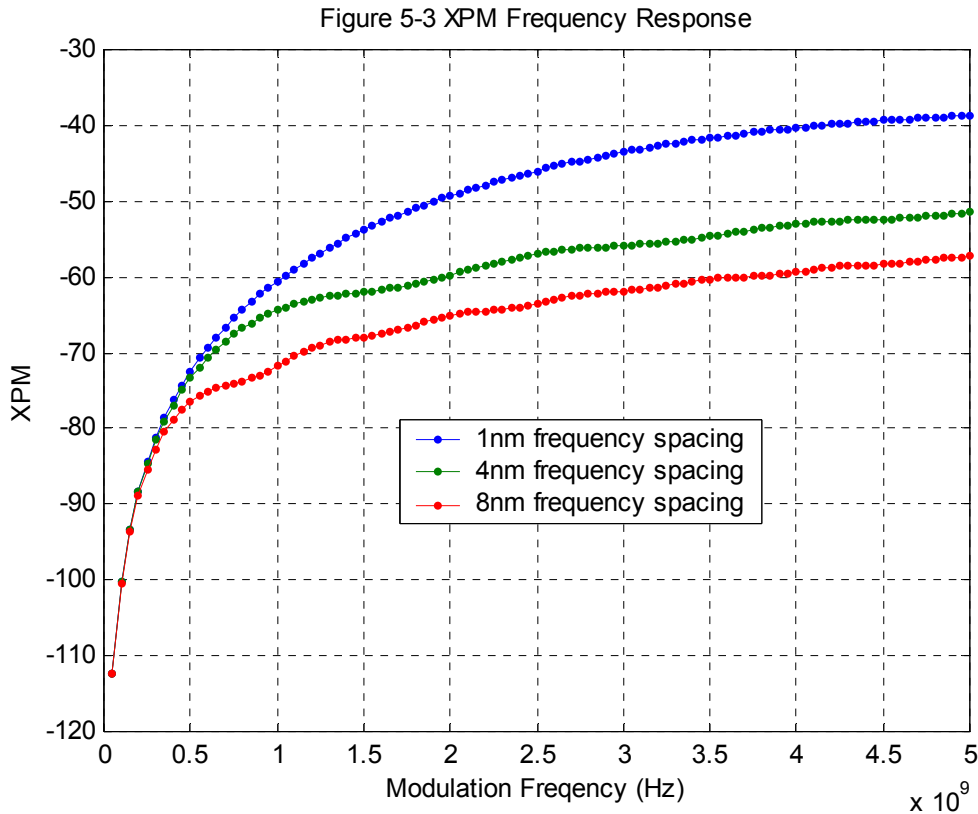
The characteristic of XPM crosstalk summarized as followed:

- As Frequency Separation (Wavelength Separation) decreases, XPM crosstalk increases with large modulation frequency.

- XPM crosstalk dominants at small frequency spacing with large modulation frequency.

- XPM has similar frequency response when frequency separation is small such as when less than 0.5nm.

## 5.3    Constructive & Destructive SRS+XPM crosstalk Concept

It is interesting to notice the magnitude of SRS transfer function is independent of which signal (modulated channel or unmodulated channel) is pumping for the Raman gain.   When considering the total crosstalk from the two effects (SRS & XPM), we must consider both their amplitude and phase.   For this assume wavelength 1 > wavelength 2, and channel 2 is a

modulated channel as illustrated below, the constructive crosstalk of SRS and XPM occurs is explained below.

Channel 2

CW
Channel 1
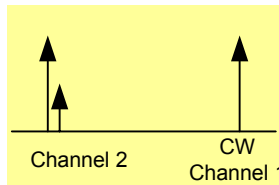
**SRS Crosstalk:** When the modulated channel is at a shorter wavelength than the CW channel, it provides Raman gain.  The CW Channel results in modulated gain through SRS interaction between subcarrier pump channel 2 and optical carrier probe channel 1.

 **XPM Crosstalk:**  Intensity modulation of pump channel 2 creates a phase modulation to probe channel 1 because of Kerr effect, and then converts to Intensity modulation with fiber dispersion. Therefore crosstalk for CW channel 1 from SRS and XPM are in-phase with each other and add constructively.

On the other hand, if channel 1 is a modulated channel as illustrated below, the destructive crosstalk of SRS and XPM occurs is explained below.

CW
Channel 2
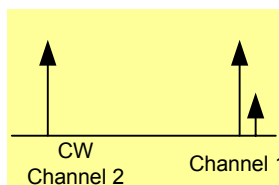
Channel 1

**SRS Crosstalk:** When the modulated channel is at a larger wavelength than the CW channel, the CW Channel looses power to channel 1. The CW Channel results in modulated depletion through SRS interaction between subcarrier channel 1 and optical carrier CW channel.  In other words, the SRS crosstalk at channel 2 is now going through power depletion rather than gain.

 **XPM Crosstalk:**  Intensity modulation of channel 1 creates phase modulation to CW channel because of Kerr effect, and then converts to Intensity modulation with fiber dispersion.

Crosstalk at CW channel 2 from SRS and XPM are out-phase with each other and add

destructively.  Figure 5-4A, 5-5A & 5-6A illustrates the constructive crosstalk frequency

response when the modulated channel is at a shorter wavelength than the CW channel, and,

Figure 5-4B, 5-5B & 5-6B illustrates the destructive crosstalk frequency response when the

modulated channel as at a longer wavelength than CW channel.

It can be clearly seen that for small modulated frequency or large wavelength separation,

crosstalk frequency response is dominated by SRS; and, for large modulated frequency or small

wavelength separation, crosstalk frequency response is dominated by XPM.  In between we must

consider whether the SRS is going through power depletion or power gain.

| Optical Ch. Power entering Fiber | 10dBm |
|---|---|
| SM Fiber distance | 10km |
| Fiber loss | 0.2 dB/km |
| Mode Effective Area | 78 $\mu m^2$ |
| SRS gain slope | $5e^{-15}$ m/W/THz |
| Dispersion | 17 ps/nm/km |

Figure 5-4A CW wavelength > Modulation wavelength (1nm Spacing)
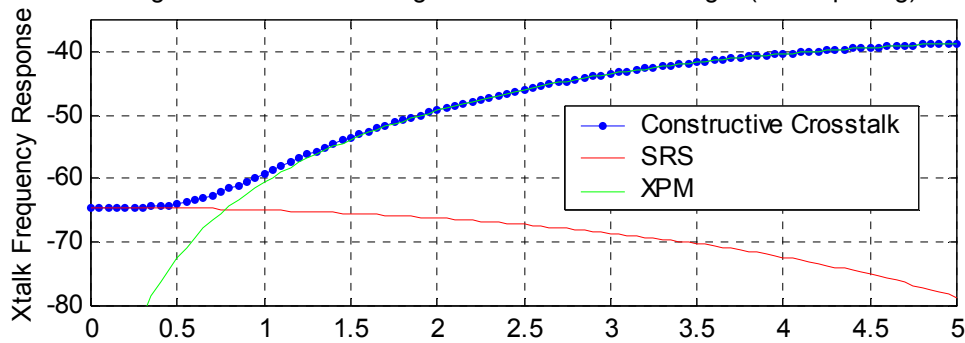


Figure 5-4B CW wavelength < Modulation wavelength
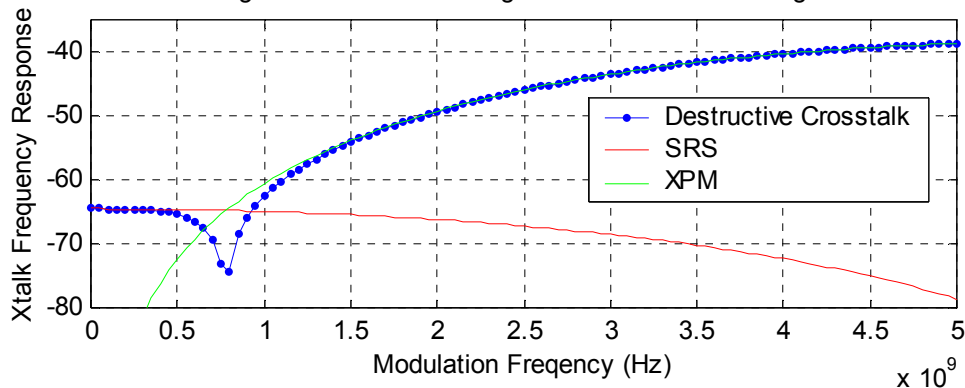
Figure 5-5A CW wavelength > Modulation wavelength (4nm Spacing)
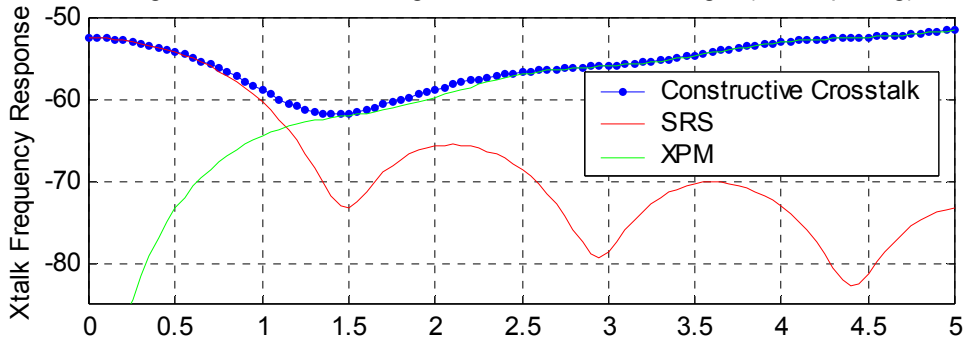
Figure 5-5B CW wavelength < Modulation wavelength
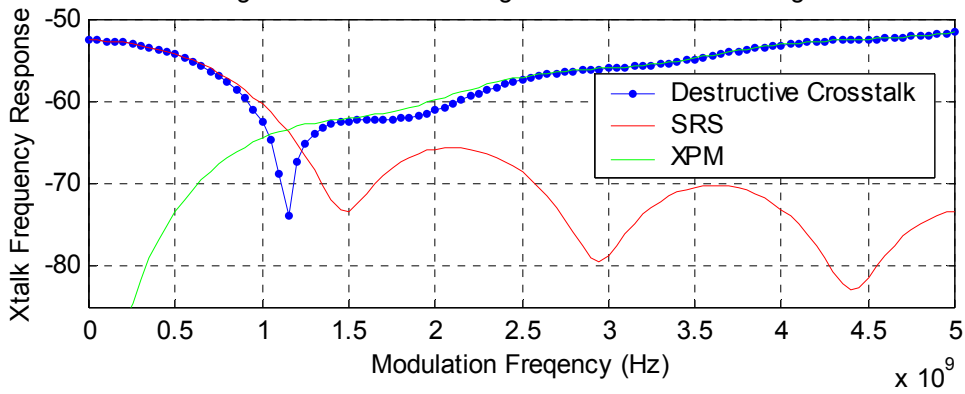
Figure 5-6A CW wavelength > Modulation wavelength (8nm Spacing)
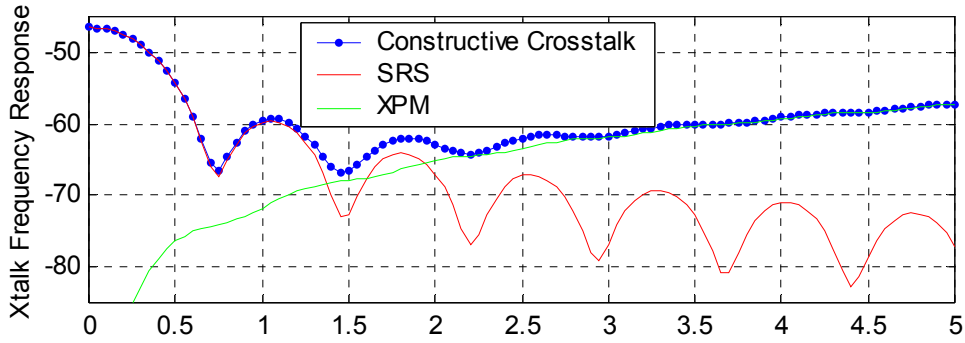
Figure 5-6B CW wavelength < Modulation wavelength
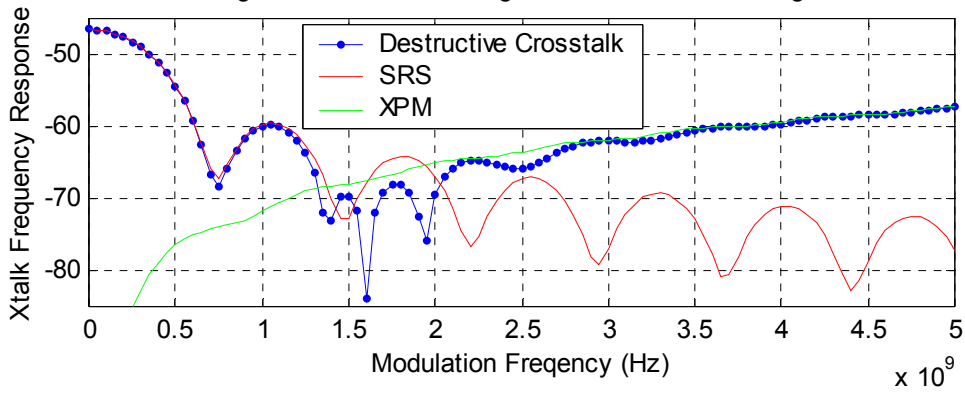
### 5.4　SRS and XPM Crosstalk in SCM externally modulated optical link

In this section, we examine SRS & XPM crosstalk interaction between subcarrier channels (analog and digital) within the same wavelength. Equation (5-4) can be re-modified by assuming the two (2) subcarrier channels are $P_2(0,t) = P_0(m\cos(\omega_2 t))$ and $P_1(0,t) = P_0(m\cos(\omega_1 t))$, which have the same average optical power and OMI. Assuming subcarrier 2 RF frequency > subcarrier 1 RF frequency: the SRS crosstalk at subcarrier 2 suffers by subcarrier channel 1

$$P_2(0,\mu_2) = P_o m\cos(\omega\mu_2)e^{-\alpha z} \cdot \left[1 + \frac{g}{A_{eff}} \int_0^z P_0 m\cos(\omega_1\mu_1 + \omega_1 d_{12}z')e^{-\alpha z'} dz'\right] \qquad \textbf{(5-13)}$$

where the first term corresponds to pump subcarrier after fiber loss and the second term is the crosstalk terms which correspond to the SRS interaction between pump and probe subcarriers. This SRS crosstalk is a result of power gain. The SRS crosstalk level in electrical domain can be expressed as following:

$$Crosstalk(SRS) = \frac{\left|P_0 m e^{-\alpha z} \dfrac{P_0 m g}{A_{eff}} \dfrac{\sqrt{1 + e^{-2\alpha z} - 2e^{-\alpha z}\cos(\omega d_{12}z)}}{\sqrt{\alpha^2 + (d_{12}\omega)^2}}\right|^2}{\left|P_0 m e^{-\alpha z}\right|^2} = \left|\frac{gP_0 m}{A_{eff}} \frac{\sqrt{1 + e^{-2\alpha z} - 2e^{-\alpha z}\cos(\omega d_{12}z)}}{\sqrt{\alpha^2 + (d_{12}\omega)^2}}\right|^2$$

**(5-14)**

where $P_0 m$ is the optical power of RF channel.

Before we analyze SRS & XPM crosstalk between analog and digital SCM/WDM system, it is important to address the sensitivity of the probe channel to SRS & XPM induced crosstalk is related on its receiver bandwidth, therefore, the crosstalk between high and low bit rate channels is comparable to the crosstalk between two low bit rate channels [10]. In this project, we have assumed that the crosstalk level between 1Gb/s digital data & 6MHz analog channel is comparable to the crosstalk between two 6MHz analog channels.

In CATV channel, 78 analog channels are packed closely with 6MHz frequency spacing between each other. Figure 5-7 shows SRS & XPM frequency response across 6MHz channel bandwidth at channel 2 suffers by channel 1 (channel 2 modulated RF frequency > channel 1 modulated RF frequency) with frequency spacing: 6MHz, 60MHz, 0.6GHz & 6GHz. We first use the optical power budget for a total of 30 end-users were connected to CO and the optical link loss at CO is 17.7dB [1dB (circulator loss) + 14.8dB (passive star coupler loss for 30 end-users) +2dB (operation margin)]. Input optical power entering SM fiber is -15.6dBm per channel using linearized MZ modulator at OMI = 4.34%.

SRS is dominant at small modulation frequency with large wavelength separation, and XPM is dominant at large modulation frequency with small wavelength separation. With small modulation frequency and small frequency separation, SRS is the dominant crosstalk compared to XPM. Figure 5-8 shows a plot of the theoretical crosstalk level at channel 1 suffered by channel 2 with same frequency spacing. The magnitude of the individual contributions from SRS and XPM remains the same; however, because the SRS crosstalk is now going through power depletion rather than gain, the SRS and XPM crosstalk adds destructively. As frequency separation increases, SRS is enhanced while XPM is mitigated for small modulation frequency. Comparing to SRS, XPM crosstalk has no impact on subcarriers channel within same wavelength.

### PARAMETERS

| | |
|---|---|
| Input Fiber Optical Power / Channel | -15.6dBm |
| SM Fiber distance and fiber loss | 10 km, 0.22dB/km |
| Mode Effective Area | $78\mu m^2$ |
| SRS gain slope | $5e^{-15}$ m/W/THz |
| Dispersion | 17 ps/nm/km |

Figure 5-7 Xtalk Frequency Response (SRS & XPM) at Channel 2
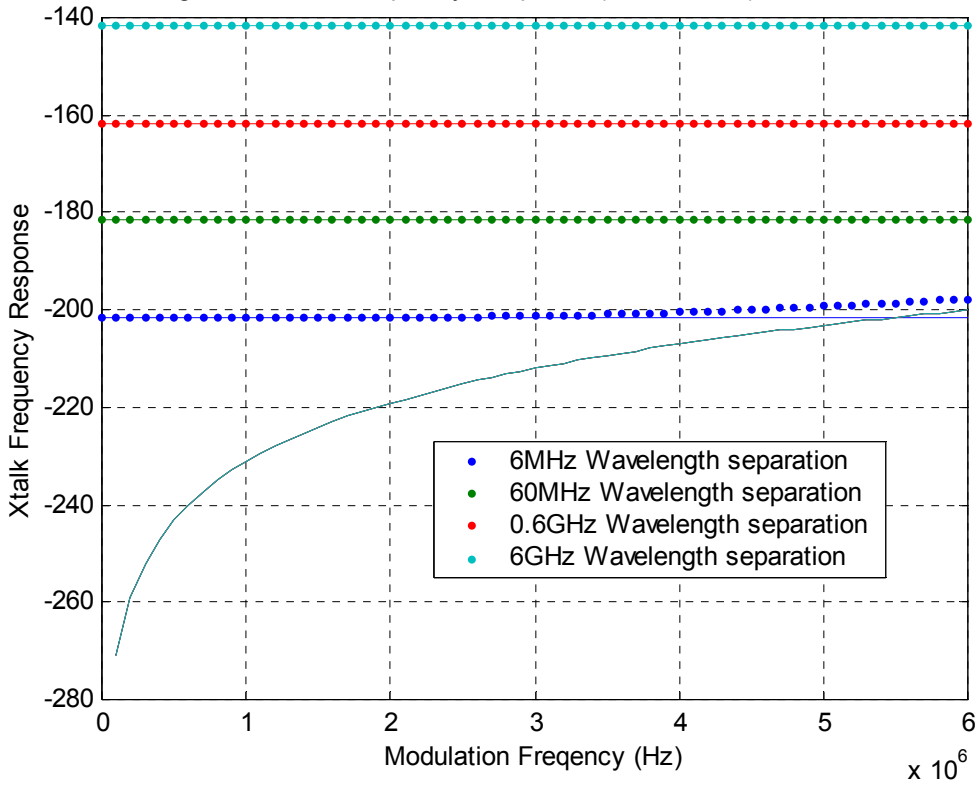


Figure 5-8 Xtalk Frequency Response (SRS & XPM) at Channel 1

62
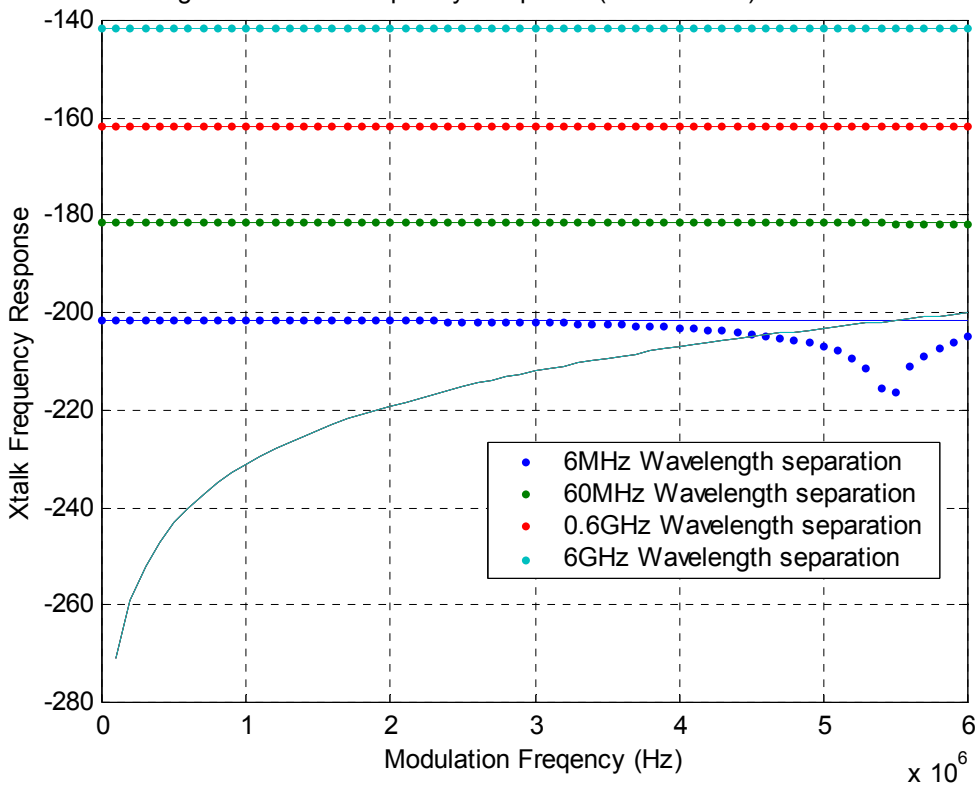
Using simple approximation to analyze crosstalk noise power, we approximate the baseband RF power spread evenly across its bandwidth. Given -15.6dBm optical power per baseband channel and 6MHz baseband bandwidth, the signal electrical power spectral density (W/Hz) is defined by dividing transmitted channel electrical power by baseband bandwidth, which is equal to 1.2643e-16(W/Hz). We obtain the crosstalk power spectral density (W/Hz) by multiplying the signal power spectrum density with the SRS & XPM crosstalk transfer functions. After obtaining the crosstalk power spectrum density, we can integrate all SRS & XPM contributions from 0 to 6MHz to obtain the total noise power. Figure 5-9 (A) plots crosstalk optical noise powers (dBm) and Figure 5-9 (B) plots the ratio of crosstalk optical power to transmitted channel power vs. wavelength spacing.



Figure 5-9A Xtalk Optical power(dBm) vs. Wavelength Separation(nm)

Figure 5-9B xtalk normalized to transmitted ch. power vs. Wavelength Separation(nm)
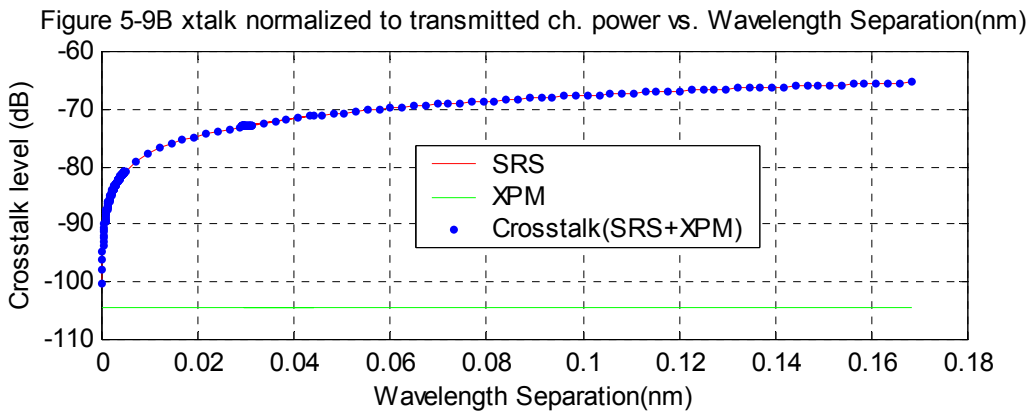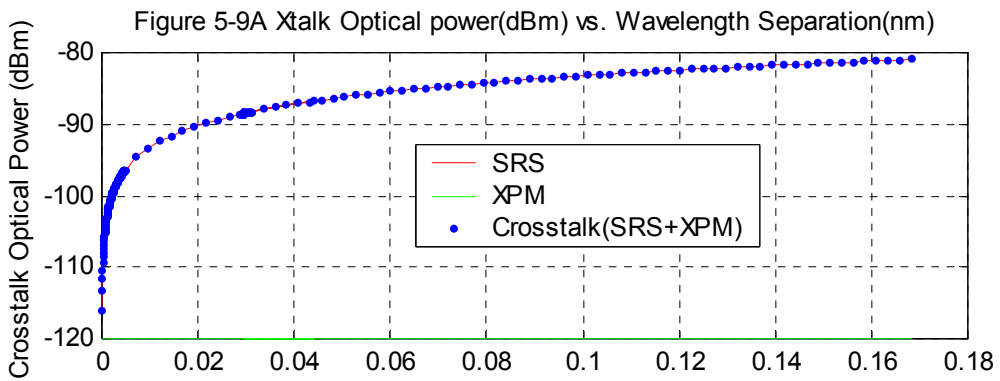
The SRS & XPM induced crosstalk between subcarriers in the same wavelength is summarized as follows:

- Compared to XPM, SRS is the dominant crosstalk in small signal bandwidth and small frequency spacing.

- Because of small channel bandwidth and small optical channel power, SRS-induced crosstalk is independent of which subcarrier channel is the pump for the Raman gain.

- Overall result, SRS & XPM Crosstalk show very minimal impact between two subcarrier channels in the same wavelength.

## 5.5    Four-wave Mixing Crosstalk in SCM externally modulated optical link

Four-wave mixing crosstalk is one of the major limiting factors in SCM/WDM optical fiber communications systems that use narrow channel spacing, low chromatic dispersion and high optical channel power.  The time-averaged optical power $P_{ijk}(L,\Delta\beta)$ generated through the FWM process for the frequency component $fijk$ is written as [13] in (esu) unit.

$$P_{ijk}(L) = \frac{1024\pi^6}{n^4\lambda^2 c^2}(DX_{1111})^2 (\frac{P_i P_j P_k}{A_{eff}^2}) \left| \frac{\{e^{(i\Delta\beta-\alpha)L}-1\}}{\{i\Delta\beta-\alpha\}} \right|^2 \qquad (5\text{-}15)$$

where $X_{1111}$ is the third-order nonlinear susceptibility, (which is related to $n_2$ nonlinear refractive index ($m^2/W$),  see Appendix 3 for detail relations between $n_2$ and $X_{1111}$ )

D as the degeneracy factor (1, 3 or 6) depends on whether three, two, or none of the frequencies $f_i$, $f_j$, and $f_k$ are the same.  The generated wave efficiency η, with respect to phase mismatch $\Delta\beta L$, is expressed as

$$\eta = \frac{P_{ijk}(L,\Delta\beta)}{P_{ijk}(L,\Delta\beta=0)} = \left| \frac{\{e^{(i\Delta\beta-\alpha)L}-1\}}{L_{eff}\{i\Delta\beta-\alpha\}} \right|^2 = \frac{\alpha^2}{\alpha^2+\Delta\beta^2}\left[1+\frac{4e^{-\alpha L}\sin^2(\frac{\Delta BL}{2})}{(1-e^{-\alpha L})^2}\right] \qquad (5\text{-}16)$$

where $\Delta\beta$ is the propagation constant difference written as

$$\Delta\beta = \frac{2\pi\lambda^2}{c}\Delta f_{ik}\Delta f_{jk}\left[D+\frac{\lambda^2 S}{2c}(\Delta f_{ik}+\Delta f_{jk})\right]$$

Assuming the equivalent frequency separation $\Delta f = (\Delta f_{ik} * \Delta f_{jk})^{1/2}$

$$\Delta\beta = \frac{2\pi\lambda^2}{c}\Delta f^2\left[D+\frac{\lambda^2 S}{2c}(\Delta f)\right] \qquad (5\text{-}17)$$

The time-average optical power generated through the FWM process can be modified in terms of generated wave efficiency as

$$P_{ijk}(L) = \frac{1024\pi^6}{n^4\lambda^2c^2}(DX_{1111})^2(\frac{P_iP_jP_k}{A_{eff}^2})L_{eff}^2\eta \qquad \textbf{(5-18)}$$

Using D = 6 (none of frequencies are the same), FWM Crosstalk optical power (dBm) vs. wavelength separation is plotted in figure 5-10A and figure 5-10B plot the ratio of generated mixing-product power to transmitted channel power versus channel spacing of two equal-power channels.

Figure 5-10A FWM optical power(dBm) vs. Wavelength Separation(nm)

Figure 5-10B Ratio of FWM power to transmitted ch. power vs. Wavelength Separation(nm)
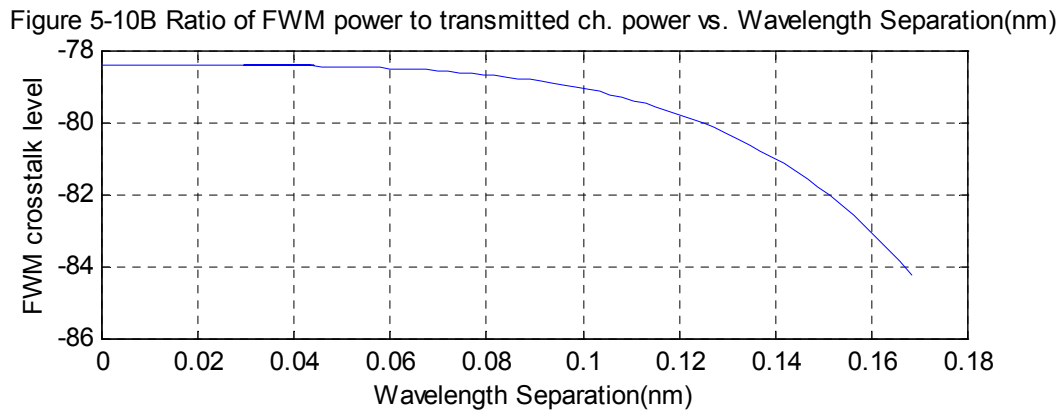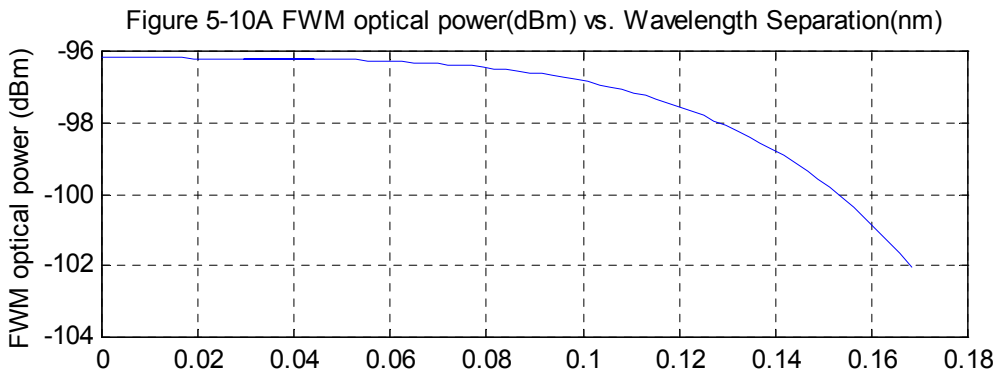
Adding all crosstalk terms (SRS, XPM & FWM) together. Figure 5-11 shows the ratio of total crosstalk (SRS+XPM+FWM) power to transmitted channel power vs. wavelength separation.  Comparing SRS and FWM crosstalk, it is evident that FWM is the major source of nonlinear crosstalk in SCM optical systems with extremely narrow spacing between RF channels.

Figure 5-11 Xtalk level vs. Wavelength Separation(nm)
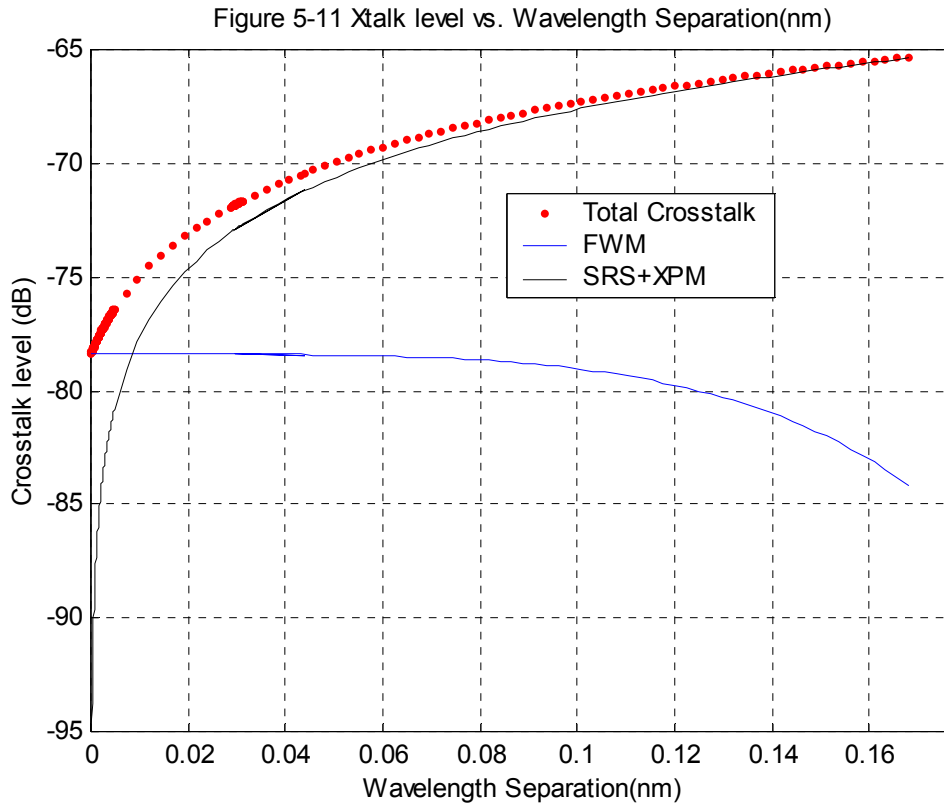
**Crosstalk level (dB) on SCM optical system over various types of fibers**

Four types of commercial available fibers are used to investigate the crosstalk level on

SCM optical system. In each case, the Raman gain coefficient is derived based on the analytical

models of [15]. The characteristic of each types of fiber is shown below.

| | Dispersion @ 1550nm | α @ 1550nm (dB/km) | Aeff (μm²) | Raman Gain (1e⁻²⁷mW⁻¹Hz⁻¹) | Length (km) | Input fiber Power per channel (dBm) |
|---|---|---|---|---|---|---|
| SMF | 17.0 ps/nm*km | 0.222 | 78 | 5.0 | 10 | -15.6dBm |
| SMF Si-Core | 19.0 ps/nm*km | 0.200 | 78 | 6.4 | 10 | -15.6dBm |
| NZDSF- | -2.3 ps/nm*km | 0.239 | 53 | 6.5 | 10 | -15.6dBm |
| NZDSF+ | 3.0 ps/nm*km | 0.205 | 53 | 6.7 | 10 | -15.6dBm |

Figure 5-12 plots the ratio of crosstalk power to transmitted channel power as a function of

channel spacing for four different types of fibers (i.e., different values of chromatic dispersion).

Among the four different types of commercial available fibers, standard single-mode fiber has

67

the best performance. This performance demonstrates that FWM crosstalk not only depends on narrow channel spacing, but also depends on fiber chromatic dispersion.



Figure 5-12 Crosstalk vs. Wavelength Separation(nm)
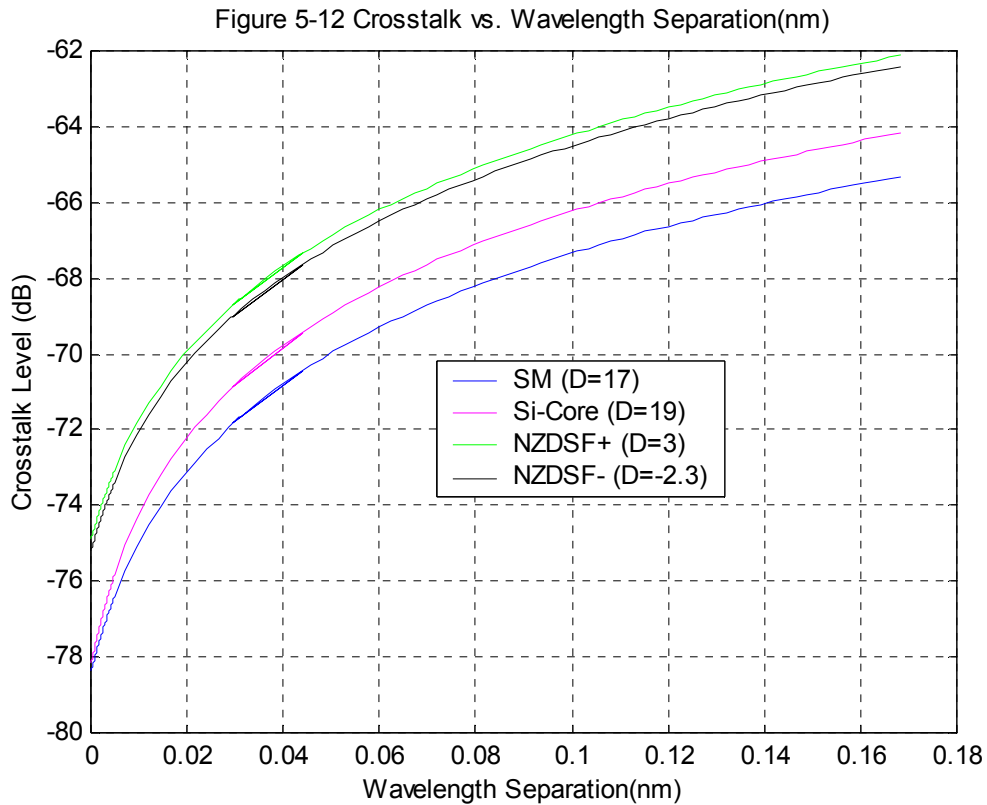
So far we have only considered the crosstalk level between two equal power subcarriers. A SCM optical system with 78 analog channels and one 1Gb/s digital channel, we add all crosstalk terms among the SCM channels to obtain total crosstalk for each individual channel. Figure 5-13 plots crosstalk for an individual CATV channel with fixed "6MHz" frequency spacing between CATV channels and "1GHz to 10GHz" frequency spacing between CATV Ch # 78 & digital Channel.

Figure 5-13 Crosstalk (dB) per CATV Channel Index
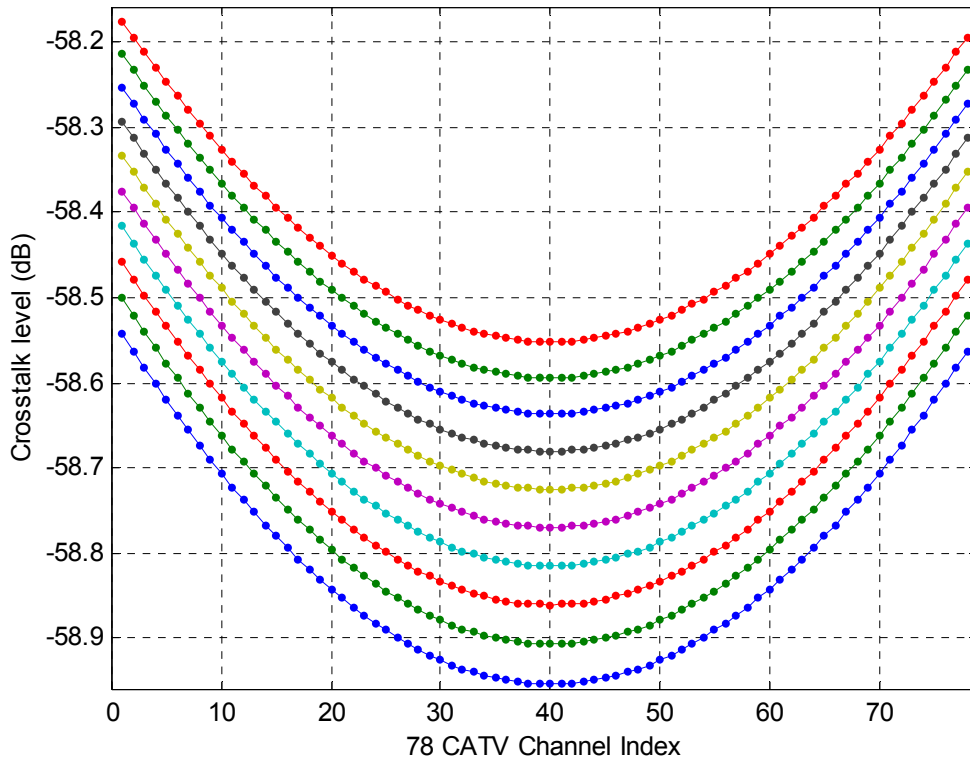


Figure 5-14 Crosstalk (dB) at Digital Channel
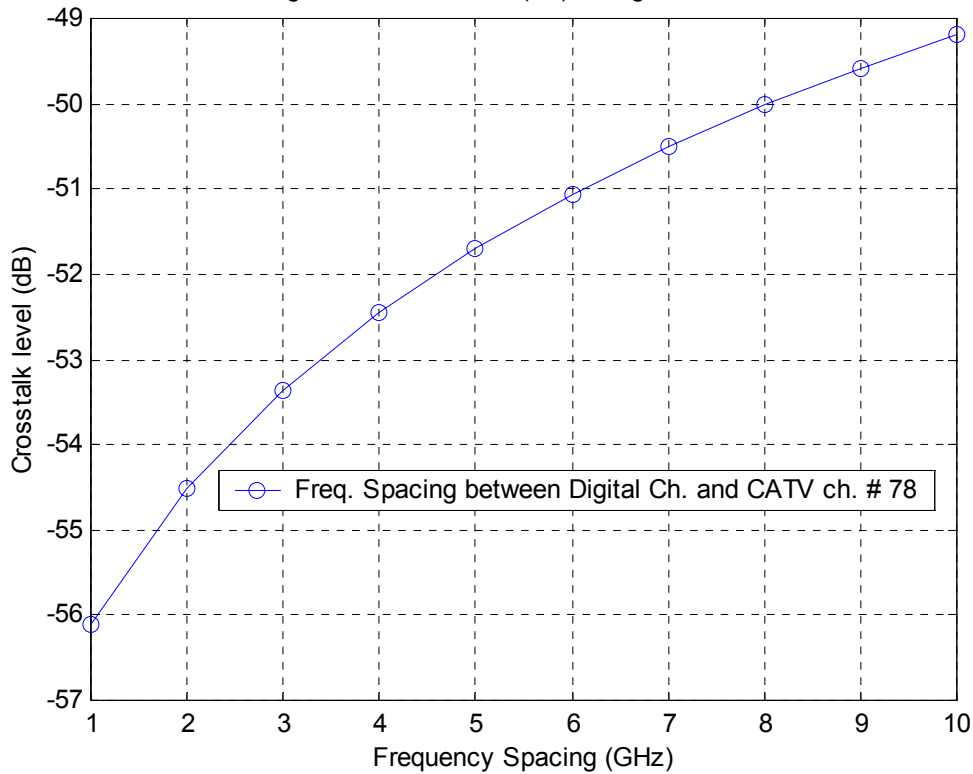
Figure 5-14 plots the crosstalk ratio (Ratio of Crosstalk power to transmitted power) at a digital channel with different frequency spacing (1GHz to 10GHz) from the CATV channel. Because SRS crosstalk becomes dominant at high frequency spacing, the crosstalk ratio at digital channel difference increases as the channel spacing increases from 1 GHz to 10GHz.

Figure 5-15 plots crosstalk ratio at CATV channel 1 vs. fiber input channel optical power. The 1GHz spacing from digital channel for CATV channel 1 crosstalk is similar to 10GHz spacing. In other words, increasing frequency spacing between CATV and digital channel has minimal impact on the change of crosstalk level for each CATV channel.

Figure 5-15 Ratio of Crosstalk power to transmitted channel power at CATV Channel 1
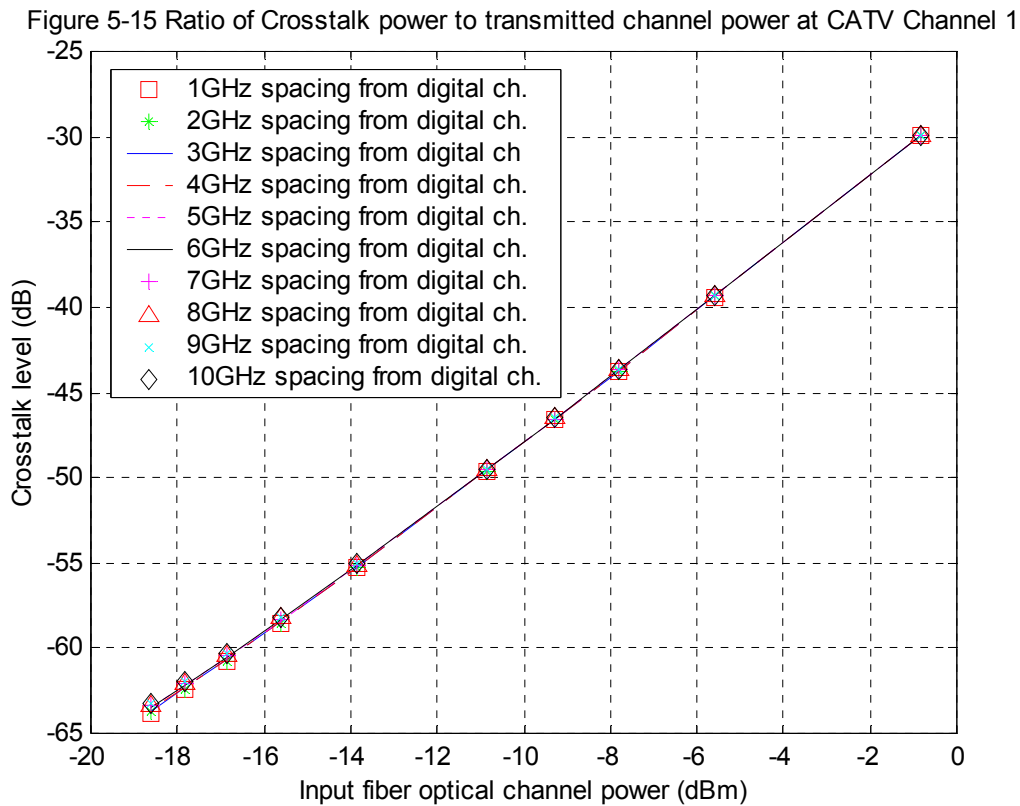


Figure 5-16 plots crosstalk ratio at Digital Channel vs. fiber input channel optical power. At high optical channel power (0dBm, for example), the FWM crosstalk becomes dominant, the overall crosstalk remains constant as frequency spacing increased.

Figure 5-16 Ratio of Crosstalk power to transmitted channel power at Digital Channel

Legend:
- 1GHz spacing from CATV
- 2GHz spacing from CATV
- 3GHz spacing from CATV
- 4GHz spacing from CATV
- 5GHz spacing from CATV
- 6Hz spacing from CATV
- 7GHz spacing from CATV
- 8GHz spacng from CATV
- 9GHz spacing from CATV
- 10GHz spacing from CATV

X-axis: Input fiber optical channel power (dBm)
Y-axis: Crosstalk level (dB)
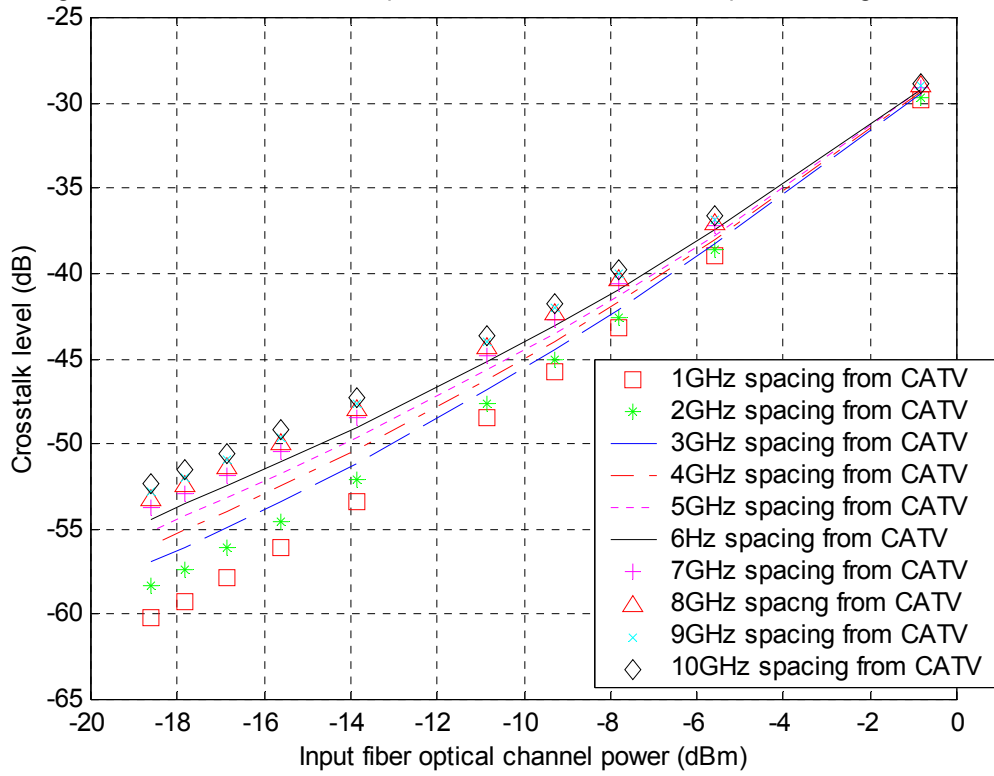
## 5.6    Impact of Signal – Crosstalk Noise on SCM optical system performance

**Signal-Crosstalk Noise Term**

Although signal-crosstalk noise term has been widely researched in the literature, the main analytical techniques can be found in [18, 19 & 20].  In a SCM optical system, if we consider a desired signal and crosstalk term injected into a photodiode, the detected photocurrent *I* at the output of a photodetector is expressed by [18]:

$$I = k\{P_s + P_x + 2\sqrt{P_sP_x}\cos(\Delta\theta)\} + n_{th} + n_{sh} \tag{5-19}$$

where $P_s$ and $P_x$ are the optical channel power of signal and crosstalk respectively, and $\Delta\theta$ is the optical phase difference between both fields.  The detectable current comprises the signal current from the first term and the crosstalk current from the second term, and an additional term due to the interaction between the two fields.  The thermal noise current and shot noise current are included in the above expression, assuming $P_s \gg P_x$, (5-19) can be rewritten as

$$I = k\{P_s + n_x\} + n_{th} + n_{sh}$$
$$n_x = 2\sqrt{P_sP_x}\cos(\Delta\theta) \tag{5-20}$$

Using Gaussian approximation, the signal-crosstalk interferometric noise variance $\sigma_x^2$ is expressed as [18, 19, 20]

$$< n_x > = 0$$
$$\sigma_x^2 = < n_x^2 > - < n_x > = 4k^2P_sP_x\cos^2(\Delta\theta) = 2k^2P_sP_x = 2I_s^2X \tag{5-21}$$

where *X* is the ratio of the crosstalk optical power to the signal optical power.

## 5.7    CATV CNR include signal-crosstalk noise term

SCM Optical transmission performance including RIN noise, Thermal noise, Shot noise, ASE noise, Clipping noise, Nonlinear Distortion as well as Signal-crosstalk noise term is analyzed in this section.  Use the best case linearized Dual parallel MZ Modulators with A=0.93 and B=2.5 and same parameter values as discussed in section 4.3., the comparison of Case I & II CATV CNR with and without signal-crosstalk noise terms versus optical channel power is plotted in figure  5-17.

| PARAMETERS | Case 1 | Case 2 |
|---|---|---|
| **Linearized MZ Modulator** | A=0.93 & B=2.5 | A=0.93 & B=2.5 |
| Input power at Booster Amplifier | -1dBm | 3dBm |
| Laser RIN | -155dB/Hz | -160dB/Hz |
| Photodiode Responsivity | 0.8 A/W | 0.9 A/W |
| Fiber distance | 10km | 10km |
| OMI | 4.343% | 4.343% |

As optical channel power increases, crosstalk noise increases and degrades system performance. The plot shows the highest CNR includes crosstalk noise term is 48.5dB using Case I model.   It indicates that as long as the receiver optical channel power is in the range of -20dBm to -17dBm, we can obtain CNR up to 48dB or higher.  Figure 5-18 plots CNR vs. number of customer premises.  It shows the SCM optical system required to connect at least 20 but no more than 40 customer units to meet 48dB CNR.  With this understanding, it is important to optimize the practical optical link budget to meet the system performance.

Figure 5-17 CNR vs. Receiver optical power per channel
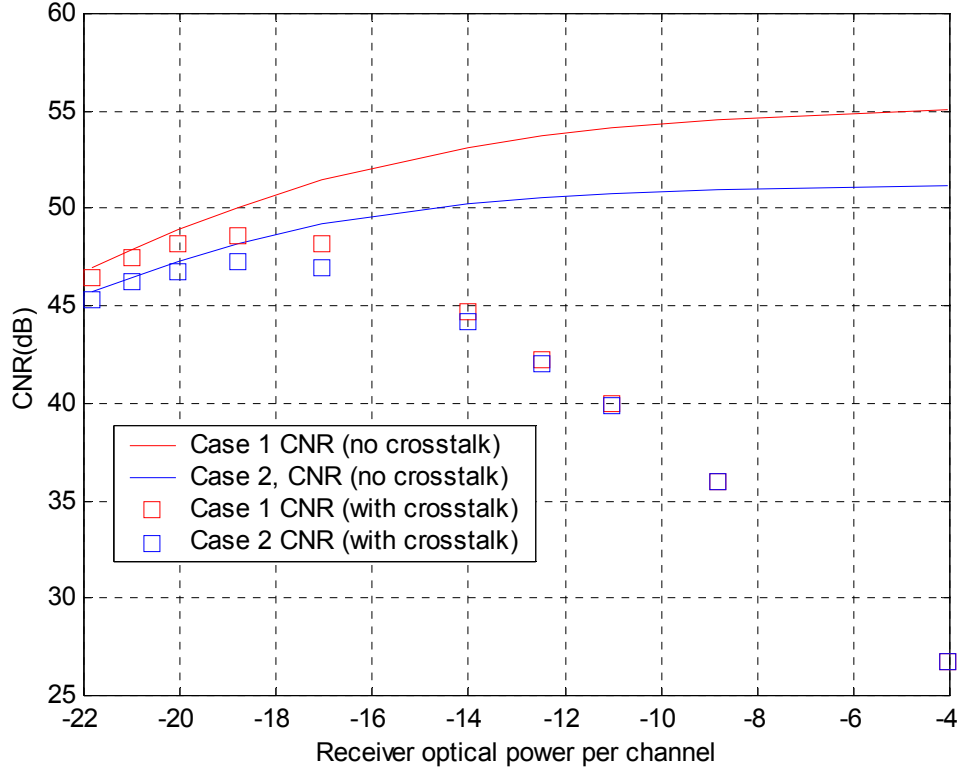


Figure 5-18 Network Scalability: CNR vs. Customer Premise
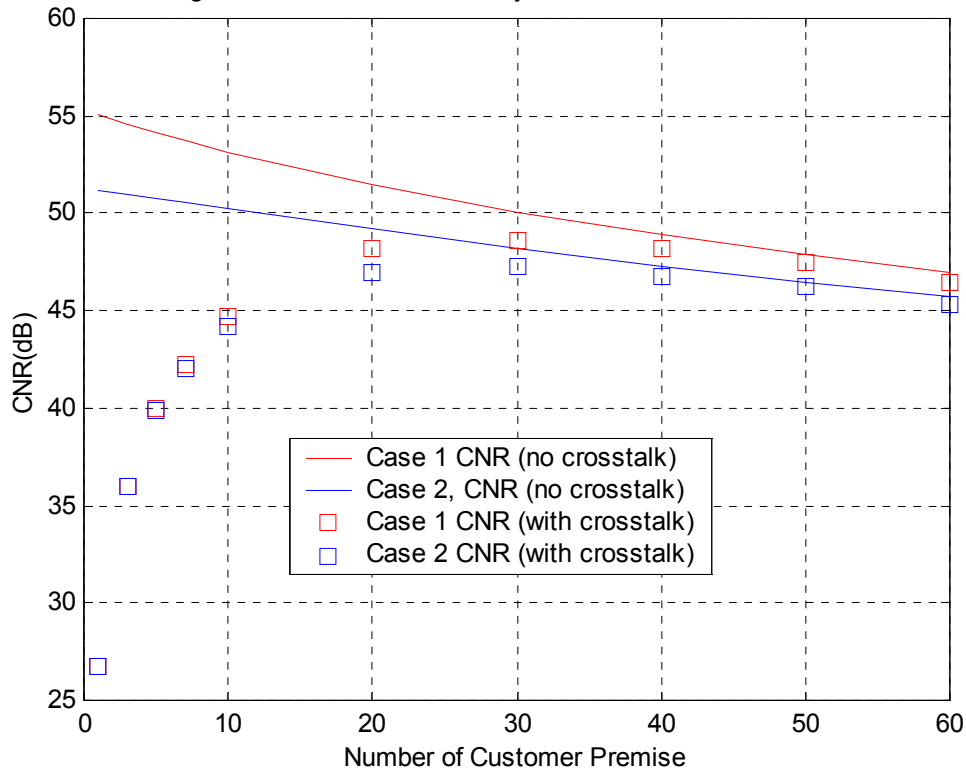
## 5.8    Digital Q-Value include signal-crosstalk noise term

The SCM optical transmission performance of 1Gb/s digital data, including RIN noise, Thermal noise, Shot noise, ASE noise, Clipping noise, Nonlinear Distortion as well as Signal-crosstalk noise term is studied in this section.  Because digital data detects only the presence or absence of a pulse rather than measure the absolute pulse shape, its signal performance requirement is more relaxed when compared to Analog CATV.  The comparison of Digital Channel Q-value with and without signal-crosstalk noise terms vs. optical channel power is plotted in figure 5-19, 5-20, 5-21 & 5-22 for BSPK, QPSK & ASK Modulation

| PARAMETERS | |
| --- | --- |
| **Linearized MZ Modulator** | A=0.93 & B=2.5 |
| Input power at Booster Amplifier | 3dBm |
| Laser RIN | -160dB/Hz |
| Photodiode Responsivity | 0.9 A/W |
| Fiber distance | 10km |
| OMI | 4.343% |



Figure 5-19 BPSK Q Value vs. optical channel power
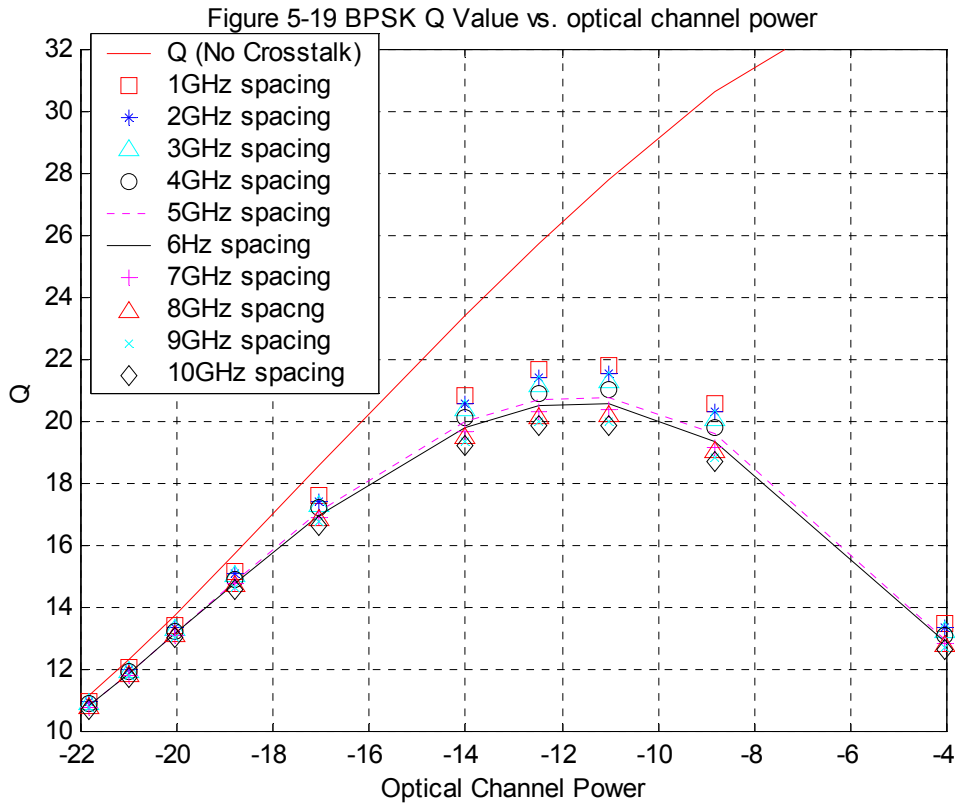
Figure 5-20 QPSK Q Value vs. optical channel power
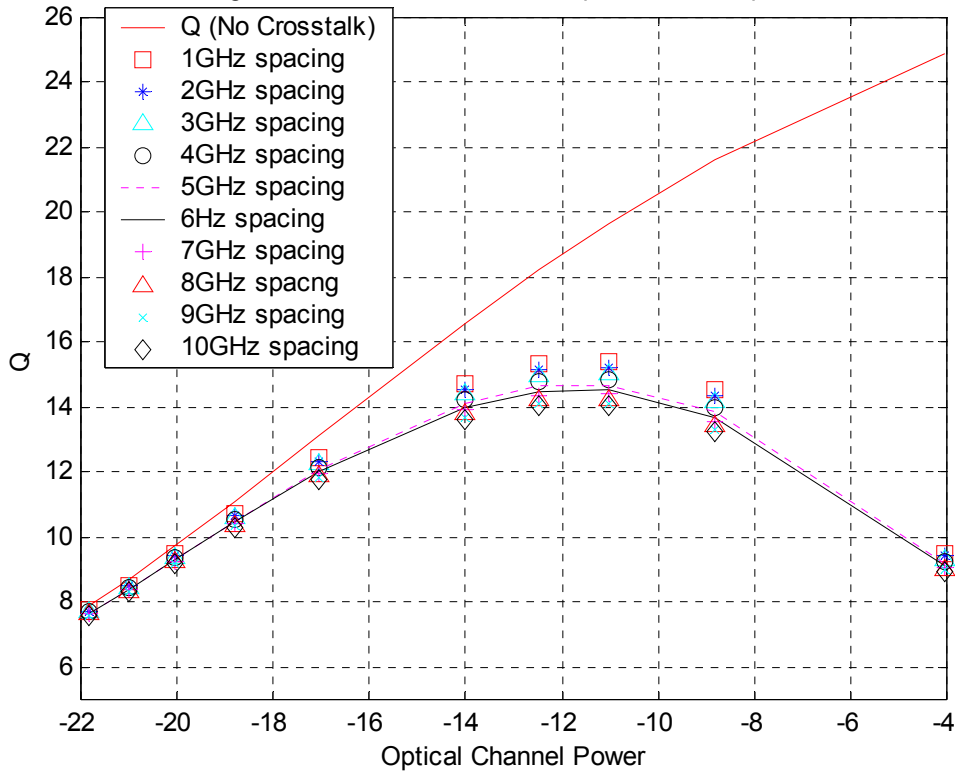


Figure 5-21 ASK Q Value vs. optical channel power
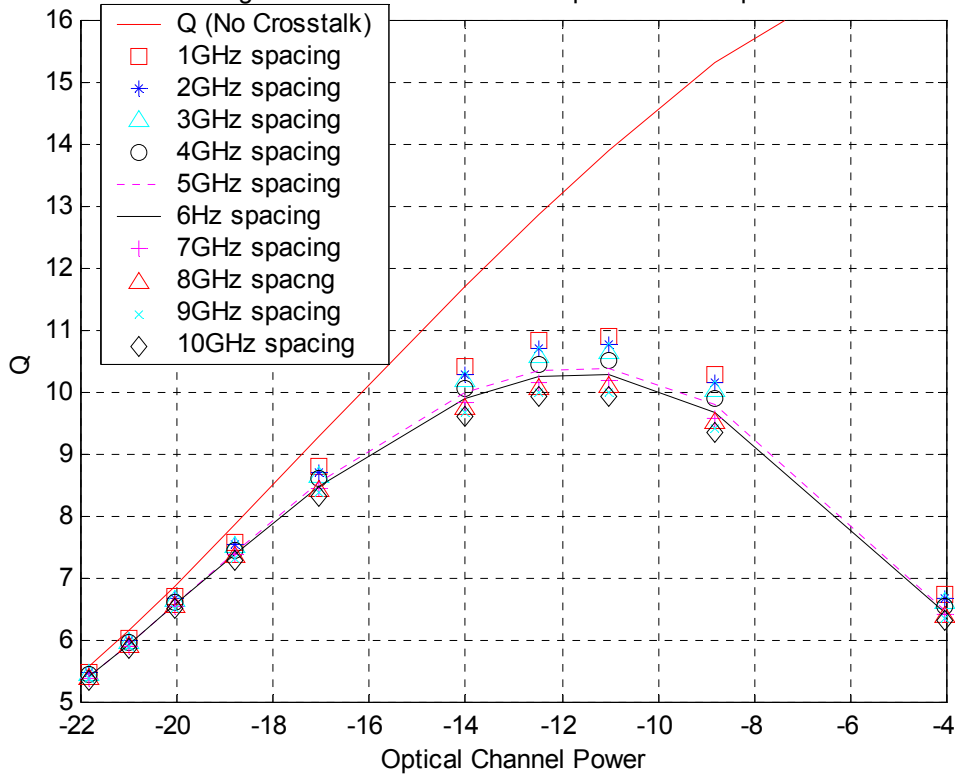
Figure 5-22 BPSK, QPSK & ASK vs. Receiver Optical power per Channel

BPSK

QPSK

ASK

Q

Receiver Optical Power per Channel
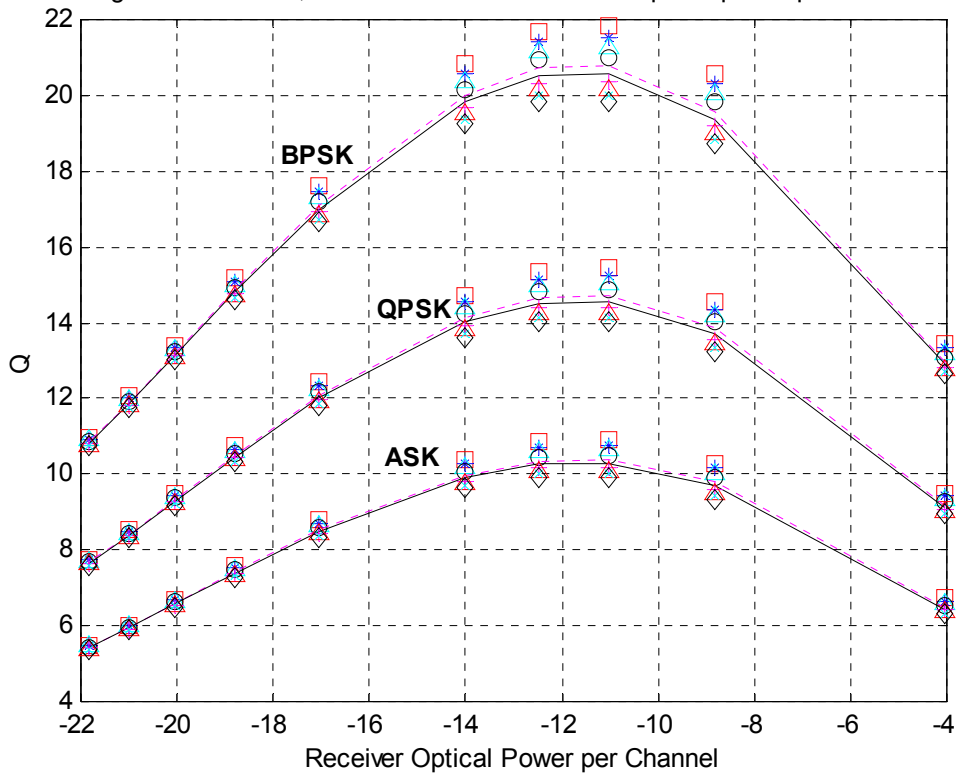


Figure 5-23 BPSK, QPSK & ASK Q Value vs. Customer Premise

BPSK

QPSK

ASK

Q
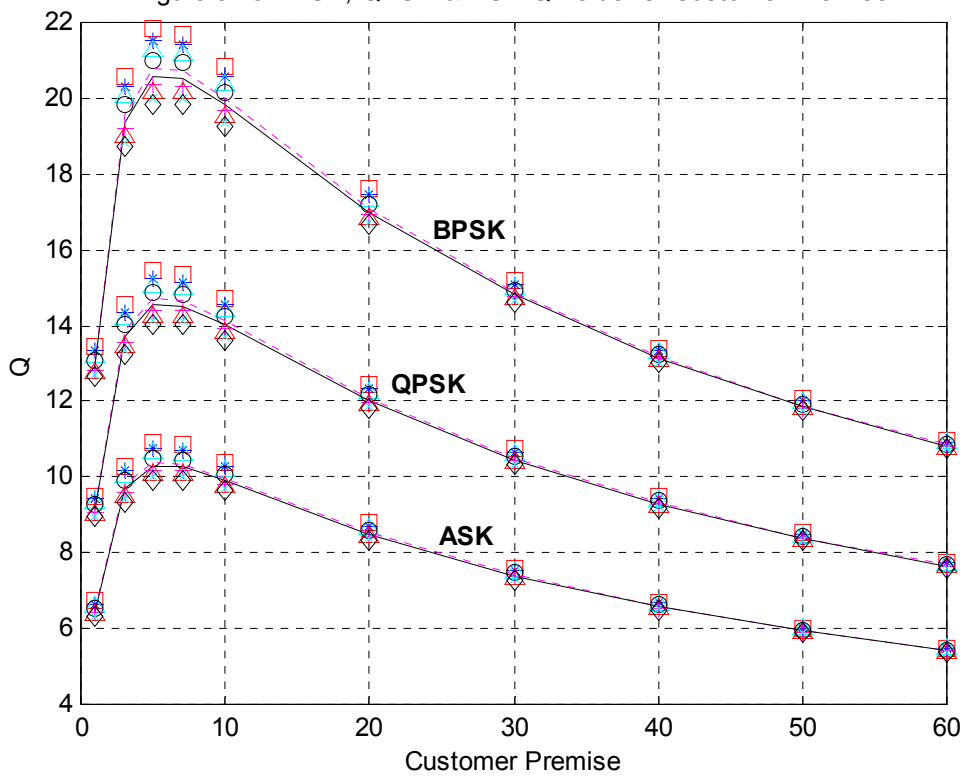
Customer Premise

Figure 5-23 plots Digital Q-value vs. number of customer premises. Based on the theoretical analysis, the transmission performance to be expected from a SCM optical system supporting 78 CATV and 1Gb/s digital data from central office to customer premises is summarized as follows:

1) The desirable receiver optical power per channel is in the range of -20dBm to -17dBm in order to achieve the maximum CNR.

2) The Optical Power (rms) contains 79 modulated RF signals at Receiver can be calculated as -10.5dBm to -7.5dBm.

3) The RF channel power at the output of photodiode is calculated as -90dBm to -84.9dBm using Responsivity =0.9 and Circuit Resistance = 50ohms.

4) CATV CNR = 48dB to 48.5dB.

5) Digital BPSK Q = 13 to 17.

6) Digital QPSK Q = 9 to 12.

7) Digital ASK Q = 6 to 8.

8) Number of Customer premises = 20 to 40.

**CHAPTER 6: Conclusion & Future Work**

**6.1     Conclusion**

This project analyzed the transmission performance of SCM Optical system transmitting 78 CATV analog and 1Gb/s digital data from CO to customer premises.  This study demonstrates that using OSSB modulation, all even-order nonlinear distortion generated by MZ modulator can be cancelled by biasing the modulator at Q point.  Also, the third order distortion generated by the MZ modulator can be suppressed using linearized dual parallel modulators.  Three scenarios were studied to optimize the CTB suppression. The best result occurs when the setting of the optical power splitting ratio is 0.93 at the primary MZ modulator and the RF power ratio is 2.5 at the secondary MZ modulator. The analytical results of this study demonstrate that the scalability of this SCM externally modulated optical network, excluding the fiber nonlinear impact, can connect as many as 30 customers. With such optical power budget, the quality of CATV can achieve 50dB CNR or higher and the third order distortion of 60dBc or higher.  In addition to CATV, the performance of downstream digital data shows good analytical results.

- BPSK modulation results in Q value equal to 15

- QPSK modulation results in Q value equal to 11

- ASK modulation results the Q value equal to 7

The results are due to the high optical power transmission in the SCM externally modulated network and because the digital signal performance requirement is a more relax compared to analog CATV.

However, we've seen in addition to noise terms such as thermal, shot, ASE, RIN, clipping, non-linear distortion generated from the system transmitter, the MZ modulator and receivers, the fiber nonlinear crosstalk plays an important role in determining the overall network

transmission performance. SRS, XPM and FWM are studied in this project. Because the sensitivity of probe channel to induced crosstalk is related on its receiver bandwidth, the crosstalk level between high and small bandwidth channels is comparable to the crosstalk between two small bandwidth channels [10]. In other words, the crosstalk level between 1Gb/s digital channel and CATV channel is comparable to the crosstalk between two CATV channels. Because of small signal bandwidth and small optical power per CATV channel, XPM demonstrates no impact on SCM system performance. On the other hand, FWM, as expected, becomes dominant crosstalk at narrow channel spacing and SRS becomes dominant at large channel spacing. This demonstrates that FWM is the main crosstalk noise term in SCM network.

Adding signal-crosstalk noise term and re-evaluating the crosstalk impact on the overall CATV and Digital data transmission performance, it is interesting to notice that as optical channel power increases, crosstalk noise power increases and seriously degrades the transmission performance. As a result, in order to optimize the maximum CATV transmission performance, the desirable receiver optical power per baseband channel is in the range of -20dBm to -17dBm.

This study concludes that by optimizing the receiver optical power, the downstream transmission quality of CATV and digital data, as well as the scalability of this SCM network, can be summarized as follows:

**A. Transmission Quality**

1) CATV CNR in the range of 48dB to 48.5dB.

2) Digital BPSK Q = 13 to 17

3) Digital QPSK Q = 9 to 12

4) Digital ASK Q = 6 to 8

### B. Network Scalability

1) Number of Customers premises = 20 to 40

and because of star network configuration, there is only 3dB optical power splitter loss difference between 20 and 40 customers. With this understanding, it is important to optimize and careful engineer the optical power link budget during practical implementation.

## 6.2     Future Work

This project analyzed the downlink transmission performance of SCM optical network transmitting 78 CATV and 1 digital channel at the lower sideband of optical carrier using OSSB modulation technique. Also, it presented the idea of transmitting an optical subcarrier at the upper sideband of optical carrier and delivering it to the end-user. Under this scenario, the optical subcarrier is used as optical source for uplink transmission to eliminate laser source.

The future study is suggest as listed below:

- Analyze the uplink transmission performance and the impact of optical crosstalk under bi-directional fiber transmission;

- Analyze uplink multiple access method such as Time Division Multiple Access (TDMA), Subcarrier Multiple Access (SCMA) and their efficiencies;

- Because Narrow-band optical filter is relative expensive compared to wide-band optical filter, further study in separate upper and lower side-band of optical carrier at end-users is suggested.

- The even-order distortion produced by a conventional modulator can be cancelled using OSSB modulation. CSO is also affected by various phenomena such as chirp, fiber chromatic dispersion and polarization-mod dispersion (PMD), self-phase modulation (SPM) as well as gain-tilt of optical amplifiers. Future study in CSO is suggested.

**REFERENCE**

[1]     R. Hui, B. Zhu, R. Huang, C. Allen, K. Demarest, D. Richards, "Subcarrier Multiplexing for High-speed Optical Transmission," *Journal of Lightwave Technology, vol. 20, no. 3, March 2002*

[2]     R. Olshansky, "Optimal Design of Subcarrier Multiplexed lightwave systems employing linearized external modulators," *Journal of Lightwave Technology, vol. 10, no.3 March, 1992*

[3]     G Keiser, *Optical fiber Communication*, Boston, 2000

[4]     W. Way, *Broadband Hybrid Fiber/Coax Access System Technologies*, San Diego, CA: Academic, 1999

[5]     G. Smith, D. Novak, Z. Ahmed, "Overcoming Chromatic-Dispersion Effects in Fiber-Wireless Systems Incorporating External Modulators," *IEEE Transactions on Microwave Theory and Techniques, vol. 45, no. 8, August 1997.*

[6]     J. Brooks, G. Maurer, R. Becker, "Implementation and Evaluation of a Dual Parallel Linearization System for AM-SCM Video Transmission," *Journal of Lightwave Technology, vol. 11, no. 1, January 1993.*

[7]     FCC Standard and Regulations: Section 76.605 "Multichannel Video and Cable Television Service"

[8]     J. Chiddix, H. Laor, D. Pangrac, L. Williamson & R. Wolfe, "AM Video on Fiber in CATV systems: Need and Implementation", *IEEE Journal on Selected Areas in Communications, vol. 8, no. 7, September 1990*

[9]     S. Bigo, S. Gauchard, A. Bertaina, & J. Hamaide, "Experimental Investigation of Stimulated Raman Scattering Limitation on WDM Transmission Over Various Types of Fiber Infrastructures," *IEEE Photonics Technology Letters, vol. 11, no. 6 June 1999.*

[10]    M Phillips & D. Ott, "Crosstalk Due to Optical Fiber Nonlinearities in WDM CATV Lightwave Systems," *Journal of Lightwave Technology, vol 17, no. 10, Oct. 1999.*

[11]    R. Hui, Y. Wang, K. Demarest, C. Allen, "Frequency Response of Cross-Phase Modulation in Multispan WDM Optical Fiber Systems," *IEEE Photonics Technology letters, vol 10, no. 9, September, 1998*

[12]    R. Hui, K. Demarest, C. Allen, "Cross-Phase Modulation in Multispan WDM Optical Fiber system," *Journal of Lightwave Technology, vol 17, no. 3, June 1999*

[13]    N. Shibata, R. Braun, R. Waarts, "Phase Mismatch Dependence of Efficiency of Wave Generation Through Four-Wave Mixing in a Single-Mode Optical Fiber," *IEEE Journal of Quantum Electronics, vol QE-23, no. 7, July 1987*

[14]    R. Tkach, A. Chraplyvy, F. Forghieri, A. Gnauck, R. Derosier, "Four-Photon Mixing and High-Speed WDM Systems," *Journal of Lightwave Technology, vol 13, no.5  May 1995.*

[15]    M. Zirngibl, "Analytical model of Raman gain effects in massive wavelength division multiplexed transmission systems, "Electron *Letter, vol. 34, no. 8, pp. 789-790, 1998.*

[16]    P. N. Butcher & D. Cotter, *The Elements of Nonlinear Optics*, Cambridge University Press, 1990

[17]    P. Gunter, *Nonlinear Optical Effects and Materials*, New York, Springer-Verlag Press, 2000.

[18]    K. Inoue, K. Nakanishi, K. Oda and H. Toba, "Crosstalk and Power Penalty due to fiber four-wave mixing in multichannel transmissions", *Journal of Lightwave Technology, vol. 12, no.8, August 1994*

[19]    P. J. Legg, M. Tur, and I. Andonvic, "Solution paths to limit interferometric noise induced performance degradation in ASK/direct detection lightwave network", *Journal of Lightwave Technology, vol. 14, pp.1943-54, 1996.*

[20]    E. L. Goldstein, L. Eskildsen, and A. F. Elrefaie, "Performance implications of component crosstalk in transparent lightwave networks", *IEEE Photonics Technology Letters, vol.6, pp. 657-60, 1004*

**Appendix 1**

**Derivation of Output MZ Modulator for composite signal**

In this Appendix, as shown in figure, the output of MZ Modulator for composite signal will be derivate. We start with the expression

78 RF Modulated Video streams: $\qquad s_i(t) = \sum\limits_{i=1}^{78} Ac_i \cdot \cos(\omega_{ci} - \omega_{mi})t$

Downstream digital data: $\qquad s_d(t) = x(t) \cdot \cos(\omega_d t)$

10GHz RF subcarrier $\qquad s_u(t) = \cos(\omega_u t)$

$$E_0 = \frac{E_i}{2}\left\{ \cos(\omega_c t + \frac{\pi}{2} + \frac{\pi}{V_\pi}\left( \sum_{i=1}^{78}\cos(\omega_i - \omega_{mi})t + x(t)\cdot\cos(\omega_d t) + \cos(\omega_u t)\right)\right\}$$

$$+ \frac{E_i}{2}\left\{ \cos(\omega_c t + \frac{\pi}{V_\pi}\left( \sum_{i=1}^{78}\cos[(\omega_i - \omega_{mi})t + \frac{\pi}{2}] + x(t)\cdot\cos(\omega_d t + \frac{\pi}{2}) + \cos(\omega_u t - \frac{\pi}{2})\right)\right\}$$

$$= \frac{E_i}{2}\left\{ \cos(\omega_c t + \frac{\pi}{V_\pi}\left( \sum_{i=1}^{78}\cos[(\omega_i - \omega_{mi})t + \frac{\pi}{2}] + x(t)\cdot\cos(\omega_d t + \frac{\pi}{2}) + \cos(\omega_u t - \frac{\pi}{2})\right)\right\}$$

$$- \frac{E_i}{2}\left\{ \sin(\omega_c t + \frac{\pi}{V_\pi}\left( \sum_{i=1}^{78}\cos(\omega_i - \omega_{mi})t + x(t)\cdot\cos(\omega_d t) + \cos(\omega_u t)\right)\right\}$$

Using Bessel function expansions

$$\sin\left[ \frac{\pi}{V_\pi}\left( \sum[S_i(t) + S_d(t) + S_u(t)]\right)\right] = \sin\left[ \frac{\pi}{V_\pi}\left( \sum_{i=1}^{78}\cos(\omega_i - \omega_{mi})t + x(t)\cdot\cos(\omega_d t) + \cos(\omega_u t + \frac{\pi}{2})\right)\right]$$

$$= \left\{ \sum_{n_1=-\infty}^{\infty}\sum_{n_2=-\infty}^{\infty}\cdots\sum_{n_{78}=-\infty}^{\infty}\sum_{n_d=-\infty}^{\infty}\sum_{n_u=-\infty}^{\infty} J_{n1}(\frac{\pi A}{V_\pi})J_{n2}(\frac{\pi A}{V_\pi})\ldots J_{n78}(\frac{\pi A}{V_\pi})\cdot J_{nd}(\frac{\pi A}{V_\pi})\cdot J_{nu}(\frac{\pi A}{V_\pi})\cdot \right.$$

$$\left. \cos[n_1(\omega_1 - \omega_{m1})t + n_2(\omega_2 - \omega_{m2})t\ldots + n_{78}(\omega_{78} - \omega_{78})t + n_d(x(t)\cdot(\omega_d t) + n_u(\omega_u t)] \right\}$$

$$= 2J_1(\frac{\pi V}{V_\pi})J_0(\frac{\pi V}{V_\pi})^{N-1}\cdot\left\{ [\sum_{i=1}^{78}\cos(\omega_i - \omega_{mi})t] + [x(t)\cos(\omega_d t)] + \cos(\omega_u t)\right\}$$

Assuming modulation index/channel is very small and by making the approximations

$$J_0(m) \approx 1$$

The output of Modulator can be rewrite as

$$E_0 = \frac{E_i}{2}\left\{\cos(\omega_c t)\cdot J_0(\frac{\pi A}{V_\pi}) - \sin(\omega_c t)\cdot 2J_1(\frac{\pi A}{V_\pi})\left(\sum_{i=1}^{78}\cos[(\omega_i - \omega_{m\,i})t + \frac{\pi}{2}] + [x(t)\cdot\cos(\omega_d t + \frac{\pi}{2}) + \cos(\omega_u t - \frac{\pi}{2}))\right)\right\}$$

$$- \frac{E_i}{2}\left\{\sin(\omega_c t)\cdot J_0(\frac{\pi A}{V_\pi}) + \cos(\omega_c t)\cdot 2J_1(\frac{\pi A}{V_\pi})\left(\sum_{i=1}^{78}\cos[(\omega_i - \omega_{m\,i})t] + x(t)\cdot\cos(\omega_d t) + \cos(\omega_u t)\right)\right\}$$

$$E_0 = \frac{E_i}{2}\left\{J_0(\frac{\pi A}{V_\pi})[\cos(\omega_c t) - \sin(\omega_c t)]\right\}$$

$$- E_i\left\{J_1(\frac{\pi A}{V_\pi})[\sin(\omega_c t)\cdot\sum_{i=1}^{78}\sin(\omega_i - \omega_{m\,i})t] + J_1(\frac{\pi A}{V_\pi})[\cos(\omega_c t)\cdot\sum_{i=1}^{78}\cos(\omega_i - \omega_{m\,i})t]\right\}$$

$$- E_i\left\{J_1(\frac{\pi A}{V_\pi})[\sin(\omega_c t)\cdot x(t)\cdot\sin(\omega_d t)] + J_1(\frac{\pi A}{V_\pi})[\cos(\omega_c t)\cdot x(t)\cdot\cos(\omega_d t)]\right\}$$

$$- E_i\left\{J_1(\frac{\pi A}{V_\pi})[-\sin(\omega_c t)\cdot\sin(\omega_u t)] + J_1(\frac{\pi A}{V_\pi})[\cos(\omega_c t)\cdot\cos(\omega_u t)]\right\}$$

$$E_0 = \frac{E_i}{2}\left\{J_0(\frac{\pi A}{V_\pi})[\cos(\omega_c t) - \sin(\omega_c t)]\right\}$$

$$- E_i\left\{J_1(\frac{\pi A}{V_\pi})\cos(\omega_c + \sum_{i=1}^{78}(\omega_i - \omega_m))t\right\}$$

$$- E_i\left\{J_1(\frac{\pi A}{V_\pi})x(t)\cos(\omega_c + \omega_d)t\right\}$$

$$- E_i\left\{J_1(\frac{\pi A}{V_\pi})\cos(\omega_c - \omega_u)t\right\}$$

Appendix 2

**Derivation of Composite Second Order (CSO) and Composite Triple Beat (CTB)**

In this Appendix, the expression of CSO and CTB will be derivate. We start with the static transfer characteristic of an MZ modulator given by

$$P_{out} = \frac{P_{in}L_a}{2}\left(1+\cos\left[\frac{V(t)}{V_\pi}\pi-\theta_b\right]\right) \tag{A2-1}$$

where Pout is the output power of the MZ modulator, Pin is the input power of the MZ modulator, La is the insertion loss due to the MZ modulator, V(t) is the modulating voltage, $V_\pi$ is the half wave voltage of the MZ modulator (the voltage required to achieve 180 degree optical phase shift), and $\theta_b$ is the static bias phase shift between the two arms of MZ modulator.

Assume that the modulating voltage V(t) is composed of multiple modulating RF signals and a DC bias voltage Vb:

$$V(t) = \sum_{i=1}^{N} A\sin(\omega_i t + \phi_i)+V_b \tag{A2-2}$$

where A is the amplitude and ωi is the angular frequency of the i-th channel. We first let the $\theta_b = 0$, and substituting Eq. (A2-1) into Eq. (A2-2), the AC output of the MZ modulator is:

$$
\begin{aligned}
P_{out} &= \frac{P_{in}L_a}{2}\cdot\cos[\frac{\pi}{V_\pi}V(t)] \\
&= \frac{P_{in}L_a}{2}\cdot\cos\left[\frac{\pi}{V_\pi}\left(\sum_{i=1}^{N}A\sin(\omega_i t+\phi_i)+V_b\right)\right] \\
&= \frac{P_{in}L_a}{2}\cdot\cos\left[\frac{\pi}{V\pi}\left(\sum_{i=1}^{N}A\sin(\omega_i t+\phi_i)\right)+\left(\frac{\pi V_b}{V_\pi}\right)\right]
\end{aligned}
\tag{A2-3}
$$

We first let the $\theta_b = 0$ and using Bessel function expansions to derivate the amplitude of second and third order intermodulation.

Bessel function expansions

$$\cos\left[\frac{\pi}{V_\pi}\left(\sum_{i=1}^{N} A\sin(\omega_i t + \phi_i)\right)\right]$$

$$= \left\{\sum_{n_i=-\infty}^{\infty}\sum_{n_2=-\infty}^{\infty}...\sum_{n_N} J_{n_2}(\frac{\pi A}{V_\pi})\cdot J_{n_2}(\frac{\pi A}{V_\pi})...J_{n_N}(\frac{\pi A}{V_\pi})\cos[n_1(\omega_1+\phi_1)+...n_N(\omega_N+\varphi_N)]\right\}$$

$$\sin\left[\frac{\pi}{V_\pi}\left(\sum_{i=1}^{N} A\sin(\omega_i t + \phi_i)\right)\right]$$

$$= \left\{\sum_{n_i=-\infty}^{\infty}\sum_{n_2=-\infty}^{\infty}...\sum_{n_N} J_{n_2}(\frac{\pi A}{V_\pi})\cdot J_{n_2}(\frac{\pi A}{V_\pi})...J_{n_N}(\frac{\pi A}{V_\pi})\sin[n_1(\omega_1+\phi_1)+...n_N(\omega_N+\varphi_N)]\right\}$$

The first Bessel expression occurs only at n = 0, 2, 4 and the second Bessel expression occurs only at n = 1, 3, 5.

The specific k-th channel can be found by setting the index $n_k$=1 and the remaining indices to zero. For example, the amplitude of output carrier at k-th channel is

$$P_k = \frac{P_{in}L_a}{2}\cdot\left\{\left|2J_1(\frac{\pi A}{V_\pi})[J_0(\frac{\pi A}{V_\pi})]^{N-1}\sin[\omega_k+\phi_k]\right|\right\}\sin[\frac{\pi}{V_\pi}V_{dc}]$$

$$P_k = \frac{P_{in}L_a}{2}\cdot\left\{\left|2J_1(\frac{\pi A}{V_\pi})[J_0(\frac{\pi A}{V_\pi})]^{N-1}\right|\right\}\sin[\frac{\pi}{V_\pi}V_{dc}]$$

The amplitude of the output carrier with frequency $\omega_i$, where $i = 1:N$ is

$$P_{out} = \frac{P_{in}L_a}{2}\cdot\left\{\left|2J_1(\frac{\pi A}{V_\pi})[J_0(\frac{\pi A}{V_\pi})]^{N-1}\sum_{i=1}^{N}\sin[\omega_i t+\phi_i]\right|\right\}\sin[\frac{\pi}{V_\pi}V_{dc}]]$$

The amplitude of an output second order intermodulation can be expressed by setting the index $n_i$=$n_j$=1, and the remain indices to zero.

$$P_{out} = \frac{P_{in}L_a}{2}\cdot\left\{\left|2[J_1(\frac{\pi A}{V_\pi})]^2[J_0(\frac{\pi A}{V_\pi})]^{N-2}\sum_{i=1}^{N}\sum_{j=1}^{N}\cos[(\omega_i+\omega_j)t+\phi_i+\phi_j]\right|\right\}\cos[\frac{\pi}{V_\pi}V_{dc}]$$

The amplitude of an output third order intermodulation can be expressed by setting the index $n_i$=$n_j$=$n_k$=1, and the remain indices to zero.

$$P_{out} = \frac{P_{in}L_a}{2} \cdot \left\{ \left\| 2[J_1(\frac{\pi A}{V_\pi})]^3 [J_0(\frac{\pi A}{V_\pi})]^{N-3} \sum_{i=1}^{N} \sum_{j=1}^{N} \sum_{k=1}^{N} \sin[(\omega_i + \omega_j + \omega_k)t + \phi_i + \phi_j + \phi_k] \right\| \sin[\frac{\pi}{V_\pi}V_{dc}]] \right.$$

Therefore, the power ratio of CSO to carrier is given by

$$\frac{CSO}{C} = \left\{ \frac{2[J_1(\frac{\pi A}{V_\pi})]^2 [J_0(\frac{\pi A}{V_\pi})]^{N-2}}{2J_1(\frac{\pi A}{V_\pi})[J_0(\frac{\pi A}{V_\pi})]^{N-1}} \right\}^2 N_{CSO} \cdot \left\{ \frac{\cos(\frac{\pi}{V_\pi}V_{dc})}{\sin(\frac{\pi}{V_\pi}V_{dc})} \right\}^2$$

where Ncso is the product-count of CSO. The power ratio of CTB to carrier is given by

$$\frac{CTB}{C} = \left\{ \frac{2[J_1(\frac{\pi A}{V_\pi})]^3 [J_0(\frac{\pi A}{V_\pi})]^{N-3}}{2J_1(\frac{\pi A}{V_\pi})[J_0(\frac{\pi A}{V_\pi})]^{N-1}} \right\}^2 N_{CTB} \cdot \left\{ \frac{\sin(\frac{\pi}{V_\pi}V_{dc})}{\sin(\frac{\pi}{V_\pi}V_{dc})} \right\}^2$$

where $N_{CTB}$ is the product-count of CTB.

It is clearly show that when the applied dc Voltage, $V_{dc}$, is set to $mV_\pi$, $(m = \pm\frac{1}{2}, \pm\frac{3}{2}, ...)$, the

CSO distortion null out. In other word, by setting the applied dc Voltage set to $\frac{V_\pi}{2}$, the

modulator is biased at quadrature point, which cancel even-order distortion, and the bias phase

shift between the two arms of modulator is $\frac{\pi}{2}$.

# Appendix 3

## Relations between $n_0$ and $\chi^3$

The polarization P induced in a medium when electric field E is applied may be expanded as a power series in the electric field vector:

$$P = \varepsilon_0 [\chi^1 E + \chi^2 EE + k\chi^3 |E|^2 ]E = \varepsilon_0 [\chi^1 + k\chi^3 |E|^2 E , \tag{A3-1}$$

where $\chi 1$ is the linear susceptibility, $\chi 2$ and $\chi 3$ are second and third order susceptibility.

For materials that have a symmetrical molecular structure such as $SiO_2$ (fiber), all even powers in the susceptibility expansion are zero [16, 17].

*K* is the numerical factor associated with third-order susceptibility, for the case of general four-wave-mixing, where $\omega_\sigma$, $\omega_1\ldots,\omega_n$ are non-zero and $\omega_1,\omega_2\ldots\omega_n$ are all different. it can be defined formally as [16, 17] $K(-\omega_\sigma;\omega_{1,}\omega_2,\ldots\omega_n) = 2^{1-n} n!,$ (A3-2)

*n* = order of nonlinearity

In the case of third order nonlinearity, $K(-\omega_\sigma;\omega_{1,}\omega_2,.\omega_3) = 2^{1-3} * 3 * 2 = \dfrac{3}{2}$ and polarization becomes

$$P = \varepsilon_0 [\chi^1 + \frac{3}{2}\chi^3 |E|^2 E \tag{A3-3}$$

Using inhomogeneous wave equation: $\dfrac{\partial^2 E}{\partial z^2} - \dfrac{1}{c^2}\dfrac{\partial^2 E}{\partial t^2} = \mu_0 \dfrac{\partial^2 P}{\partial t^2}$

Substituting the polarization into the wave equation

$$\frac{\partial^2 E}{\partial z^2} - \frac{1}{c^2}\frac{\partial^2 E}{\partial t^2} = \mu_0\varepsilon_0 \frac{\partial^2 E}{\partial t^2}\left[ \chi^1 + \frac{3}{2}\chi^3 |E|^2 \right]$$

$$\frac{\partial^2 E}{\partial z^2} = \frac{\left[ 1 + \chi^1 + \dfrac{3}{2}\chi^3 |E|^2 \right]}{c^2} \frac{\partial^2 E}{\partial t^2} \tag{A3-4}$$

So the refractive index is: $n = \sqrt{1 + \chi^1 + \frac{3}{2}\chi^3 |E|^2}$, which contains linear and nonlinear

polarizations. The usual refractive index is $n_0 = \sqrt{1 + \chi^1}$

So:
$$n = \sqrt{n_0^2 + \frac{3}{2}\chi^3 |E|^2} = n_0 \sqrt{1 + \frac{3}{2n_0^2}\chi^3 |E|^2} \qquad \text{(A3-5)}$$

Assume that the nonlinear term $<< n_0$:

$$n \approx n_0 \left[ 1 + \frac{3}{4n_0^2}\chi^3 |E|^2 \right] \approx n_0 + \frac{3}{4n_0}\chi^3 |E|^2 \approx n_0 + \frac{3\chi^3}{4n_0} I \qquad \text{(A3-6)}$$

Therefore the nonlinear refractive index $n_2$ [m$^2$/V$^2$] $= \frac{3}{4n_0}\chi^3{}_{[esu]}$

The relationship between esu and SI unit can be expressed as following [16, 17]

Convert the unit of $n_2$ [m$^2$/V$^2$] to $n_2$ [esu],

$$n_2[esu] = 4\pi \cdot n_2[m^2 / V^2] = \frac{3\pi}{n_0}\chi^3{}_{[esu]} \qquad \text{(A3-7)}$$

$$n_2[m^2 / W] = \frac{80\pi}{cn_0}n_2[esu] = \frac{240\pi^2}{cn_0^2}\chi^3{}_{[esu]} \qquad \text{(A3-8)}$$

# Appendix 4  Matlab Program

```matlab
clear all;
close all;
index=0;
index1=0;
index2=0;
index3=0;
index4=0;
%CTB Product Counts
channel=[2:79]
for N=78;
    for r=channel;
        index1=index1+1;
        D(index1)=((r./2)*(N-r+1))+((1/4)*((N-3)^2-5-(0.5.*(1-(-1)^N))*(-
1)^(N+r)));
    end
end

%CATV IF carrier
run c:\eecs891\ber_cnr_pwr\channel_freq.m;

d=6;
%CSO (fa-fb) Product Counts
channel1=[2:79]
for N=78;
    for r=channel1;
        index2=index2+1;
    D1(index2)=(N-1)*(1-((ch_freq(r-1)-d)./(ch_freq(78)-ch_freq(1))));
    end
end
%CSO (fa+fb) Product Counts

channel2=[2:79]
for N=78;
    for r=channel2;
        index3=index3+1;
    D2(index3)=(N-1)*((ch_freq(r-1)-2*ch_freq(1)+d)./(2*(ch_freq(78)-
ch_freq(1))));
    end
end
figure(1)
plot(D);grid;hold;
[Nctb,ch]=max(D);
plot(ch,Nctb,'*r');
title('Figure 2-3 Third order product count vs. Channel Number)')
xlabel('Channel Number')
ylabel('Number of Terms')

figure(2)
plot(D1,'.-r');grid;hold;
plot(D2,'o-b');
title('Figure 2-2 Second order product count vs. Channel Number)')
```

91

```matlab
xlabel('Channel Number')
ylabel('Number of Terms')
axis([0,80,0,70])
h = legend('fa-fb','fa+fb',2);

for omi=0.05;
    for t=[-1.5:0.001:1.5];
        index4=index4+1;
        CONV_IMD(index4)=128./(3*omi^4*N^2);
        CONV_IMD2(index4)=(1/69)*(2/omi)^2*(tan(pi*t))^2;
    end
end
voltage=[-1.5:0.001:1.5];
figure(3)
plot(voltage,-10*log10(CONV_IMD2),'r');grid;hold;
plot(voltage,-10*log10(CONV_IMD),'b');
title('Figure 2-4 CTB/C, CSO/C vs. Applied DC bias voltage with OMI=5%)')
xlabel('Applied Bias DC Voltage normalized to Vpi')
ylabel('CTB/C, CSO/C (-dBc)')
h = legend('CSO/C','CTB/C',2);
axis([-1,1,-90,30])

%Program 2: CNR analysis with Conventional MZ Modulator
%Plot Figure 2-5, 4-3, 4-4
%%Figure 4-3 Parameter: RIN=-155, R=0.8, P=-1dBm

clear all;
close all;
load c:\eecs891\BER_CNR_pwr\data.mat;
q=1.60218e-19;
B=4e6;                              %CATV Channel bandwidth
N=78;                              %Assume 80 CATV Channel
rin=10^(-160/10);                  %RIN = -155, -160
length = 10;                       %fiber distance
delta = 0.22;                      %fiber loss
R = 0.9;                           %Responsivitiy = 0.8, 0.9
irx = 1e-12;
Kb=1.38e-23;
T=300;
Resistance=1000;
Ft=10^(5/10);
h=6.625e-34;
freq=3e8/1550e-9;
nsp=10^((5-3)/10);
I=current';
index=0;
index1=0;
index2=0;
index3=0;
index4=0;
index5=0;

mod1=[0.01:0.0001:0.03];
mod2=[0.03:0.001:0.04];
mod3=[0.04:0.0001:0.05];
mod=[0.0001,0.001,0.005,0.006,0.007,0.008,0.009,0.001,0.0015,mod1,mod2,mod3,0
.051,0.08,0.09,0.1,0.12,0.15,0.17,0.2,0.3,0.4,0.5,0.6,0.7...
```

```
,0.8,0.9,1,1.5,2,2.5,3,3.5,4,4.5,5,5.5,6,6.5,7,7.5,8,8.5,9,9.5,10,10.5,13,15,
17,20];
Ipt=10^(-1/10)*1e-3*R;      %Optical Power Entering Booster Amp.
                            %-1dBm, 1dBm, 3dBm
Id=4e-9;    %Dark Current
for Ip=I;
    for m=mod;
        index=index+1;
        thermal_noise=((4*Kb*T)/Resistance)*B*Ft;
        ASE_noise(index)=(4*h*freq*nsp*B*R);
        shot_noise(index)=(2*q*B).*(Ip+Id);
        RIN_noise(index)=rin*B;
        u(index)=m*sqrt(N/2);
        IMD(index)=3072./(2^4*m^8*N^4);
        CONV_IMD(index)=128./(3*m^4*N^2);
        carrier(index)=2*(m/2)^2;
    end
end
clipping=sqrt(2*pi)*((1+6*u.^2)./u.^3).*exp(1./(2*u.^2));
for Ip=I;
    for m1=mod;
        index1=index1+1;
        source(index1,:)=0.5*((m1.^2).*Ip.^2);
        source1(index1,:)=0.5*((m1.^2).*Ipt);
        source2(index1,:)=0.5*((m1.^2));
    end
end

CNR_shot=source'./shot_noise;
CNR_RIN=source2'./RIN_noise;
CNR_Thermal=source'./thermal_noise;
CNR_ASE=source1'./ASE_noise;
CNR_noise=source'./(thermal_noise+shot_noise+RIN_noise);
CNR_clipping=clipping;
CNR_IMD=IMD;
CNR_CONV_IMD=CONV_IMD;

[a,b]=size(CNR_noise);
[c,d]=size(mod);

for n=0:(b/d)-1
    index2=index2+1;
    Noise_rx_shot_rin_thermal(index2,:)=CNR_noise(n*d+1:n*d+d);
    Noise_clipping(index2,:)=CNR_clipping(n*d+1:n*d+d);
    Noise_IMD(index2,:)=CNR_IMD(n*d+1:n*d+d);
    Noise_CONV_IMD(index2,:)=CNR_CONV_IMD(n*d+1:n*d+d);
    Noise_ASE(index2,:)=CNR_ASE(n*d+1:n*d+d);
    Noise_shot(index2,:)=CNR_shot(n*d+1:n*d+d);
    Noise_Thermal(index2,:)=CNR_Thermal(n*d+1:n*d+d);
    Noise_RIN(index2,:)=CNR_RIN(n*d+1:n*d+d);
end
Noise_total=(1./Noise_ASE)+(1./Noise_shot)+(1./Noise_Thermal)+(1./Noise_RIN)+
(1./Noise_CONV_IMD);
Noise_total2=(1./Noise_ASE)+(1./Noise_shot)+(1./Noise_Thermal)+(1./Noise_RIN)
;
Noise_total=(1./Noise_total);
```

```matlab
[m,n]=size(Noise_total);
for n1=1:m
    index3=index3+1;
    total=[Noise_total(n1,:);Noise_clipping(n1,:)];
    total_CNR(n1,:)=min(total);
end
[e,f]=size(I)
for n2=1:f
    index4=index4+1;
    DR(index4)=max(total_CNR(n2,:));
end
hubs=1:f;
figure(1)
semilogx(mod, 10*log10(Noise_ASE(1,:)),'g');grid;hold;
semilogx(mod, 10*log10(Noise_shot(1,:)),'c');
semilogx(mod, 10*log10(Noise_RIN(1,:)),'b');
semilogx(mod, 10*log10(Noise_Thermal(1,:)),'m');
semilogx(mod, 10*log10(Noise_clipping(1,:)),'k');
semilogx(mod, 10*log10(Noise_CONV_IMD(1,:)),'r');
semilogx(mod, 10*log10(total_CNR(1,:)),'.-');
semilogx(mod, 10*log10(Noise_total2(1,:)));
axis([0,10,0,80])
title('Figure 4-3 CNR vs OMI with one Remote Unit');
xlabel('OMI');
ylabel('CNR');
h = legend('ASE Noise','Shot Noise','RIN Noise','Thermal Noise','Laser
Clipping','CTB','CNR');

[m2,n2]=size(total_CNR);
for n3=1:m2
    index5=index5+1;
    CNR_predistortion(n3,:)=max([total_CNR(n3,:)]);
end
figure(2)
plot(hubs, 10*log10(CNR_predistortion));grid;hold
plot(hubs, 10*log10(CNR_predistortion),'*');
title('Figure 4-4 CNR vs. Number of End-Users')
xlabel('Number of End-Users')
ylabel('CNR')
figure(3)
semilogx(mod, 10*log10(Noise_CONV_IMD(1,:)),'r');grid;
axis([0,10,0,80])
title('Figure 2-5 CTB/C vs. OMI');
xlabel('OMI');
ylabel('CTB/C');
h = legend('CTB/C for 78 CATV channels');

%Program 3: Dual Parallel Linearized MZ Modulator
%Figure 4-6 to 4-11
clear all;
close all

index=0;
index1=0;
index2=0;
index3=0;
%Modulation Index
```

```matlab
mod1=[[0.01:0.0005:0.05],[0.051:0.005:0.11]];
mod2=mod1;
m=mod2;

M=mod1.*sqrt(78);
M1=mod2.*sqrt(78);

B=[2,2.5,3]
for n=1:length(B)
index=index+1;
A1(index,:)=(B(n)*(mod1./2)).^3;
A2(index,:)=exp(-B(n)^2*(M.^2)./4);
A3(index,:)=(mod1./2).^3;
A4(index,:)=exp(-(M.^2)./4);
end

for n=1:length(B);
    index1=index1+1;
    A(index1,:)=(A1(n,:).*A2(n,:))./((A3(n,:).*A4(n,:))+(A1(n,:).*A2(n,:)));
end

CONV_IMD=128./(3*m.^4*78^2);
CONV_IMD5=(m./2).^8*(78^4/12);

figure(1)
plot(mod1,A);grid;hold;
title('Figure 4-6 DPMZ Power Divider Ratio vs. OMI');
xlabel('Optical Modulation Index m');
ylabel('Power Divider Ratio(A)');
h = legend('B=2','B=2.5','B=3');
axis([0.01,.1,0.8,1])

a=[0.88,0.93,0.96];
b=[2,2.5,3];

for n1=1:length(b)
index2=index2+1;
IMD1(index2,:)=a(n1).*(m./2).^3;
IMD2(index2,:)=exp(-(M1.^2)./4);
IMD3(index2,:)=(1-a(n1)).*(b(n1).^3*(m./2).^3);
IMD4(index2,:)=exp(-b(n1).^2*(M1.^2)./4);
C1(index2,:)=a(n1).*(m./2);
C2(index2,:)=exp(-(M1.^2)./4);
C3(index2,:)=(1-a(n1)).*(b(n1)*(m./2));
C4(index2,:)=exp(-b(n1).^2*(M1.^2)./4);
IMD5_1(index2,:)=a(n1).*(m./2).^5;
IMD5_2(index2,:)=exp(-(M1.^2)./4);
IMD5_3(index2,:)=(1-a(n1)).*(b(n1).^5*(m./2).^5);
IMD5_4(index2,:)=exp(-b(n1).^2*(M1.^2)./4);
test_imd5(index2,:)=(b(n1).^4)*(m./2).^8*(78^4/12);
end

total_IMD=(IMD1.*IMD2)-(IMD3.*IMD4);
total_IMD_5=(IMD5_1.*IMD5_2)-(IMD5_3.*IMD5_4);
total_C=(C1.*C2)-(C3.*C4);
CTB=(total_IMD./total_C).^2*(3*78^2/8);
CTB_5=(total_IMD_5./total_C).^2*((78^4)/12);
```

```
CTB_IMD5=CTB+test_imd5;

figure(2)
plot(m, 10*log10(1./CTB));grid;hold
plot(m, -10*log10(1./CONV_IMD),'r');
figure(3)
plot(m, -10*log10(CTB(1,:)),'b');grid;hold
plot(m, -10*log10(test_imd5(1,:)),'b.');
plot(m, -10*log10(CTB(2,:)),'r');
plot(m, -10*log10(test_imd5(2,:)),'r.');
plot(m, -10*log10(CTB(3,:)),'k');
plot(m, -10*log10(test_imd5(3,:)),'k.');
axis([0.01,.1,0,120])
title('Figure 4-11 Carrier to Third & Fifth order distortion vs. OMI');
xlabel('Optical Modulation Index m');
ylabel('C/CTB & C/CIR5(dB)');
h = legend('Case I: Third Order Distortion','Case I: Fifth Order
Distortion','Case II: Third Order Distortion','Case II: Fifth Order
Distortion','Case III: Third Order Distortion','Case III: Fifth Order
Distortion');

%Program 4: Carrier-to-Noise Ratio Analysis with Linearized Modulator
%Plot Figure 4-12 to 4-18
%Figure 4-13 Parameter: a=0.88, b=2, RIN=-155, R=0.8, P=-1dBm
%Figure 4-14 Parameter: a=0.93, b=2.5, RIN=-155, R=0.8, P=-1dBm
%Figure 4-15 Parameter: a=0.96, b=3, RIN=-155, R=0.8, P=-1dBm

clear all;
close all;
load c:\eecs891\BER_CNR_pwr\data.mat;
load c:\eecs891\BER_CNR_pwr\linear_imd.mat;
load c:\eecs891\BER_CNR_pwr\imd5.mat;
load c:\eecs891\BER_CNR_pwr\total_linear_imd.mat;

mod_index=164;                         %0.0448 OMI
Number=30;                             %No. of Customer
q=1.60218e-19;
B=4e6;                                 %CATV Channel bandwidth
N=78;                                  %Assume 80 CATV Channel
rin=10^(-160/10);                      %RIN = -155, -160
length = 10;                           %fiber distance
delta = 0.22;                          %fiber loss
R = 0.9;                               %Responsivitiy =0.8, 0.9
irx = 1e-12;
Kb=1.38e-23;
T=300;
Resistance=1000;
Ft=10^(5/10);
h=6.625e-34;
freq=3e8/1550e-9;
nsp=10^((5-3)/10);
gain=10^(0/10);
I=current';

index=0;
index1=0;
index2=0;
```

```
index3=0;
index4=0;
index5=0;

mod1=[0.01:0.001:0.03];
mod2=[0.03:0.0001:0.04];
mod3=[0.04:0.0001:0.046];
mod=[0.0001,0.001,0.005,0.006,0.007,0.008,0.009,mod1,mod2,mod3,0.051,0.08,0.0
9,0.1,0.12,0.15,0.17,0.2,0.3,0.4,0.5,0.6,0.7...
      ,0.8,0.9,1];

Ipt=10^(3/10)*1e-3*R;        %Optical Power Input at Booster Amp.
                             %-1dBm, 1dBm, 3dBm
Id=4e-9;

for Ip=I;
   for m=mod;
      index=index+1;
      thermal_noise=((4*Kb*T)/Resistance)*B*Ft;
      ASE_noise(index)=(4*h*freq*nsp*B*R);
      shot_noise(index)=(2*q*B).*(Ip+Id);
      RIN_noise(index)=rin*B;
      u(index)=m*sqrt(N/2);
      CONV_IMD(index)=128./(3*m^4*N^2);
      carrier(index)=2*(m/2)^2;
   end
end
clipping=sqrt(2*pi)*((1+6*u.^2)./u.^3).*exp(1./(2*u.^2));

A=0.93;        %A=0.88, 0.93, 0.95
B=2.5;         %B=2, 2.5, 3
for Ip=I;
   for m1=mod;
      index1=index1+1;
      source(index1,:)=0.5*(Ip.^2).*(((A^2).*(m1.^2))-(((1-
A)^2).*(B.*m1).^2));
      source1(index1,:)=0.5*(Ipt).*(((A^2).*(m1.^2))-(((1-
A)^2).*(B.*m1).^2));
      source2(index1,:)=(((0.5*A^2).*(m1.^2))-((0.5*(1-A)^2).*(B.*m1).^2));
      source3(index1,:)=2*R^2*(10^(-63.5/10))*(10^(-21.8138/10)*1e-3)^2;
   %Signal-Crosstalk Terms
   end
end

CNR_shot=source'./shot_noise;
CNR_RIN=source2'./RIN_noise;
CNR_Thermal=source'./thermal_noise;
CNR_ASE=source1'./ASE_noise;
CNR_noise=source'./(thermal_noise+shot_noise+RIN_noise);
CNR_clipping=clipping;
CNR_xtalk=source'./source3';
CNR_CONV_IMD=CONV_IMD;

[a,b]=size(CNR_noise);
[c,d]=size(mod);

for n=0:(b/d)-1
```

```
    index2=index2+1;
    Noise_rx_shot_rin_thermal(index2,:)=CNR_noise(n*d+1:n*d+d);
    Noise_clipping(index2,:)=CNR_clipping(n*d+1:n*d+d);
    Noise_xtalk(index2,:)=CNR_xtalk(n*d+1:n*d+d);
    Noise_CONV_IMD(index2,:)=CNR_CONV_IMD(n*d+1:n*d+d);
    Noise_ASE(index2,:)=CNR_ASE(n*d+1:n*d+d);
    Noise_shot(index2,:)=CNR_shot(n*d+1:n*d+d);
    Noise_Thermal(index2,:)=CNR_Thermal(n*d+1:n*d+d);
    Noise_RIN(index2,:)=CNR_RIN(n*d+1:n*d+d);
end
te=ones(1,60);
te=te';
Noise_IMD=te*(1./CTB);
Noise_IMD5=te*(1./test_imd5);
Noise_IMD3_IMD5=te*(1./CTB_IMD5);

Noise_total=(1./Noise_ASE)+(1./Noise_shot)+(1./Noise_Thermal)+(1./Noise_RIN)+
(1./Noise_IMD)+(1./Noise_xtalk);
Noise_total=(1./Noise_total);
[m,n]=size(Noise_total);
for n1=1:m
    index3=index3+1;
    total=[Noise_total(n1,:);Noise_clipping(n1,:)];
    total_CNR(n1,:)=min(total);
end
[e,f]=size(I)
for n2=1:f
    index4=index4+1;
    DR(index4)=max(total_CNR(n2,:));
end
hubs=1:f;
figure(1)
semilogx(mod, 10*log10(Noise_ASE(1,:)),'g');grid;hold;
semilogx(mod, 10*log10(Noise_shot(1,:)),'c');
semilogx(mod, 10*log10(Noise_RIN(1,:)),'b');
semilogx(mod, 10*log10(Noise_Thermal(1,:)),'m');
semilogx(mod, 10*log10(Noise_clipping(1,:)),'k');
semilogx(mod, 10*log10(Noise_IMD(1,:)),'r');
semilogx(mod, 10*log10(Noise_IMD5(1,:)),'.-g');
semilogx(mod, 10*log10(total_CNR(1,:)),'.-');
semilogx(mod, 10*log10(total_CNR(30,:)),'.-r');
semilogx(mod, 10*log10(total_CNR(60,:)),'.-k');
axis([0,10,0,80])
title('Figure 4-15:CNR vs OMI using Case III linearized Modulator');
xlabel('OMI');
ylabel('CNR');
h = legend('ASE Noise','Shot Noise','RIN Noise','Thermal Noise','Laser
Clipping','CTB','CIR5','CNR 1 end-users','CNR 30 end-users','CNR 60 end-
users');
[m2,n2]=size(total_CNR);
for n3=1:m2
    index5=index5+1;
    CNR_predistortion(n3,:)=max([total_CNR(n3,:)]);
end
figure(2)
plot(hubs, 10*log10(CNR_predistortion));grid;hold
plot(hubs, 10*log10(CNR_predistortion),'*');
```

```matlab
title('CNR vs. Number of Remote Unit')
xlabel('Number of Hubs (Remote Units) in a passive optical star network')
ylabel('CNR')
%Program 5: Q Value analysis with Linearized Modulator
%Plot figure 4-19 to 4-20
%Figure 4-19 Parameter: a=0.88, b=2, RIN=-155, R=0.8, P=-1dBm, Number=27
%Figure 4-14 Parameter: a=0.93, b=2.5, RIN=-155, R=0.8, P=-1dBm, Number=30
%Figure 4-15 Parameter: a=0.96, b=3, RIN=-155, R=0.8, P=-1dBm, Number=18

clear all;
close all;
load c:\eecs891\ber_cnr_pwr\data.mat;
load c:\eecs891\ber_cnr_pwr\star_hub;
Number=60;
ix=164;                                 %177, 164, 72
q=1.60218e-19;
B_total = 1e9;                          %Digital data rate is 1Gbps
N=1;                                    %1 digital Channel
Be=0.7*B_total/N;                       %Electrical Bandwidth
length = 10;                            %fiber distance
delta = 0.22;                           %fiber loss
R = 0.9;                                %Responsivitiy= 0.8 & 0.9

Kb=1.38e-23;
T=300;
Resistance=1000;
Ft=10^(5/10);
h=6.625e-34;
freq=3e8/1550e-9;
F=5;
nsp=10^((F-3)/10);
rin=10^(-160/10);                       %RIN = -155 & -160
Id=2e-9;

index=0;
index1=0;
index2=0;

mod1=[0.01:0.001:0.03];
mod2=[0.03:0.0001:0.04];
mod3=[0.04:0.0001:0.046];
mod=[0.0001,0.001,0.005,0.006,0.007,0.008,0.009,mod1,mod2,mod3,0.051,0.08,0.09,0.1,0.12,0.15,0.17,0.2,0.3,0.4,0.5,0.6,0.7...
     ,0.8,0.9,1];

Ipt=sqrt(10^(3/10)*1e-3);               %Input Optical Power at Booster
                                        %-1dBm, 1dBm & 3dBm

for Ip=current'*gain;
    for m=mod;
    index=index+1;
    thermal_noise=sqrt(((4*Be*Kb*T*Ft)/Resistance));
    %ASE_noise(index)=sqrt(4*R*Ip*nsp*freq*h*(gain)*Be);
    ASE_noise(index)=sqrt(4*nsp*freq*h*Be*R);
    shot_noise(index)= sqrt(2*q*Be*(Ip+Id));
    RIN_noise(index)=sqrt(Ip^2*rin*Be);
    end
```

```matlab
    end


A=0.93;  %A=0.88, 0.93, 0.96
B=2.5;   %B=2, 2.5, 3

for Ip=current';
   for m1=mod;
      index1=index1+1;
      source(index1,:)=(Ip).*((A.*m1*exp(-m1^2*80/4))-((1-A)*B.*m1*exp(-
B^2*m1^2*80/4)));
      source1(index1,:)=(Ipt).*((A.*m1*exp(-m1^2*80/4))-((1-A)*B.*m1*exp(-
B^2*m1^2*80/4)));
      source3(index1,:)=sqrt(2*R^2*(10^(-52.3845/10))*(10^(-21.8138/10)*1e-
3)^2);
%Signal-Crosstalk Noise Term
   end
end
pwr=source';


BPSK_Q_shot=source'./shot_noise;
BPSK_Q_RIN=source'./RIN_noise;
BPSK_Q_Thermal=source'./thermal_noise;
BPSK_Q_ASE=source1'./ASE_noise;
BPSK_Q_xtalk=source'./source3';
BPSK_Q_noise=(1./BPSK_Q_ASE)+(1./BPSK_Q_shot)+(1./BPSK_Q_Thermal)+(1./BPSK_Q_
RIN)+(1./BPSK_Q_xtalk);
BPSK_Q_noise=(1./BPSK_Q_noise);
BPSK_Q_noise_ASE=source1'./(ASE_noise);

[a,b]=size(BPSK_Q_noise);
[c,d]=size(mod);

for n=0:(b/d)-1
   index2=index2+1;
   BPSK_Q(index2,:)=BPSK_Q_noise(n*d+1:n*d+d);
   ASK_Q(index2,:)=0.5*(BPSK_Q_noise(n*d+1:n*d+d));
   QPSK_Q(index2,:)=(1/sqrt(2))*(BPSK_Q_noise(n*d+1:n*d+d));
   BPSK_ASE(index2,:)=BPSK_Q_noise_ASE(n*d+1:n*d+d);
   power(index2,:)=pwr(n*d+1:n*d+d);
end

Q_Various=[BPSK_Q(Number,:); QPSK_Q(Number,:); ASK_Q(Number,:)];
Q_ASE=[BPSK_ASE(Number,:);0.5*BPSK_ASE(Number,:);(1/sqrt(2))*BPSK_ASE(Number,
:)];
figure(1)
semilogx(mod, Q_Various);grid;
title('Q Value at BPSK, QPSK & ASK Modulation vs Modulation Index')
xlabel('Optical Modulation Index')
ylabel('Q Value')
axis([0.01,0.06,0,60])
figure(2)
plot(mod, Q_Various);grid
title('Q Value at BPSK, QPSK & ASK Modulation vs. Modulation Index')
xlabel('Optical Modulation Index')
ylabel('Q')
```

```
h = legend('BPSK','QPSK','ASK');
axis([0,0.05,0,20])
figure(3)
plot(mod,Q_ASE);grid;hold;
title('Q Value (Signal-ASE Noise only) Vs. Modulation Index')
BPSK_value=BPSK_Q(Number,ix)
QPSK_value=QPSK_Q(Number,ix)
ASK_value=ASK_Q(Number,ix)
p=10*log10((power(:,ix)./R)/1e-3);
set=[BPSK_Q(:,ix),QPSK_Q(:,ix),ASK_Q(:,ix)];
figure(4)
subplot(2,1,1)
plot(mod, Q_Various);grid
axis([0,0.05,0,20])
title('Figure 4-20 "Set 2"')
xlabel('OMI at 30 End-Users Optical Power Budget')
ylabel('Q')
h = legend('BPSK','QPSK','ASK');
subplot(2,1,2)
plot(p, set);grid;hold;
xlabel('Optical Channel Power at 4.34% OMI')
ylabel('Q')
h = legend('BPSK','QPSK','ASK');

%Program 6: FWM
%Plot figure 5-10A, 5-10B
run c:\eecs891\Crosstalk\SM_fiber_narrow_spacing;

clear all;
close all;
index=0;
index1=0;
index2=0;
index3=0;
index4=0;
index5=0;

load c:\eecs891\Crosstalk\freq_spacing;
load c:\eecs891\Crosstalk\smallwavelength;

wavelength=1550;                            %nm
c=3e8/1e-9;                                 %nm/s
Aeff =78*(1e-6)^2;                          %m^2
delta =0.22/4.343;                          %/km  = 0.25dB/km
l=10;                                       %km
leff=(1/delta)*(1-exp(-delta*l));           %km
D=(17e-12);                                 %(Dispersion) s/(nm*km)
S=0.08e-12;                                 %(Dispersion) s/(nm^2*km)
n2=2.68e-20;                                %(non-linear refractive index)
m^2/W
n=1.4645;                                   %SM fiber refractive index
df=df*1e6;                                  %Convert MHz to Hz
P1=10^(-0.77/10)*1e-3;
Ip=P1*0.9;
a=0.93;
b=2.5;
m1=0.0434;
```

```
source=(Ip)*((a*m1*exp(-m1^2*80/4))-((1-a)*b*m1*exp(-b^2*m1^2*80/4)));
P=source/0.9
%Receiver Optical Power per channel
save('power','P');
B=((2*pi*wavelength^2)/c)*df.^2*D+((2*pi*wavelength^4)/c^2)*df.^3*S;
N1=delta^2./(delta.^2+B.^2);
N2=4*exp(-delta*l)*sin(B*l/2).^2;
N3=(1-exp(-delta*l)).^2;
N=N1.*(1+(N2./N3));

FWM=(32*pi*n2*(leff*1000)*6)/(240*(wavelength*1e-9)*Aeff);
FWM1_sm=(FWM*P)^2*N;

figure(1)
plot(dw, 10*log10(FWM1_sm));grid
FWM2_sm=(FWM*P)^2*N*P*exp(-delta*l);

figure(2)
subplot(2,1,1)
plot(dw, 10*log10(FWM2_sm/1e-3));grid
title('Figure 5-10A FWM optical power(dBm) vs. Wavelength Separation(nm)')
ylabel('FWM optical power (dBm)')
subplot(2,1,2)
plot(dw, 10*log10(FWM1_sm));grid
title('Figure 5-10B Ratio of FWM power to transmitted ch. power vs.
Wavelength Separation(nm)')
xlabel('Wavelength Separation(nm)')
ylabel('FWM crosstalk level')
save('fwm_sm_ratio','FWM1_sm');
save('fwm_sm_power','FWM2_sm');

%Program 7: SRS,XPM+FWM
%Plot Figure 5-7,5-8,5-9A&B,5-11 & 5-12
run c:\eecs891\Crosstalk\SM_fiber_narrow_spacing;
clear all;
close all;
index=0;
index1=0;
index2=0;
index3=0;
index4=0;
index5=0;
index6=0;

load c:\eecs891\Crosstalk\smallgain;
load c:\eecs891\Crosstalk\smallwavelength;
load c:\eecs891\ber_cnr_pwr\data.mat;
load c:\eecs891\crosstalk\freq_spacing;

[m,number]=size(gain);

p=1                  %effective polarization
%Note: If the polarizations of the two (2) fields are closed to perpendicular
(p=0.00001). Crosstalk mininal.
%Note: If the polarizations of the two (2) fields are parallel (p=1),
Crosstalk mininal.
```

```matlab
Aeff = 78*(1e-6)^2;   %m^2
Aeff1=78*(1e-6)^2;        %m^2
delta =0.222/4.343;   %/km  = 0.25dB/km
l=10;                 %km
leff=(1/delta)*(1-exp(-delta*l));
Dispersion=(17e-12); %s/nm/km
Dispersion1=17 ;      %ps/nm/km
P1=10^(-0.77/10)*1e-3;
Ip=P1*0.9;

a=0.93;
b=2.5;
m1=0.0434;
source=(Ip)*((a*m1*exp(-m1^2*80/4))-((1-a)*b*m1*exp(-b^2*m1^2*80/4)));
P=source/0.9;  %Optical Power per Channel

d=Dispersion*(dw);

freq=[0:.01:6];
freq=freq*1e6;

for n=1:number
   %%%%%%%%%%%%%%%
   index=index+1;
   %%%%%%%%%%%%%%%
A(index,:)=((p*gain(n).*P)/(Aeff/1000)).^2;                 %1/km^2
B(index,:)=1+exp(-2*delta*l)-2*exp(-delta*l).*cos(2*pi*freq*d(n)*l);
C(index,:)=(delta)^2+(2*pi*freq*d(n)).^2;            %1/km^2
D(index,:)=(1+((p*gain(n)*P*leff*1000)/Aeff1)).^2;
srs(index,:)=(A(n,:)).*(B(n,:)./(C(n,:)));
end

n2=2.68e-20 ;         %m^2/W
wavelength=1550;      %nm
wavelength=wavelength*(1e-9/1000);  %convert to km
wavelength1=1550  ;  %nm

c=3e8 ;              %m/s
c=3e8*(1e-12/1e-9);  %convert to ps/nm
b2=-((wavelength1)^2/(2*pi*c))*Dispersion1;      %ps^2/km

alpha=2*pi*n2/(wavelength*Aeff1);             %1/km

dt=dw*Dispersion1;

for n1=1:number
   %%%%%%%%%%%%%%%%%%%%%
   index1=index1+1;
   %%%%%%%%%%%%%%%%%%%%%
A1(index1,:)=2*alpha*P;
B1(index1,:)=exp(i*b2*(2*pi*freq*1e-12).^2*l*1/2)-exp(-
delta*l+i*(2*pi*freq*1e-12).*dt(n1)*l);
B2(index1,:)=i.*(delta-i.*2*pi*freq*1e-12.*dt(n1)+(i.*b2*(2*pi*freq*1e-
12).^2*0.5));
C1(index1,:)=exp(-i*b2*(2*pi*freq*1e-12).^2*l*1/2)-exp(-
delta*l+i*(2*pi*freq*1e-12).*dt(n1)*l);
```

```matlab
C2(index1,:)=i.*(delta-i.*2*pi*freq*1e-12.*dt(n1)-(i.*b2*(2*pi*freq*1e-
12).^2*0.5));
xpm(index1,:)=abs(A1(n1,:).*((B1(n1,:)./B2(n1,:))-(C1(n1,:)./C2(n1,:)))).^2;
end

xtalk_srs_xpm=abs(((srs)+(xpm)));
xtalk_srs_xpm1=abs(((srs)-(xpm)));
srs_6MHz=(P^2/freq(length(freq))).*srs;

%%%%%%%%%%%%%%%%%%%%%%%%%%%%%%%%%%%%%%%%%%%%%%%%%%%%%%%%%%%%%%%%%
%example:
%The modulation frequency is 1GHz
%The bandwidth_range is 0.1GHz
%The count will be starting at
%0Hz, 0.1GHz,0.2GHz,0.3GHz....0.9GHz
%srs_6MHz(1), srs_6MHz(1000+1),srs_6MHz(2000+1)...srs_6MHz(9000+1)
%%%%%%%%%%%%%%%%%%%%%%%%%%%%%%%%%%%%%%%%%%%%%%%%%%%%%%%%%%%%%%%%%
n2=1
modulation_frequency=freq(length(freq));  %modulation frequency bandwidth,
6MHz
%count=modulation_frequency/((length(freq)-1)/n);
bandwidth_range=n2*1e6             %if n2=1, bandwidth_range is 1e6
                                   %if n2=0.01, bandwidth range is 10000Hz
count=(length(freq)-1)/(modulation_frequency/bandwidth_range);

for number1=1:number
    for number2=0:(modulation_frequency/bandwidth_range)-1
        %%%%%%%%%%%%%%%%%%%%
        index3=index3+1;
        %%%%%%%%%%%%%%%%%%%%

srs_6MHz_total(number1,index3)=srs_6MHz(number1,(count*number2+1))*bandwidth_
range;
    end
end

for number3=1:number
    %%%%%%%%%%%%%%%%
    index4=index4+1;
    %%%%%%%%%%%%%%%%%%
    srs_total(index4)=sum(srs_6MHz_total(index4,:));
end

xpm_6MHz=(P^2/freq(length(freq))).*xpm;

for number4=1:number
    for number5=0:(modulation_frequency/bandwidth_range)-1
        %%%%%%%%%%%%%%%%%%
        index5=index5+1;
        %%%%%%%%%%%%%%%%%%

xpm_6MHz_total(number4,index5)=xpm_6MHz(number4,(count*number5+1))*bandwidth_
range;
    end
end

for number6=1:number
```

```matlab
    %%%%%%%%%%%%%%%
    index6=index6+1
    %%%%%%%%%%%%%%%%
    xpm_total(index6)=sum(xpm_6MHz_total(index6,:));
end

xtalk_srs_xpm_6MHz=abs((srs_total+xpm_total));

figure(1)
plot(freq,10*log10((srs)));grid;
title('Crosstalk (SRS) vs. Modulation Frequency')
xlabel('Modulation Freqency (Hz)')
ylabel('Crosstalk (SRS)')
figure(2)
plot(freq, 10*log10(xpm),'.-');grid
title('Crosstalk (XPM) vs. Modulation Frequency')
xlabel('Modulation Freqency (Hz)')
ylabel('Crosstalk (XPM)')
figure(3)
plot(freq,10*log10(xtalk_srs_xpm));grid
title('Figure 5-7 Crosstalk (SRS+XPM) vs. 6MHz Modulation Frequency')
xlabel('Modulation Freqency (Hz)')
ylabel('Crosstalk (SRS+XPM)')
figure(4)
plot(freq,10*log10(xtalk_srs_xpm1));
title('Figure 5-8 Crosstalk (SRS+XPM) vs. 6MHz Modulation Frequency')
xlabel('Modulation Freqency (Hz)')
ylabel('Crosstalk (SRS,XPM)')
figure(6)
plot(dw,10*log10(srs_total/1e-3),'r');hold
plot(dw,10*log10(xpm_total/1e-3),'g');
plot(dw,10*log10(xtalk_srs_xpm_6MHz/1e-3),'.-');grid
title('Crosstalk Electrical power (dBm) vs. Wavelength Separation (nm)')
xlabel('Wavelength Separation(nm)')
ylabel('Crosstalk (SRS,XPM& SRS+XPM)')
h = legend('SRS','XPM','Crosstalk(SRS+XPM)',3);
figure(7)
subplot(2,1,1)
plot(dw,10*log10(sqrt(srs_total)/1e-3),'r');hold
plot(dw,10*log10(sqrt(xpm_total)/1e-3),'g');
plot(dw,10*log10(sqrt(xtalk_srs_xpm_6MHz)/1e-3),'.');grid
title('Figure 5-9A Xtalk Optical power(dBm) vs. Wavelength Separation(nm)')
ylabel('Crosstalk Optical Power (dBm)')
h = legend('SRS','XPM','Crosstalk(SRS+XPM)',3);
subplot(2,1,2)
plot(dw,10*log10(sqrt(srs_total)/(P)),'r');hold
plot(dw,10*log10(sqrt(xpm_total)/(P)),'g');
plot(dw,10*log10(sqrt(xtalk_srs_xpm_6MHz)/(P)),'.');grid
title('Figure 5-9B xtalk normalized to transmitted ch. power vs. Wavelength
Separation(nm)')
xlabel('Wavelength Separation(nm)')
ylabel('Crosstalk level (dB)')
h = legend('SRS','XPM','Crosstalk(SRS+XPM)',3);

load c:\eecs891\crosstalk\fwm_sm_ratio;
load c:\eecs891\crosstalk\fwm_sm_power;
```

```matlab
ctalk=abs((sqrt(xtalk_srs_xpm_6MHz)+FWM2_sm));
ctalk_ratio=abs((sqrt(xtalk_srs_xpm_6MHz)/P+FWM1_sm));


figure(8
plot(dw, 10*log10(ctalk/1e-3),'.r');grid;hold
plot(dw, 10*log10(FWM2_sm/1e-3),'b');
plot(dw, 10*log10(sqrt(xtalk_srs_xpm_6MHz)/1e-3),'k');
title('Xtalk Optical Power (dBm) vs. Wavelength Separation(nm)')
xlabel('Wavelength Separation(nm)')
ylabel('Crosstalk Optcal Power (dBm)')
h = legend('Total Crosstalk','FWM','SRS+XPM');
axis([0 0.18 -100 -70])

figure(9)
plot(dw, 10*log10(ctalk_ratio),'.r');grid;hold
plot(dw, 10*log10(FWM1_sm),'b');
plot(dw, 10*log10(sqrt(xtalk_srs_xpm_6MHz)/P),'k');
title('Figure 5-11 Xtalk level vs. Wavelength Separation(nm)')
xlabel('Wavelength Separation(nm)')
ylabel('Crosstalk level (dB)')
h = legend('Total Crosstalk','FWM','SRS+XPM');
axis([0 0.178 -95 -65])

%%%%%%%%%%%%%%%%%%%%%%%%%%%%%%%%%%%%%%%%%%%%%%%%%%%%%%%%%%%%%%%%%%%%%%%%%%
%This portion program is to analysis different type of fibers
%
%                 NZDSF+         NZDSF-          SM Si-Core     SMF
%Fiber Eff.Area   53e-12 m^2     53e-12 m^2      78e-12 m^2     78e-12 m^2
%Fiber Loss       0.205 dB/km    0.239 dB/km     0.2 dB/km      0.25 dB/km
%Dispersion       3 ps/nm*km     -2.3 ps/nm*km   19 ps/nm*km    17 ps/nm*km
%%%%%%%%%%%%%%%%%%%%%%%%%%%%%%%%%%%%%%%%%%%%%%%%%%%%%%%%%%%%%%%%%%%%%%%%%%
load c:\eecs891\Crosstalk\ctalk_sicore;
load c:\eecs891\Crosstalk\ctalk_NZDSF1;
load c:\eecs891\Crosstalk\ctalk_NZDSF2;

load c:\eecs891\Crosstalk\ctalk_sicore1;
load c:\eecs891\Crosstalk\ctalk_NZDSF11;
load c:\eecs891\Crosstalk\ctalk_NZDSF21;

figure(10)
plot(dw,10*log10(ctalk_ratio),'b');grid;hold;
plot(dw,10*log10(ctalk_ratio_sicore),'m');
plot(dw,10*log10(ctalk_ratio_NZDSF1),'g');
plot(dw,10*log10(ctalk_ratio_NZDSF2),'k');
title('Figure 5-12 Crosstalk vs. Wavelength Separation(nm)')
xlabel('Wavelength Separation(nm)')
ylabel('Crosstalk Level (dB)')
h = legend('SM (D=17)','Si-Core (D=19)','NZDSF+ (D=3) ','NZDSF- (D=-2.3)');
```

```
%Program 8 Total Crosstalk vs Channel Index
%Plot Figure 5-13 & 5-14
clear all
close all
load c:\eecs891\Crosstalk\te\ctalk_ratio_sm;
load c:\eecs891\Crosstalk\te\ctalk_ratio_sm1g;
load c:\eecs891\Crosstalk\te\ctalk_ratio_sm2g;
load c:\eecs891\Crosstalk\te\ctalk_ratio_sm3g;
load c:\eecs891\Crosstalk\te\ctalk_ratio_sm4g;
load c:\eecs891\Crosstalk\te\ctalk_ratio_sm5g;
load c:\eecs891\Crosstalk\te\ctalk_ratio_sm6g;
load c:\eecs891\Crosstalk\te\ctalk_ratio_sm7g;
load c:\eecs891\Crosstalk\te\ctalk_ratio_sm8g;
load c:\eecs891\Crosstalk\te\ctalk_ratio_sm9g;
load c:\eecs891\Crosstalk\te\ctalk_ratio_sm10g;
ctalk_ratio_g=[ctalk_ratio_1g;ctalk_ratio_2g;ctalk_ratio_3g;ctalk_ratio_4g;..
.
ctalk_ratio_5g;ctalk_ratio_6g;ctalk_ratio_7g;ctalk_ratio_8g;ctalk_ratio_9g;ct
alk_ratio_10g];
%%%%%%%%%%%%%%%%%%%%%%%%%%%%%%%%%%%%%%%%%%%%%%%%%%%%%%
%This section is to calcuate the total crosstalk on
%individual CATV channel(2to77), High-speed data channel
%%%%%%%%%%%%%%%%%%%%%%%%%%%%%%%%%%%%%%%%%%%%%%%%%%%%%%
index=0;
index1=0;
index2=0;
index3=0;
index4=0;

a=[ctalk_ratio(1:77)];   %78 CATV Channel
b=[-sort(-a),0,a];
c=(length(a)+1);
ch=1:78;
for number=0:77
   index=index+1;
   channel_side1(index,:)=sum(b(c:(length(b)-number)))
   channel_side2(index,:)=sum(b((c-number):c));
 end

 for num=1:10
    index1=index1+1;
       channel78(index1,:)=channel_side1'+channel_side2'+(-sort(-
       ctalk_ratio_g(num,:)));
       channel79(index1,:)=sum(ctalk_ratio_g(num,:));
 end
 figure(1)
 plot(ch,10*log10(channel78),'.-');grid;
 title('Figure 5-13 Crosstalk (dB) per CATV Channel Index')
 ylabel('Crosstalk level (dB)')
 xlabel('78 CATV Channel Index')
 axis([0 79 -58.96 -58.16])
 figure(2)
 plot(10*log10(channel79),'o-');grid;
 title('Figure 5-14 Crosstalk (dB) at Digital Channel')
 xlabel('Frequency Spacing (GHz)')
 ylabel('Crosstalk level (dB)')
 h = legend('Freq. Spacing between Digital Ch. and CATV ch. # 78');
```